



12-1997

Supercritical carbon dioxide extraction of lipids from *Pythium irregulare*

Terry Hill. Walker

Follow this and additional works at: https://trace.tennessee.edu/utk_graddiss

Recommended Citation

Walker, Terry Hill., "Supercritical carbon dioxide extraction of lipids from *Pythium irregulare*. " PhD diss., University of Tennessee, 1997.
https://trace.tennessee.edu/utk_graddiss/7501

This Dissertation is brought to you for free and open access by the Graduate School at TRACE: Tennessee Research and Creative Exchange. It has been accepted for inclusion in Doctoral Dissertations by an authorized administrator of TRACE: Tennessee Research and Creative Exchange. For more information, please contact trace@utk.edu.

To the Graduate Council:

I am submitting herewith a dissertation written by Terry Hill. Walker entitled "Supercritical carbon dioxide extraction of lipids from *Pythium irregulare*." I have examined the final electronic copy of this dissertation for form and content and recommend that it be accepted in partial fulfillment of the requirements for the degree of Doctor of Philosophy, with a major in Biosystems Engineering.

Luther R. Wilhelm, Major Professor

We have read this dissertation and recommend its acceptance:

Greg Hulbert, Hank Cochran, F. Ann Draughon

Accepted for the Council:

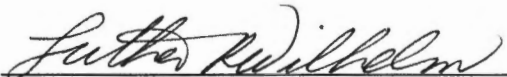
Carolyn R. Hodges

Vice Provost and Dean of the Graduate School

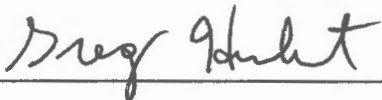
(Original signatures are on file with official student records.)

To the Graduate Council:

I am submitting herewith a dissertation written by Terry H. Walker entitled "Supercritical Carbon Dioxide Extraction of Lipids from *Pythium irregulare*." I have examined the final copy of this dissertation for form and content and recommend that it be accepted in partial fulfillment of the requirements for the degree of Doctor of Philosophy, with a major in Biosystems Engineering.


Luther R. Wilhelm, Major Professor


We have read this dissertation
and recommend its acceptance:







Accepted for the Council:


Associate Vice Chancellor and
Dean of The Graduate School

SUPERCRITICAL CARBON DIOXIDE EXTRACTION OF LIPIDS
FROM *PYTHIUM IRREGULARE*

A Dissertation
Presented for the
Doctor of Philosophy
Degree
The University of Tennessee, Knoxville

Terry H. Walker
December, 1997

Ag-VetMed

Thesis
97b
.w34

Copyright © Terry H. Walker, 1997
All rights reserved

DEDICATION

**This dissertation is dedicated to Debbie Patton
for her endurance and continuing support
during the completion of this project.
The dedication is also extended to my parents,
George and Pamela Walker.**

ACKNOWLEDGEMENTS

My sincere appreciation is extended to my committee members for their encouragement throughout this endeavor. The support and invaluable advice from Drs. Greg Hulbert, Hank Cochran, Luther Wilhelm and Ann Draughon greatly exceeded my expectations. However, the friendship and contact was most important and will hopefully continue in my next ventures. I would like to thank Dr. Paul Bienkowski, Justin Shingleton and members of the Chemical Engineering machine shop who gratefully assisted me with the apparatus. Also, I thank Paul Elliot, Walker Garner and Greg Wagoner from the Biosystems engineering machine shop for their excellent work on parts of the apparatus.

My gratitude is extended to the faculty from the Department of Biosystems Engineering (including Drs. Raj Raman and Willie Hart) and the Department of Food Science and Technology (including Drs. Sharon Melton and Sam Beattie). Their excellent correspondence and friendship made the collaboration between the departments a strong relationship that has important potential for higher learning and research. Finally, I would like to thank my fellow students, Charlie Lin, Harvey Drews, Ming Cheng, Wayne Liao and Yusuf Yilmaz for their support, advice and friendship. My correspondence with the three departments at the University of Tennessee and Oak Ridge National Laboratory proved to be most valuable and my luck for meeting truly genuine people among these groups has been a pleasure during my work experience at the University.

ABSTRACT

Lipids that contain polyunsaturated fatty acids (PUFA) have therapeutic value. Supercritical carbon dioxide extraction of PUFA from the lower fungi, *Pythium irregulare* was attempted for freeze-dried material in the presence of an aqueous phase. Extraction showed some success at moisture contents up to 30% (wb) and with the addition of a novel CO₂-philic surfactant. Equilibrium and kinetic data are presented. Equilibrium data were taken for the fungal oil in a flow-through apparatus at a low flow rate for two isotherms (40 and 60 °C) over a pressure range of 13.7 to 27.5 MPa. Equilibrium data were also taken for pure naphthalene at 40 °C to test the system. The compressed-gas model utilizing the Peng-Robinson equation of state was then applied to the data. The kinetic data portrayed three types of mass transfer behavior including an initial surface-film regime where pseudo steady-state conditions prevailed, a diffusion-controlled regime where unsteady-state conditions were evident and a temporary transition region. For tests with extraction times of 5 to 6 hours, data for the diffusion-controlled region were modeled with an analytical solution to Fick's Second Law assuming the particles were spherical shaped. The models worked well for both equilibrium and kinetic data, however the physical property values for the equilibrium data were altered substantially to obtain a reasonable fit with the compressed-gas model.

TABLE OF CONTENTS

Chapter

I. INTRODUCTION.....	1
1.1 Objectives.....	3
II. LITERATURE REVIEW.....	4
2.1 Polyunsaturated Fatty Acids.....	4
2.2 Fungal Production of Lipids.....	5
2.3 Waste Treatment Potential.....	7
2.4 Supercritical Carbon Dioxide.....	8
2.5 Solubility Considerations.....	13
2.6 Extraction from Aqueous Suspensions.....	14
2.7 Surfactant Technology.....	15
2.8 Extraction of Fungal Lipids.....	16
2.9 Enzyme-Catalyzed Reactions in Supercritical CO ₂	21
III. THEORY AND MODEL DEVELOPMENT.....	24
3.1 Solubility Modeling.....	24
3.2 Compressed Gas Model (PR-EOS).....	26
3.3 Physical Properties.....	31
3.3.1 Estimation of Vapor Pressure.....	32
3.3.2 Estimation of Critical Properties and Other Physical Properties.....	34
3.4 Application of Physical Properties.....	34

3.5 Mass Transfer Modeling	38
IV. METHOD DEVELOPMENT	42
4.1 Fungal Biomass Cultivation and Preparation	42
4.2 CO ₂ Extraction Apparatus	47
4.3 Extraction Procedure.....	50
4.3.1 Flow-rate Kinetic Tests.....	51
4.3.2 Single-flow Kinetic Tests.....	53
4.3.3 Equilibrium Tests.....	54
4.4 Lipid Analysis.....	55
V. RESULTS AND DISCUSSION	58
5.1 Fungal Production.....	58
5.2 Equilibrium Results.....	61
5.2.1 Application of the Compressed-Gas Model	68
5.3 Mass Transfer Results	70
VI. CONCLUSIONS AND RECOMMENDATIONS	83
REFERENCES	87
APPENDIXES.....	99
A. PROCESS CONTROL AND FILTRATION DATA	100
B. KINETIC AND EQUILIBRIUM DATA.....	103

C. COMPUTER PROGRAMS.....	116
Program A. Compressed-Gas Model.....	117
Program B. Kinetic Model (Fick's Second Law).....	128
VITA.....	132

LIST OF TABLES

Table 3.1	Estimated physical properties for use in the PR-EOS model.....	37
Table 5.1.	Growth of <i>P. irregulare</i> and production of fungal oil.....	59
Table 5.2.	Typical fatty acid methyl ester distribution in <i>P. irregulare</i>	60
Table 5.3.	Comparison of solubilities (wt%) of <i>P. irregulare</i> oil with selected literature values.	66
Table 5.4.	Peng-Robinson EOS parameters estimated for fungal lipids.....	69
Table 5.5.	Effective diffusivities for <i>P. irregulare</i> obtained from Equation 32 at 20.6 Mpa.	74
Table B.1.	Raw data for flow-rate kinetic experiments	104
Table B.2.	Raw data for moisture-content kinetic experiments	109
Table B.3.	Raw data from equilibrium experiments.....	113

LIST OF FIGURES

Figure 2.1. Triacylglycerols containing PUFA (e.g. EPA).....	5
Figure 2.2. Pressure-temperature diagram for a pure component.	9
Figure 2.3. Diffusivity behavior of carbon dioxide.	11
Figure 2.4 Schematic of the supercritical CO ₂ extraction mechanism of fungal lipid from fragments of mycelium.	18
Figure 4.1. Photomicrograph (10X) of <i>P. irregulare</i> particle (0.15 mm radius) after cell mastication.	45
Figure 4.2. Photomicrograph (40X) of intact <i>P. irregulare</i> mycelium and sporangium.....	46
Figure 4.3. Schematic of continuous-flow supercritical CO ₂ system.	48
Figure 5.1. Sample chromatogram of fatty acid methyl ester distribution in <i>P.</i> <i>irregulare</i>	60
Figure 5.2. Experimental and literature solubility values for naphthalene at 40 °C. P-R Model is the fitted values from the compressed-gas model. M-K (1994) is McHugh and Krukonis (1994).....	62
Figure 5.3. Equilibrium data of fungal oil at 40 °C. The dehydrated fungi had a 0.15 mm particle radius and 10% moisture content.....	64
Figure 5.4. Equilibrium data of fungal oil at 60 °C. The dehydrated fungi had a 0.15 mm particle radius and 10% moisture content.....	64

Figure 5.5. Equilibrium data for fungal oil extracted from dehydrated fungi with 10% moisture content and 0.15 mm particle radius.	65
Figure 5.6. Density of carbon dioxide as a function of pressure for several isotherms.	67
Figure 5.8. Sample-loop mole fractions of fungal oil at 50 °C, 20.7 MPa, 10% moisture content and 0.15 mm particle radius.	71
Figure 5.9. Effect of flow rate on the extraction rate of fungal oil at 50 °C, 20.6 MPa, 10% moisture content and 0.15 mm particle radius.	73
Figure 5.10. Effect of moisture content and particle size on the extraction rate of fungal oil at 40 °C and 20.6 Mpa.	74
Figure 5.11. Extraction of lipids at selected flow rates from fungi with a particle size of 0.15 mm verses total moles of CO ₂ consumed.	77
Figure 5.12. Effect of flow rate and moisture content on the extraction rate of fungal oil at 50 °C and 20.6 MPa.	78
Figure 5.13. Fatty acid methyl ester fraction for fungi with a 10% MCwb extracted at 50 °C and 20.6 MPa.	79
Figure 5.14. Fatty acid methyl ester distribution 30% MCwb extracted at 50 °C and 20.6 MPa.	79
Figure 5.15. Effect of surfactant (10% w/w PFPE) on diffusion of fungal oil in <i>P. irregulare</i> with a 95% moisture content.	82
Figure A.1. Temperature data taken for experiment K1 (40 °C and 20.7 MPa) for the bath, cold trap and heating tape.	101

Figure A.2. Pressure data taken for experiment K1 (40 °C and 20.7 MPa) for the bath, cold trap and heating tape.....	101
Figure A.3. Filtration flux and energy consumption as a function of time for the fungal biomass.	102

CHAPTER I

INTRODUCTION

Beneficial health effects of consuming polyunsaturated fatty acids (PUFA) that include the ω -3 fatty acids, eicosapentaenoic acid (EPA) and docosahexaenoic acid (DHA) have been well publicized since the late 1980s. They are thought to reduce risk for coronary heart disease, arthritis, inflammation, hypertension, psoriasis, other autoimmune disorders and cancer. Algae are the dietary source of the fatty acids for marine fish and are a possible resource. However, fungi are also capable of producing EPA and are better suited for bioconversion of food processing wastes or other agricultural byproducts.

Microorganisms produce many complex macromolecules such as PUFA and enzymes. When compared to chemical synthesis, microorganisms are analogous to very efficient chemical factories that may significantly reduce the cost of production. Many simple compounds such as ethanol are also efficiently produced, making the bioconversion of grains a feasible option. Filamentous fungi such as *Pythium irregulare* produce large amounts of long-chain PUFA (e.g. EPA) and show potential for mass production of these valuable compounds. These fungi also degrade waste streams high in organic material such as food-processing waste streams making this bioprocess even more beneficial.

Although the filamentous fungi are capable of producing valuable compounds such as enzymes and PUFA, the separation and purification steps impose significant restraints particularly because these products are thermally labile, fragile or unstable (Shuler and Kargi, 1992). Carbon dioxide (CO₂) is a potentially feasible alternative solvent for the extraction of sensitive lipids because it becomes supercritical at 31.1 °C and 73.8 bar. The temperature is ideal for thermally labile compounds and the lack of oxygen prevents potentially harmful oxidation reactions. Supercritical CO₂ also has the advantages of low cost, nontoxicity, high diffusivities, low viscosity, and the capability of solubilizing many heavy organic compounds at reasonably low temperatures. Separation of the solvent after extraction is easily accomplished by reducing the pressure.

Unfortunately, polar compounds soluble in aqueous environments (e.g. enzymes) typically have limited solubility in supercritical CO₂ leaving vacant a broad number of useful applications. Supercritical CO₂ would be the ideal solvent for many valuable biological compounds except for the challenge of the aqueous phase. Water is also known to be inhibitory to the extraction rates of lipids from biological matrices, therefore, the extraction has been typically applied to freeze-dried material. Freeze-drying is an expensive process that may inhibit the economical savings that supercritical extraction offers. Also, the presence of an aqueous phase maybe important for swelling the biological matrix for better access of the CO₂ to the solute of interest as long as the phase does not produce a significant resistance to mass transfer. In this research we have attempted to optimize the supercritical extraction

process for removal of EPA from the fungal biomass in the presence of an aqueous phase adsorbed to the fungi.

1.1 Objectives

The specific objectives of the research included:

1. determine the phase equilibrium conditions with supercritical CO₂ for the fungal oil contained in the biomass suspensions and attempt to apply the compressed gas model for a simplified binary system.
2. conduct a series of experiments to determine the effect of CO₂ flow rate and moisture content on the mass transfer of the system containing fungi and attempt to model the diffusion process with Fick's Second Law.
3. determine the effect of the addition of a novel CO₂-soluble surfactant and its potential application to aqueous suspensions such as fermentation broth.

CHAPTER II

LITERATURE REVIEW

2.1 Polyunsaturated Fatty Acids

Beneficial health effects from consumption of certain fish oils have been attributed to the presence of the essential PUFA, EPA and DHA (see Figure 2.1). These ω -3 fatty acids have been linked to a reduced risk for coronary heart disease, arthritis, inflammation, hypertension, psoriasis, other autoimmune disorders and cancer (Simopoulos, 1989). The ω -6 fatty acids have also gained increasing interest for health benefits; examples include arachidonic acid (ARA) and γ -linolenic acid (ALA), which is recommended for relief of eczema (Ratledge, 1993). ALA is a precursor of ARA by means of an important rate-limiting D6-desaturase reaction (Yokochi, 1990). PUFA are currently marketed as dietary supplements at health food stores in the form of concentrated fish oils. Supplementation into baby foods has lately received greater interest. PUFA are also prescribed medications for humans and pets. The U.S. market alone in 1987 was estimated to be \$100 million per year, and the projected market was \$790 million per year (Van Der Wende, 1988). The European market is even greater.

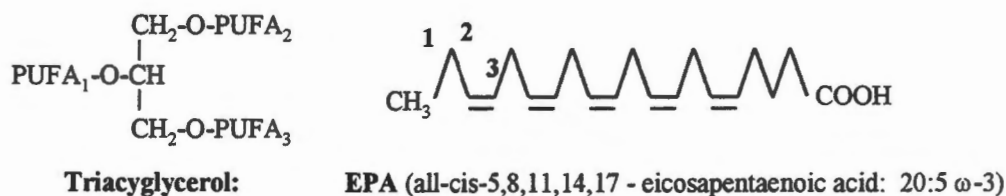


Figure 2.1. Triacylglycerols containing PUFA (e.g. EPA).

2.2 Fungal Production of Lipids

Declining marine resources and an increasing demand for PUFA have prompted the search for alternative sources of EPA and DHA. Also, concentrated fish oils contain additional, less desirable, fatty acids, cholesterol, and sometimes heavy metals and pesticides (Wessinger et al., 1990). Possible alternative sources of PUFA include algae and filamentous fungi. Commercialization of fungal oils has already taken place in the EEC and Japan for production of GLA from *Mucor circinelloides* and *Mortierella isabellina*, respectively (Ratledge, 1993).

Algae are the dietary source of the fatty acids for the marine fish and are consumed directly by some Asian populations (Radmer and Parker, 1994; Dunstan et al., 1993; Grima et al., 1993). In fact, Martek Corp. has proposed the production of EPA and DHA in the absence of other PUFA using two types of algae, one producing EPA and the other DHA, thus allowing for greater purification of each PUFA (Ratledge, 1993).

Filamentous fungi have the potential to produce large amounts of EPA within the mycelial walls when grown at optimal conditions (Radwan, 1991; Ghandi and Weete, 1991). These fungi are also capable of being genetically engineered to produce large amounts of fungal oil. Target fungal oils may contain specific fatty acids by altering the production of important desaturase enzymes that participate in the conversion of fatty acids (Ratledge, 1993). Shimizu et al. (1988) found that the genus *Mortierella* accumulated large amounts of EPA (29 mg/g dry mycelia) when grown at low temperature (12 °C). Previously, Yamada et al. (1987) determined that an isolate of *M. elongata* at higher temperatures produced a large amount of arachidonic acid (ARA), which is a possible precursor fatty acid to EPA in the presence of $\Delta 17$ -desaturase. Prior to this research, *Penicillium cyaneum* IAM 7302 was the only microorganism found to accumulate ARA intracellularly, although the amounts (on the order of 0.2 mg/g dry cells) were not industrially significant (Yamada et al. 1987). Bajpai and Bajpai (1993) reported that *M. alpina* 20-17 produced up to 103 mg EPA L⁻¹d⁻¹ when the cultures were allowed to age.

Mortierella species are also known to convert oils high in α -linolenic acid to EPA and are able to utilize various nitrogen sources such as soybean meal (Shinmen et al., 1992). Other works focused on the conversion of natural oils high in α -linolenic acid (e.g. linseed, soybean, and olive oil) to EPA where yields became as high as 66.6 mg/g dry mycelia (Shimizu et al., 1989a; Shimizu et al., 1989b). With fish oil as the main carbon source, the same species, *M. alpina* 1S-4, increased the amount of EPA

and DHA from the original amounts already present in the fish oil (Shinmen et al., 1992).

2.3 Waste Treatment Potential

Fungal bioconversions are well suited for treatment of processing waste from U.S. food industries. Fungi are heterotrophic and require carbon sources such as fats or carbohydrates for growth. These and other carbon sources are typically found in food processing waste streams. Fungi are particularly useful in treating "difficult to treat waste" such as low pH wastewaters from wineries or cheese processors, waste liquors from the pulp and paper industry containing ligninsulfonate, or waste streams containing heavy metals. Filamentous organisms, however, often disrupt conventional waste treatment methods because of their poor filtration properties and slower growth rates. Therefore, these organisms would have to be incorporated separately from conventional waste treatment systems (e.g. activated sludge systems).

Bioconversions of organic waste streams to useful products provide the possibility of reducing waste disposal cost. For instance, worldwide production of cheese whey is greater than 90 million tons per year, and cheese production is increasing at a rate of approximately 3%/yr (Zall, 1984). Approximately 47% of the whey which is produced is not utilized (Flatt et al., 1988), resulting in significant disposal costs. Little or no new technology for producing additional whey products has been created in the past several years, and many of the available whey utilization schemes are not economically justifiable (Boersma et al., 1995). Conversion of organic substances (e.g. food processing waste and oils) to a useful and needed

product such as ω -3 fatty acids and enzymes is especially alluring. O'Brien et al. (1993) demonstrated that the filamentous fungus *P. irregulare* could convert sweet whey permeate to large amounts of EPA (24.9 mg EPA/ g dry biomass). This organism also produces pectin depolymerase (Domsch and Gams, 1972), which is the fundamental enzyme for breakdown of pectin substances.

Cellulolytic enzymes produced by fungi are important for the breakdown of lignocellulostic compounds, which are extremely abundant in agriculture (Kirk, 1976). These enzymes produce suitable substrates for many other fermentations such as alcohol production, or the production of other important enzymes (Turker and Mavituna, 1987). The cost of producing cellulase is as high as 50% of the total cost of producing glucose (Hendy et al., 1984). Therefore, low-costing substrates that include such agricultural byproducts as rice straw, sawdust, cheese whey and wheat straw are needed for the production of cellulase (Kirk, 1976). These substrates may also support the production β -D-glucosidase and D-xylanase (Shamala and Sreekantiah, 1987).

2.4 Supercritical Carbon Dioxide

Biomaterials are often thermally labile, fragile or unstable complicating their separation and purification (Shuler and Kargi, 1992). Carbon dioxide becomes supercritical at 31.1 °C and 73.8 bar (see Figure 2.2). This temperature is ideal considering the instability of the extractants at higher temperatures. A supercritical fluid is defined as a fluid at or above its critical temperature and pressure. It is neither a liquid nor a gas but simultaneously exhibits both characteristics. Supercritical

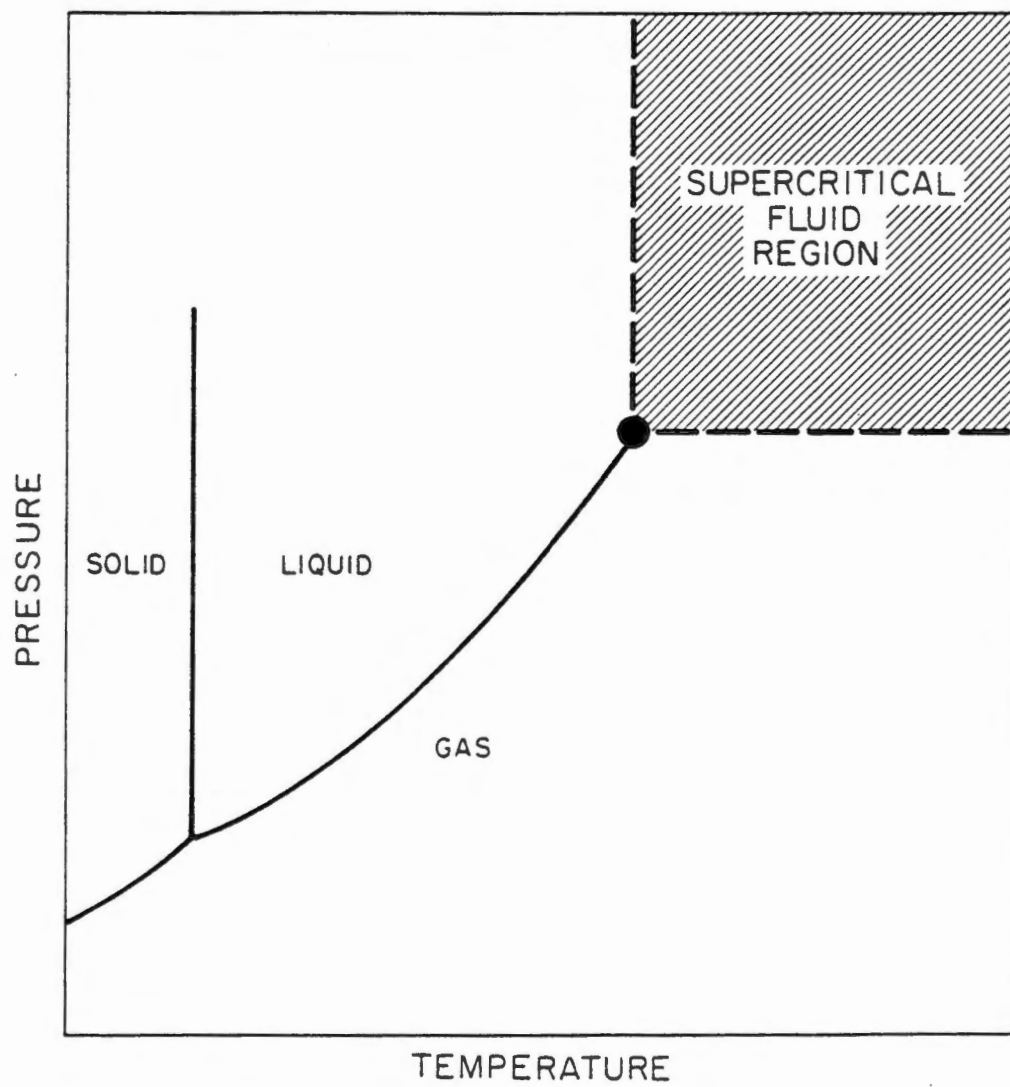


Figure 2.2. Pressure-temperature diagram for a pure component.

Source: McHugh and Krukonis (1994)

extraction has an advantage over liquid extraction because the supercritical fluid has "gas-like" properties that allow the solvent to diffuse more readily through the extraction medium. For instance, the typical diffusivities (see Figure 2.3) of supercritical fluids are in the range of 10^{-4} cm²/sec, which is 1 to 2 orders of magnitude greater than the diffusivities of liquids (10^{-5} - 10^{-6} cm²/sec). Yet the "liquid-like" properties allow compounds to be highly soluble in the supercritical fluid. Therefore, the solvent power is directly related to the thermodynamic state of the solvent, and may be controlled by manipulating the temperature and/or pressure. Disadvantages of supercritical extraction systems include the high capital cost for industrial batch systems and the lack of necessary technology for continuous systems (Friedrich and Pryde, 1984). Continuous systems have been designed only recently for pilot-scale processing of soybean oil (McHugh and Krukoniš, 1994).

Carbon dioxide is most commonly used for industrial supercritical extractions and has gained popularity because of its low toxicity and low cost compared to organic solvents commonly employed in liquid extractions. Also no solvent residues are left in the extracted product because the carbon dioxide vaporizes when brought to atmospheric conditions. For example, large amounts of industrial solvents are often required to complete extractions, thus producing high initial cost; however, even greater cost is often realized for their disposal (Rizvi et al., 1986b). Therefore, supercritical CO₂ is currently the leading choice for replacement of toxic organic solvents that are used in food and agricultural separation processes.

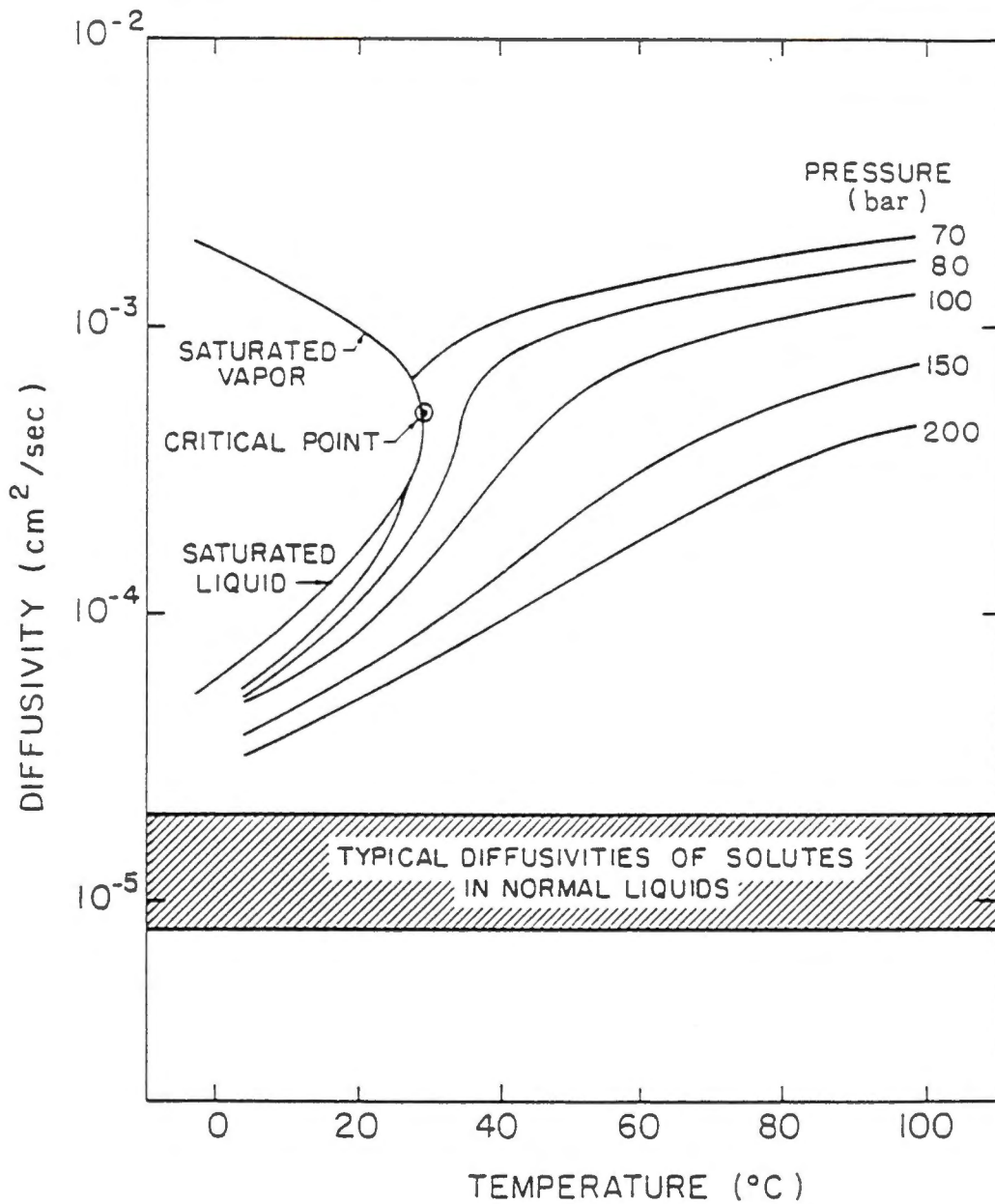


Figure 2.3. Diffusivity behavior of carbon dioxide.

Source: McHugh and Krukonis (1994)

The first commercial process to use supercritical fluid extraction (SFE) was the M.W. Kellogg Company in 1946, which utilized near-critical propane to extract and fractionate edible oils (Dickinson and Meyers, 1952). Edible oils today are extracted with hexane; however, supercritical CO₂ is presently being considered to replace hexane extractions of soybean oil because of the flammability and toxicity hazards associated with hexane (McHugh and Krukonis, 1994; Reverchon and Osséo, 1994). Also solvent extractions of fish oil result in protein denaturation (Pariser et al., 1978), whereas use of SFE has minimal effects on protein properties (Eldridge et al., 1986).

The main costs involved for implementing supercritical extraction is the high capital cost for high-pressure equipment and the operating cost determined by the required pressures (Rizvi et al., 1986b). Temperature considerations have little effect on cost, and more of an effect on the quality of extraction when thermally sensitive compounds are of interest. These high costs, however, may not be justified for some extraction processes; therefore, the extraction kinetics and phase equilibria studies are extremely important for design of supercritical extraction systems and economic analyses required to justify implementation. Unfortunately, equilibrium data are sparse for most biomolecular compounds under high pressures. The ability to predict these data with phase equilibrium relationships such as equations of state and statistical mechanics is hampered by the extreme nonideal nature of gases under high pressure (Mühlbauer and Raal, 1995). Therefore, more phase equilibrium and kinetic data are required to obtain more feasible systems for food and bioprocessing applications.

2.5 Solubility Considerations

Solubilities of soybean triglycerides in supercritical CO₂ may range from 0.1 to over 25 weight percent (wt%) depending on the temperature and pressure conditions (King, 1993). Sakaki et al. (1990) reported solubilities of fungal lipids to be higher in N₂O (2.3 wt%) than CO₂ (0.48wt%) at 333 K and 24.5 MPa. Maheshwari et al. (1992) determined the solubilities of six pure fatty acids using a flow-through equilibrium apparatus. They obtained solubilities of about 2.7 wt% for pure oleic and linoleic acids. The equilibrium data were modeled by Chrastil's equation (Chrastil, 1982), which gives a simple linear relationship for density and solubility at equilibrium conditions. Also, the presence of triglycerides (e.g. vegetable and fungal oils) or entrained impurities may cause significant interactions with pure fatty acids, which could possibly increase or decrease solubility (Nilsson and Hudson, 1993).

Even though the nonpolar and neutral lipids are soluble in supercritical CO₂, the polar lipids (e.g. phospholipids in the cell membrane) are less soluble, and proteins (e.g. enzymes) are mostly insoluble (McHugh and Krukoni, 1994). Therefore, edible oils can be easily separated from proteins. The more polar lipid fractions may be significantly solubilized in CO₂ with the addition of small amounts of polar entrainers such as ethanol (Temelli, 1992). Hardardottir and Kinsella (1988) reported that SFE could remove up to 97% of fish lipids with the addition of 10% ethanol compared to 78% lipids without ethanol. Also cholesterol removal was about 99.5%. Mendes et al. (1994b) extracted hydrocarbons from a slightly crushed, freeze-dried algae and discovered that the polar phospholipids were not extracted (verified by thin layer

chromatography). Cygnarowicz-Provost et al. (1992), however, noted that an SFE with 10% ethanol gave a recovery of 89% lipids from the filamentous fungi, *Saprolegnia parasitica*, which contains 25% polar lipids. This compared to only 49% lipids extracted with pure CO₂.

2.6 Extraction from Aqueous Suspensions

Water is only slightly soluble in CO₂ (Hedrick and Taylor, 1989), however, Eggers and Sievers (1989) found that toward the end of the extraction process of oilseed (mass transfer was diffusion-controlled) more water was coextracted than oil. They noted that the mass transfer of water was less inhibited than oil. They also found that a pressure of 75 MPa extracted the oil faster than 30 MPa, because of greater solvent density and a decreased amount of coextracted water. Staby et al. (1993) found that selectivity of fish oil fatty acid ethyl esters was high at lower pressures, and at high pressure the selectivity was low, but the solubility was high.

The moisture content of various biological materials also affects the extraction rates using supercritical fluids (McHugh and Krukoniš, 1994). Coffee beans soaked with water to about 45% moisture content enhanced diffusion of caffeine from the bean, which is considered the rate-determining step. The extraction rate increases with increased moisture content possibly because of the release of bound caffeine allowing greater overall desorption from the coffee matrix. The effect of water is certainly beneficial for caffeine extraction; however, because of the immiscibility of oil in water, the effect would be expected to be much different in the extraction of oils from aqueous suspensions.

2.7 Surfactant Technology

Techniques for producing aqueous dispersions in supercritical CO₂ have been sought for over a decade, and only recently (DeSimone et al., 1993, Maury et al., 1993, Guan and DeSimone, 1994, Fulton et al., 1995, Beckman, 1996, Johnston et al., 1996) have a few successful surfactants been found that result in reverse micelles in supercritical CO₂ with small quantities of water in their cores. Harrison et al. (1994) designed a hybrid fluorocarbon-hydrocarbon surfactant capable of incorporating up to 10 times the amount of water normally soluble in CO₂, thus giving a water-to-surfactant ratio of 32 at room temperature. Most other surfactants give ratios near zero.

Water-free reverse micelles consisting of a novel fluorinated sulfosuccinate surfactant were found to incorporate a moderately polar dye, thymol blue, under supercritical conditions (Hoefling et al., 1991). Hoefling et al. (1993) later designed a fluorether (molecular weight of 2500) that showed relatively high solubility in supercritical CO₂ at moderate pressures. The amount of water capable of being incorporated, however, was not determined. Water is required to solubilize proteins within the microemulsions (Johnston et al., 1996). Kaler et al. (1991) determined that sodium bis(2-ethylhexyl) sulfosuccinate (AOT) and D₂O formed swollen reverse micelles in near-critical propane. They determined by small-angle neutron scattering that the droplet sizes at the same water-surfactant ratios were pressure independent. These droplets would be large enough to incorporate biological macromolecules.

Chittofrati et al. (1989) verified the structural aggregates of quaternary mixtures of perfluoropolyether (PFPE) oil, PFPE surfactant, isopropyl alcohol and

water with light-scattering measurements. Johnston et al. (1996) found that PFPE surfactant forms reverse micelle cores swollen with water that form microemulsions that are soluble in supercritical CO₂. These microemulsions were shown to incorporate the protein BSA. This finding is very significant and possibly opens up many avenues for extraction of polar compounds in supercritical CO₂. Unfortunately, the water-to-surfactant ratio attained to date has been too small for most potential applications, and the known surfactants (perfluoro- polymers) are very costly.

2.8 Extraction of Fungal Lipids

The extraction of lipids, fatty acids, or derivatized forms of fatty acids from a microbial mass requires knowledge of the various barriers to mass transfer of these compounds to the supercritical phase. Some barriers include bulk movement and diffusion of solute within the cell. Other barriers include diffusion through and from the complex membrane and mass transfer through the external part of the cell mass. This may include diffusion through the stagnant film layer around the solid and diffusion through a water layer to the solvent phase as in the case of a moist biomass. Physically crushing the cell walls provides a means for releasing the lipids into the surrounding media thus decreasing the cell wall barrier (Sakaki et al. 1990; Cygnarowicz-Provost et al., 1992). This may be accomplished on a small scale by ultrasonic disintegration, shearing with glass beads, mastication, crushing with a ball mill (Sakaki et al., 1990), or freeze drying combined with crushing (Cygnarowicz-Provost et al., 1992). Because the physical distribution of oils in processed biomass is

not accurately known, understanding the controlling mass transfer step in extraction is challenging.

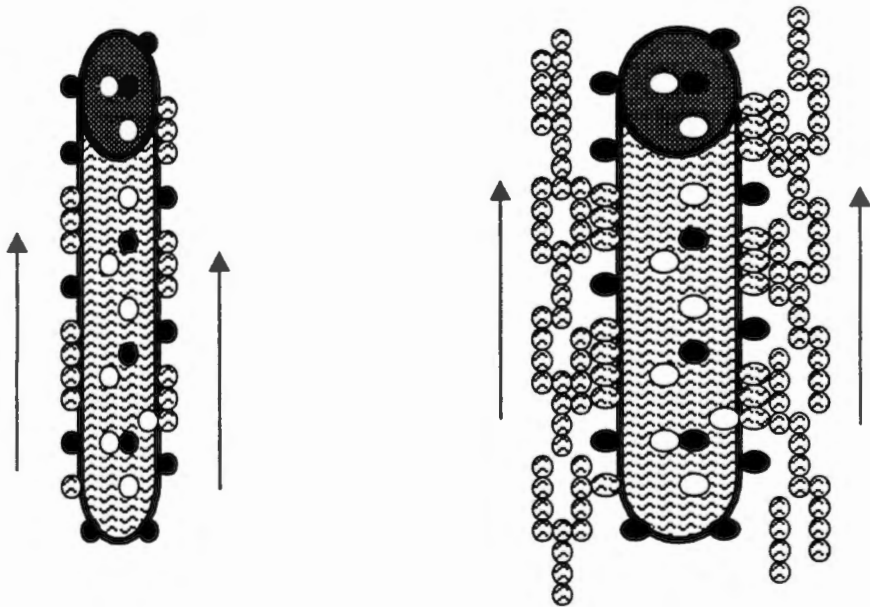
Observation of equilibrium and kinetic behavior of the fungal-oil system in supercritical CO₂ gives valuable insight to the overall extraction picture. This complex picture is primarily represented by four constituents including:

1. the inert solid phase (branched mycelium) containing the fungal cell wall (made primarily of polysaccharides, ~0.5 μm thick), intracellular proteins, lipoproteins, etc.
2. the moisture present after freeze-drying the fungi to 10% moisture content and the adsorbed moisture in the fungi with moisture contents of 20 and 30%. When moisture is reabsorbed to the fungal biomass, the effect of hysteresis may occur. This effect would increase the water activity allowing greater ease in the removal of moisture from the surface.
3. the condensed oil phase containing mainly neutral triacylglycerols that exists as both individual molecules and small droplets.
4. the supercritical CO₂ solvent phase.

One could picture these constituents in contact with each other as a heterogeneous mixture. Figure 2.4 shows schematics of the fragments of partially crushed mycelium with moisture contents of 10 and 30% in contact with supercritical CO₂. The dehydrated and shrunken fungal debris consists of both crushed and

10% Moisture Content

30% moisture content



○ Trapped Oil Droplet ● Surface Oil Droplet ⊕ Water Droplets

Figure 2.4 Schematic of the supercritical CO₂ extraction mechanism of fungal lipid from fragments of mycelium.

whole mycelia. The degree of cell fragmentation would be important in determining how much oil could be extracted before diffusion became the main form of resistance to mass transfer (Cygnarowicz-Provost et al., 1992). Greater fragmentation is expected to increase the amount of oil on the surface of the particle, which would make the oil easily available for intimate contact with the CO₂ phase. This would be the case only after the barrier of surface moisture, having highly repulsive interactions with oil, is removed. Once the oil is depleted from the surface, oil trapped within the tough cell walls would diffuse very slowly through this barrier to the solvent phase.

The extraction of lipids from fungi and algae using supercritical fluids has been accomplished for freeze-dried materials (Choi et al., 1987; Polak et al., 1989; Cygnarowicz-Provost et al., 1992; Mendes et al., 1995). In most cases, increasing pressures enhanced solubility of lipids in CO₂. Choi et al. (1987) noted that lipid solubilities in freeze-dried algae reached a maximum at 24 MPa. Temperature generally had little effect, however, decreases in solubilities were noted at 20 MPa with increasing temperature (Mendes et al., 1995). This effect is known as "retrograde" behavior where decreasing solubilities at constant pressure are associated with increasing temperature due to decreasing densities near the critical point. The temperature effect far from the critical point, however, is opposite because of the increased vapor pressure of the solute (Cygnarowicz and Seider, 1989).

The flow rate of CO₂ is an important consideration for industrial purposes since faster flow rates typically result in greater extraction rates up to an optimum value. Sakaki et al. (1990), however, noted that a flow rate of 8.4 g CO₂ /min showed

lower extraction rates than 2.0 or 5.0 g CO₂ /min in a 120 mL cylindrical extraction cell. Adverse flow effects that may cause channeling in the extractor bed is a possible explanation. Temperature is known to have less effect on extraction rates at constant pressure (Mishra, 1993), except in the retrograde region of supercritical fluids, where a decrease in solubility of the oil occurs with increasing temperature.

Concentration and fractionation of the PUFA may be accomplished during the extraction process (Nilsson et al., 1988; Rizvi et al., 1986a; Zosel, 1978). Friedrich and Pryde (1984) noted that more polar and high molecular weight compounds tend to appear at higher concentrations in the later fractions. Zosel (1978) separated up to 50 fractions of triglycerides from cod-liver oil based on increasing molecular weight and degree of unsaturation. McHugh and Krukonis (1994) and Eisenbach (1984) noted that by first transesterifying the triglycerides to EPA ethyl esters, fractionation of individual fatty acids would be possible during the SFE process. Transesterification also increases volatility that would correspond to an increase in solubility of the fatty acids in supercritical CO₂ (Harrison et al., 1994). Chromatography methods provide another alternative for fractionation of triacylglycerols. Ikushima et al. (1989) noted that a column packed with AgNO₃-doped silica and ethyl acetate entrainer was capable of fractionating oleic (C18-1), linoleic (C18-2) and linolenic (C18-3) acid methyl esters, which would otherwise be very difficult to separate with supercritical CO₂. Bharath et al. (1992) found that triglyceride mixtures in palm and sesame oils were fractionated on the basis of the total carbon number of the constituent fatty acids. Staby et al. (1993) noted that the molar equilibrium ratios (K-value) were strongly

dependent on system pressure and carbon number, but weakly dependent on degree of saturation and position of double bonds.

2.9 Enzyme-Catalyzed Reactions in Supercritical CO₂

The filamentous fungi are also major enzyme producers. Lambert (1983) noted that the *Aspergillus* species are filamentous fungi that produce many important industrial enzymes, which include glucose oxidase (used in blood glucose analysis), catalase (H₂O₂ removal from milk), amylases (maltose syrup production), pectinase (clarification of fruit juices), lactase (whey processing). Cellulolytic enzymes produced by fungi are important for the breakdown of lignocellulostic compounds, which are extremely abundant in agriculture (Kirk, 1976). The enzymes produce suitable substrates for many other fermentations such as alcohol production, or the production of other important enzymes (Turker and Mavituna, 1987). Lipase is another useful industrial enzyme that catalyzes lipolysis and interesterification of oils. Although enzymes are insoluble in CO₂, there is recent interest in developing systems for extracting and immobilizing enzymes in supercritical CO₂ (Ikushima et al., 1996; Shishikura et al., 1994; Vermuë et al., 1992; Steytler et al., 1991; Erickson et al. 1990). Enzymes show significant stability when immobilized in CO₂. The stability is partially attributed to the absence of oxidation reactions (Shishikura et al., 1994). Fungal enzymes are typically more stable in nonaqueous environments than bacteria-derived enzymes due to the functionality of fungi at lower water activities (Svensson et al., 1994). Fungal lipases are particularly well suited to catalyze reactions in nonaqueous environments. This is not only due to this enzyme's stability, but the

reacting substrates and products are usually soluble in the nonaqueous phase.

Therefore, the equilibrium of the enzyme-catalyzed reaction may be improved by the facilitated removal of byproducts with CO₂ (Shishikura et al., 1994).

An important group of lipases include the 1,3 regiospecific enzymes (e.g. *Mucor miehei*, *Rhizopus arrhizus*) that produce diacylglycerols, 2-monoacylglycerols and free fatty acids. This leads to a number of important reactions that include transesterification and interesterification of lipids. For instance, Shishikura et al. (1994) found that lipase-catalyzed interesterification (using the immobilized *Mucor miehei* lipase, LIPOZYME) between medium chain length triglycerides and free long-chain fatty acids may be accomplished, while the byproducts of the reaction (medium chain length fatty acids) are simultaneously extracted with CO₂.

Enzymes require an aqueous phase directly adjacent to the enzyme to remain active. Therefore the water activity is an important parameter for the enzymes functionality in nonaqueous environments and should be controlled to optimize the reaction kinetics (Svensson et al., 1994).

Supercritical CO₂ extraction of highly polar compounds such as enzymes or the simultaneous extraction of enzyme-catalyzed products may be possible in dispersed aqueous systems created by surfactants (Kaler et al., 1991). If such dispersions exist, a large number of applications with enzymes in supercritical fluids could result. For instance, one approach might include the formation of reverse micelles that contain the enzyme and maintains the enzyme's activity in an aqueous environment dispersed in the nonaqueous phase. Giovenco et al. (1987) used reverse

micelles to disintegrate bacterial cells and extract the enzymes into the reverse micellar phase for later purification into an aqueous phase. Particular interests have been devoted to lipases combined with surfactant in organic media (Pabai et al., 1995; Stamatis et al., 1993; Prazeres et al., 1993; Sabastião et al., 1993; Chang et al. 1991). Aqueous phases are required for enzyme reactions, but also cause unwanted hydrolysis reactions during interesterification with the lipase enzyme (Shishikura et al., 1994). Therefore it is advantageous to contact the reaction mixture with CO₂ to extract fatty acid moieties produced during the interesterification to improve equilibrium conditions.

CHAPTER III

THEORY AND MODEL DEVELOPMENT

3.1 Solubility Modeling

Numerous approaches for modeling solubility include theories from both classical thermodynamics and statistical mechanics. Such approaches include the compressed -gas models that utilize cubic equations of state (e.g. Soave-Redwich-Kwong EOS and Peng-Robinson EOS), excluded volume and local composition models (Kirkwood-Buff models) and more complex hard-sphere models (e.g. mixed hard-sphere van der Waals model).

Compressed-gas models that utilize cubic equations of state are commonly employed to model binary and multicomponent phase equilibria because of their relative simplicity and reasonable accuracy, but they show inaccuracies at supercritical conditions (Shah et al., 1994). The Peng-Robinson equation of state (PR-EOS, Peng and Robinson, 1976) is commonly used because it has been generalized and offers reasonable predictive capabilities. Therefore, the PR-EOS has been used for a wide range of mixtures of nonpolar compounds and a limited range of polar compounds. Eubank et al. (1994) used the PR-EOS to predict three-phase water-hydrocarbon behavior using van der Waals mixing rules. The accuracy, however, becomes questionable when molecules form a combination of polar-nonpolar mixtures or volatile-nonvolatile mixtures. Shah et al. (1996) utilized a quartic equation of state to better model these repulsive interactions of unlike molecules when compared to PR-

EOS. This model requires only four properties (critical volume, critical temperature, acentric factor and dipole moment) to model the fluid equilibria over a wide range of temperatures and pressures. Although cubic equations are effective curve-fitting tools, they cannot predict behavior outside of the range of the data and have limited use for predicting phase behavior for polar compounds.

Cochran et al. (1987) and Cochran et al. (1990) proposed models for binary and multicomponent systems, respectively, that were based on the Kirkwood-Buff theory for solutions approaching infinite dilution. Other attempts for modeling binary and multicomponent systems are mentioned by Jonah and Cochran (1994). Although models have been successfully developed for many binary systems that include a solvent in the supercritical state, much less success is evident for supercritical fluids at or near the critical point. The supercritical solvent structure tends to show striking behavior near the critical point where the density of the fluid changes rapidly as pressure is increased and the solubility of solute in fluid phase increases dramatically. Such behavior has been recently attributed to the formation of massive solvent clusters around the solute molecules. Several small angle neutron scattering (SANS) studies of pure noble gases were conducted to better understand the complex physical interactions between solvent-solvent pairs in dilute solutions of noble gases (Londono et al., 1993a; Londono et al., 1993b). The small-angle data was then directly correlated with thermodynamic properties using an equation of state.

Several multicomponent biosystems have been successfully modeled with various equations of state. The Peng-Robinson equation of state was applied to

systems containing caffeine in coffee (Peker et al., 1992) and guaraná seeds (Mehr, 1996). This equation of state was also applied to the fungi system containing PUFA (Cygnarowicz-Provost et al., 1992). The phase equilibria for an enzyme-catalyzed transesterification of oil, which included five components was predicted by the Soave-Redlich-Kwong equation of state (Chisochoou and Bolz, 1995).

3.2 Compressed Gas Model (PR-EOS)

An exact thermodynamic relationship exists for compounds in all phases at equilibrium. This relationship states that the fugacity, which is directly related to the chemical potential of a component, in one phase is equal to the fugacity of the same species in any other phase at equilibrium. The fugacity can be thought of in terms of “corrected pressure” of a pure component or “corrected-partial pressure” of a component in a mixture. In other words, the fugacity is equal to the partial pressure of components in an ideal gas mixture, but is the corrected partial pressure for nonideal compounds. The equilibrium relationship is a function of system temperature, T , and pressure, P , for the component having the concentration, y , in the supercritical CO₂ phase and a concentration, c , in the condensed phase. The relation is

$$f_i^c(T, P, c) = f_i^f(T, P, y) \quad (3.1)$$

where

$f_i^c(T, P, c)$ = fugacity of component i in the condensed phase

$f_i^f(T, P, y)$ = fugacity of the component i in the fluid phase

$$f_i^f = \Phi_i^f y_i P \quad (3.2)$$

The fugacity coefficient Φ_i^f is simply the ratio of the fugacity of a compound over the saturation (vapor or sublimation) pressure p_i^{sat} of the compound at the system temperature. This coefficient accounts for the deviation of the saturated vapor from ideal gas behavior (Prausnitz et al., 1986).

Assuming that the solvent has negligible solubility in the solid phase, the thermodynamic relationship presented by Prausnitz et al. (1986) for the fugacity of a pure component i (fungal oil, etc.) in the condensed phase is

$$f_i^c = p_i^{sat} \Phi_i^{sat} \exp \int_{p_i^{sat}}^P \frac{v_i^c dP}{RT} \quad (3.3)$$

where Φ_i^{sat} is the fugacity coefficient of component i at p_i^{sat} , v_i^c is the molar volume of solute in the condensed phase and R is the gas constant. Assuming the condensed phase is incompressible and the fugacity coefficient for the component at the saturation pressure is approximately unity (because the vapor pressures are typically low enough to assume an ideal gas), equations (3.2) and (3.3) may be equated from the relation in equation (3.1) to obtain the solubility,

$$y_i = \frac{p_i^{sat}}{P} \frac{1}{\Phi_i^f} \exp \left[\frac{v_i^c (P - p_i^{sat})}{RT} \right] \quad (3.4)$$

The exponential term is simplified to the form above from the assumption that the condensed phase is incompressible. This term is often known as the Poynting correction factor, which is the correction of the fugacity of the condensed phase and takes into account the difference of the system pressure from the saturation pressure. The enhancement factor, which expresses the enhancement in the solubility with respect to solubility for an ideal gas mixture, can be derived from equation (3.4),

$$E = y_i \frac{P}{p_i^{sat}} = \frac{1}{\Phi_i^f} \exp \left[\frac{v_i^c (P - p_i^{sat})}{RT} \right] \quad (3.5)$$

The fugacity coefficient of the component in the supercritical fluid can be obtained by applying the exact thermodynamic relationship in pressure-explicit terms to the PR-EOS. This expression for the fugacity coefficient is given as

$$\ln \Phi_i^f = \frac{1}{RT} \int_v^\infty \left[\left(\frac{\partial P}{\partial n_i} \right)_{T,v,n_j} - \frac{RT}{v} \right] dv - \ln Z \quad (3.6)$$

where n_i is the number of moles of component, i , v is the molar volume and Z is the compressibility factor that is defined by

$$Z = \frac{Pv}{RT} \quad (3.7)$$

The PR-EOS is written as

$$P = \frac{RT}{v-b} - \frac{a(T)}{v(v+b) + b(v-b)} \quad (3.8)$$

The PR-EOS can be rewritten in terms of the compressibility factor, Z :

$$Z^3 - (1-B)Z^2 + (A-3B^2-2B)Z - (AB-B^2-B^3) = 0 \quad (3.9)$$

where A and B are defined as

$$A = \frac{a(T) \cdot P}{R^2 T^2} \quad (3.10)$$

$$B = \frac{bP}{RT} \quad (3.11)$$

The parameter $a(T)$ is related to the intermolecular attraction forces dependent on temperature. The constant b is related to repulsive forces, which depends on the molecular size. This cubic equation yields up to three roots depending on the number of phases in the system. For two-phase, vapor-liquid equilibria, the largest root corresponds to the compressibility factor of the vapor (e.g. CO₂) and the smallest positive root corresponds to the liquid compressibility factor (Peng and Robinson, 1976).

At the critical point,

$$a(T_c) = 0.45724 \frac{R^2 T_c^2}{P_c^2} \quad (3.12)$$

$$b(T_c) = 0.0778 \frac{RT_c}{P_c} \quad (3.13)$$

and at other temperatures,

$$a(T) = a(T_c) \cdot \alpha(T_r, \omega) \quad (3.14)$$

$$b = b(T_c) \quad (3.15)$$

$$T_r = \frac{T}{T_c} \quad (3.16)$$

where $\alpha(T_r, \omega)$ is a function of the reduced temperature, T_r , and the acentric factor, ω .

The acentric factor is defined as

$$\omega = -\log P_r (@T_r = 0.7) - 1.0 \quad (3.17)$$

where

$$P_r = \frac{P}{P_c} \quad (3.18)$$

or the reduced vapor pressure at the reduced temperature of 0.7.

This function can be expressed as

$$\alpha(T_r, \omega) = \left[1 + \kappa_i \sqrt{1 - T_r} \right]^2 \quad (3.19)$$

where $\kappa = 0.37464 + 1.54226\omega - 0.26992\omega^2$ (3.20)

and κ_i is a characteristic constant of each compound based on its acentric factor.

To apply the PR-EOS for a component in a mixture that includes the supercritical fluid, several mixing rules have been proposed (Peng and Robinson, 1976; Panagiotopoulos and Reid, 1987). The van der Waals mixing rules used by Peng and Robinson (1976) were given by

$$a = \sum_i \sum_j c_i c_j a_{ij} \quad (3.21)$$

$$b = \sum_i c_i b_i \quad (3.22)$$

where $a_{ij} = (1 - k_{ij}) \sqrt{a(T)_i a(T)_j}$ (3.23)

Substituting equation (3.9) into equation (3.6) yields the expression for the fugacity coefficient of the supercritical fluid phase,

$$\ln \Phi_i^f = \frac{b_i}{b} (Z - 1) - \ln(Z - B) + \frac{A}{2\sqrt{2}B} \left[\frac{2 \sum_j y_j a_{ij}}{a} - \frac{b_i}{b} \right] \ln \frac{Z + (1 - \sqrt{2})B}{Z + (1 + \sqrt{2})B} \quad (3.24)$$

The solubility of component i may be determined by the following procedure, which was applied in a computer program written in Microsoft QuickBASIC (see Appendix C). First the physical properties of all pure components must be specified, which will be discussed further in the following sections. A range must be set for binary interaction parameter, k_{ij} , in equation (3.23) to determine a_{ij} . At this point the

PR-EOS (equation 3.9) may be applied to obtain the largest root, Z . After establishing an initial guess for the solubility, y_i , the fugacity of the solute in the fluid phase is then determined from equation (3.24) and a new y_i is calculated from equation (3.4). The process is iterated for y_i until the convergence criterion is met (tolerance of 0.0001).

The optimum value for k_{ij} is then obtained by minimizing the average absolute deviation (AAD) over the set range of k_{ij} . The average absolute deviation is defined as

$$AAD = \frac{1}{n} \sum_1^n \frac{|y_i^{predict} - y_i^{exp}|}{y_i^{exp}} \quad (3.25)$$

3.3 Physical Properties

There are a number of important pure-component, physical properties required to accurately model the solubility of a compound in supercritical fluids using the compressed-gas model that in turn utilizes PR-EOS. Unfortunately the physical properties are only known for a relatively small number of compounds (mostly petrochemical in nature).

Many physical properties of complex biomolecules are not usually available in literature possibly because of difficulties in purification, lack of availability or sensitivity to the environment such as thermal or chemical decomposition. Therefore, most of the required pure-component, physical properties for biomolecules must be estimated either based on empirical formulations, molecular structure (group contribution methods) or classical theories of corresponding states that utilize critical properties. Physical properties of simple compounds can be obtained from literature

including Daubert and Danner, (1993), Reid et al., (1987), CRC Handbook of Chemistry and Physics (1990) and the Handbook of Physical Properties of Organic Chemicals (1997), which contains a large data base of organic compounds.

3.3.1 Estimation of Vapor Pressure

Perhaps the most important physical property in the compressed-gas model for solubility in supercritical fluids is the vapor pressure of the solute, which is a strong function of system temperature. Vapor pressure and boiling point data are difficult to collect for biomolecules such as triglycerides because these molecules often decompose at temperatures at or below the boiling point (Ko et al., 1991). Mishra et al. (1994) estimated the vapor pressure of fatty acid esters using a gas chromatography method; however, this method is limited to volatile compounds in a narrow temperature range.

D'Souza and Teja (1987) accurately predicted the vapor pressures for 31 carboxylic acids with an overall AAD of 2.26%. Carboxylic acids contain the strongly reactive $-\text{COOH}$ group that contributes to vapor pressure reduction. The method utilizes the Wagner equation, which requires the effective carbon number (ECN) and the critical temperature and pressure.

$$\ln(P_R) = \frac{(A^*(1-T_R) + B^*(1-T_R)^{1.5} + C^*(1-T_R)^3 + D^*(1-T_R)^6)}{T_R} \quad (3.26)$$

and A^* , B^* , C^* and D^* are constants specific to the compound.

The determination of ECN requires the normal boiling point. Because boiling point data are not often available at normal pressure due to decomposition of the acid,

the boiling point at the reduced pressure of 1.3 kPa is sometimes available and may be correlated with the normal boiling point by the following expression,

$$T_{101.3} = 204.5462 + 0.02T_{1.3}^{1.61} \quad (3.27)$$

Several other empirical equations exist for various compounds such as the Lee-Kesler relation or the Benson vapor pressure equation (Daubert and Danner, 1993).

The Benson relation is stated as

$$Y = \exp \left[A + \frac{B}{T} + C \ln T + DT^E \right] \quad (3.28)$$

where Y is the vapor pressure in Pa and the constants A,B,C,D and E are specific to the compound, which include many of the fatty acids of interest. Unfortunately very few vapor pressure data exists for triglycerides, which are the principal component of fungal oil. Therefore much of the estimation of physical properties of fungal oil are based on the constituent fatty acids, which are also present in the “free” (detached from the glycerol unit of the triacylglycerol) form (Schaeffer et al., 1989). Saturated fatty acids are typically solid at the temperatures described for supercritical extraction with carbon dioxide. Therefore, the sublimation pressure for these fatty-acid constituents is required in the compressed-gas model. Schaeffer et al. (1988) suggested that the sublimation pressure may be estimated from the relationship of the fugacity of the solid (equal to the sublimation pressure) and the fugacity of the liquid (equal to the vapor pressure). This relation is

$$\ln \left(\frac{f^L}{f^S} \right) = \frac{\Delta h_f}{RT_t} \left(\frac{T_t}{T} - 1 \right) \quad (3.29)$$

where Δh_f = heat of fusion

T_t = triple point temperature.

Triglycerides containing unsaturated fatty acids are typically liquid at room temperature. For instance, soybean oil is high in triolein that contributes to making it liquid at room temperature (e.g. solidification point for soybean oil is -16 to -10 °C).

3.3.2 Estimation of Critical Properties and Other Physical Properties

Various methods are available for reasonable estimation of the critical properties and molar volume that often depend on group contribution methods. These methods include the Lydersen, Joback and Ambrose methods for critical temperature, pressure and volume and the Fedor's Method for critical temperature (Reid et al., 1987) and critical volume (Daubert and Danner, 1993). The Joback group contribution method also estimates the normal boiling point, T_b , and the freezing point. The acentric factor is often estimated by the Lee-Kesler vapor pressure relation

$$\omega = \frac{\alpha}{\beta} \quad (3.30)$$

where $\alpha = -\ln P_c - 5.92714 + 6.09648 \frac{1}{\theta} + 1.28862\theta - 0.169347\theta^6$ (3.31)

$$\beta = 15.2518 - 15.6875 \frac{1}{\theta} - 13.4721 \ln \theta - 0.43577\theta^6 \quad (3.32)$$

and $\theta = \frac{T_b}{T_c}$ (3.33)

3.4 Application of Physical Properties

The compressed-gas model has a distinctive advantage in that only four physical properties are required, T_c , P_c , ω and p^{sat} . The compressed-gas model was

applied to the fungal-oil system, which was simplified to a binary system with the following assumptions:

1. the system was modeled on a moisture-free basis. Water is very polar and is only slightly soluble in CO₂ compared to the fungal oil components.
2. The fungal system contains many proteins (including enzymes) that are also polar and have negligible solubility in CO₂; therefore, these constituents were neglected from the model.
3. Other constituents including polysaccharides that make up the cell wall were considered inert to the fluid phase and were neglected in defining the binary pseudo-component.
4. The CO₂-soluble portion of the fungal system contains a large number of components including neutral triglycerides, free fatty acids, sterols, etc. and were considered to be a single pseudo-component to simplify the analysis. The physical properties of the pseudo-component required to solve the compressed-gas model were then represented by a single compound.

The individual compounds that were chosen to represent the pseudo-component physical properties included palmitic acid, oleic acid and tetradecane. Their physical properties are listed in Table 3.1. Palmitic acid and oleic acid are major constituents of the fungal lipids and represent the saturated and unsaturated portions, respectively. All physical property data for the fatty acids with the exception of the heat of fusion was obtained from Daubert and Danner (1993). The heat of fusion was

used in Equation (3.29) to estimate the sublimation pressure of palmitic acid.

Tetradecane, which is similar in carbon number to myristic acid, was chosen to represent the neutral portion of the lipids that mainly constituted the triacylglycerols. The physical properties of tetradecane were obtained from Reid et al. (1987). The physical properties of naphthalene were obtained from Daubert and Danner (1993), which are also listed in Table 3.1.

The vapor pressures of oleic acid were estimated using the Benson equation (Equation 3.28) where the constants $A=186$, $B=-20315$, $C=-22.472$, $D=6.1199e^{-6}$ and $E=2$. The sublimation pressures of palmitic acid were estimated using Equation (3.29), which utilized the vapor pressure estimated from Equation (3.28), where the constants, $A=186$, $B=-20315$, $C=-22.472$, $D=6.1199e^{-6}$ and $E=2$. The vapor pressures of tetradecane were estimated using the Frost-Kalkwarf-Thodos equation (Reid et al., 1987) where the constants, $A^*=84.552$, $B^*=11322.9$, $C^*=-10.07$ and $D^*=-4.81238$. The vapor pressures of naphthalene were estimated using the Wagner equation (Equation 3.26) where the constants, $A^*=-7.85178$, $B^*=2.17172$, $C^*=-3.70504$ and $D^*=-4.81238$. Two vapor pressures of all compounds at 25 °C are shown for comparison with literature values. The vapor pressures for palmitic acid at 25 °C indicate a rather large deviation in the predicted values.

Hypothetical physical properties within the range of the physical properties for long-chain hydrocarbons and fatty acids were also applied to generate a better fit of the compressed-gas model to the equilibrium data. The ranges of the physical properties were 600 to 800 °K for the critical temperature, 10 to 20 MPa for the

critical pressure and 0.5 to 1.1 for the acentric factor. From these ranges, optimum values were regressed from the compressed-gas model by adjusting the values for the vapor pressure and k_{ij} to obtain the lowest %AAD. The results from these hypothetical properties could then be applied to search for a possibly better compound to represent the pseudo-component in the simplified binary mixture.

Goodrum and Eiteman (1996) estimated the vapor pressures for tricaprins, which consists of three 10-carbon fatty-acid units. This molecule is considerably smaller than the triglycerides associated with fungal oil, but is much larger than the fatty acid pseudo-components in Table 3.1. The estimated vapor pressure was $3.7e^{-10}$ bar at 40 °C, which is in the same range as oleic acid.

Table 3.1 Estimated physical properties for use in the PR-EOS model.

Physical Property	Oleic Acid	Palmitic Acid	tetradecane	Naphthalene
T_c (K)	781.0 ⁽¹⁾	776.0 ⁽¹⁾	693.0	748.4
P_c (bar)	13.9 ⁽¹⁾	15.1 ⁽¹⁾	14.4	40.5
V_c (mol/cm ³)	1000.0 ⁽²⁾	917.0 ⁽²⁾	830.0	413.0
v^c (mol/cm ³)	157.0	300.8		130.8
ω ⁽³⁾	1.187	1.08	0.581	0.302
T_m (K)	286.5	336.0		353.4
T_b (K)	633.0 ⁽⁴⁾	624.2 ⁽⁴⁾	526.7	491.1
T_i (K) ⁽⁵⁾	286.5	336.0		
p^{sat} (25 °C) ⁽⁶⁾	$7.28e^{-10}$	$2.65e^{-12}$	$1.55e^{-5}$	$1.13e^{-4}$
p^{sat} (25 °C)	$7.27e^{-10}$	$1.11e^{-8}$	$2.04e^{-5}$	$2.71e^{-4}$
p^{sat} (40 °C)	$6.67e^{-9}$	$1.23e^{-7}$	$7.67e^{-5}$	$8.27e^{-4}$
p^{sat} (60 °C)	$8.83e^{-8}$	$2.13e^{-6}$	$3.61e^{-4}$	$3.01e^{-3}$
ΔH_{fusion} (J/mol) ⁽⁷⁾		42037.0		

1. estimated by Lydersen's method
2. estimated by Fedor's method
3. all values estimated using the Lee-Kesler relation (Equation 3.30)
4. substance decomposes at boiling point
5. estimated to be equal to melting point temperature
6. vapor pressure data at 25 °C (Handbook of Physical Properties of Organic Chemicals, 1997)
7. heat of fusion was obtained from CRC Handbook of Physics and Chemistry (1990).

3.5 Mass Transfer Modeling

The economic and technical feasibility of a supercritical extraction process requires knowledge of the thermodynamic and mass transfer properties of the system. Process models using the equilibrium and mass transfer properties are necessary to obtain conclusions concerning equipment size, operating conditions, extraction yields and solvent flow rates (Rizvi et al. 1986a).

A combined thermodynamic/mass transfer model first developed by Schaeffer et al. (1989) applied a simple mathematical relationship based on the unsteady-state extraction of monocrotaline and lipids from *Crotalaria spectabilis* with supercritical CO₂ and an ethanol entrainer in a fixed-bed extractor. A similar model for the extraction of canola oil also showed reasonable predictions for both distance and time relationships at 55 °C and 36 MPa (Lee et al., 1986). The model equation is a second order nonlinear, unsteady-state relationship that requires the density obtained from the Peng-Robinson or other appropriate equations of state. These models are empirical fits to the overall mass transfer performance of a specific extraction system and offer little in the way of fundamental understanding or transferable knowledge.

Mendes et al. (1994a) and Cygnarowicz-Provost et al. (1992) used a similar model proposed by Lee et al. (1986) for oil from soybean flakes to predict the mass transfer of lipids from dried algae and fungi, respectively. The experiments were conducted in a flow apparatus. The main assumptions include plug flow, negligible axial dispersion, and constant temperature, pressure and flow rate. Material balances

on the solute with y and x the solute mole fraction in the fluid and solid phase, respectively, are as follows:

$$A\varepsilon\rho\left(\frac{\delta y}{\delta t}\right) = -\rho UA\left(\frac{\delta y}{\delta z}\right) + AA_p K(y^* - y) \quad (3.34)$$

$$A(1-\varepsilon)\rho_s\left(\frac{\delta x}{\delta t}\right) = -AA_p K(y^* - y) \quad (3.35)$$

where

- A = the cross-sectional area of the packed bed
- A_p = the surface area of the particle per unit volume
- ε = the void fraction of the packed bed
- ρ = the density of the fluid
- ρ_s = the density of the solid
- K = the solute mass transfer coefficient
- y^* = the equilibrium solute concentration in the fluid phase at the solid surface

Mendes et al. (1994a) predicted that the extraction shifts from a regime controlled by mass-transfer in the fluid phase to a regime controlled by diffusion in the condensed phase at 25% of the total lipids extracted for the partially crushed algae. The shift occurred near 55% of the total lipids extracted for the fully-crushed algae, showing that initially more lipids were easily accessible during the extraction when the algae were fully crushed. The initial extraction indicates that the resistance to mass transfer may occur at the surface of the submerged object. This implies that the mass transfer rate is dependent on velocity. Therefore, the mass transfer coefficient may be derived from forced-convection relations (Bird et al., 1960).

If diffusion occurs primarily within the mycelium structure of the biomass and the fungi are assumed to be spherical in geometry after mastication, an analytical solution to Fick's second law of diffusion can be obtained for a spherical geometry (Crank, 1975). Because diffusion appears in the condensed phase to limit the rate of mass transfer later in the extraction after approximately 30 to 50% of the lipids are removed, this model would possibly describe data in this region of interest. Fick's Second Law for a sphere may be written in spherical coordinates as:

$$\frac{\partial C}{\partial t} = D \left(\frac{\partial^2 C}{\partial r^2} + \frac{2}{r} \frac{\partial C}{\partial r} \right) \quad (3.36)$$

with initial condition: $C = C_0$ when $t = 0$ (3.37)

and boundary conditions: $\frac{dC}{dr} = 0$ when $r = 0$ (3.38)

$$C = C_\infty \text{ when } r = R \text{ and } t = \infty \quad (3.39)$$

where C = the concentration of solute in the sphere at time t

C_∞ = the final concentration of solute at the surface

D = the diffusion coefficient

r = distance from center of sphere

R = the radius of the sphere

The analytical solution (Crank, 1975) takes the form of an infinite series for the total amount of a species diffusing from the sphere:

$$\frac{M_t}{M_\infty} = 1 - \frac{6}{\pi^2} \sum_{n=1}^{\infty} \frac{1}{n^2} \exp \frac{Dn^2\pi^2 t}{a} \quad (3.40)$$

where M_t and M_∞ represent the total amount of solute (lipid) leaving the sphere at time t and the total amount of solute extracted over infinite time (approximately the initial amount of solute in the sphere), respectively. The effective diffusivity is represented by D for porous media having a void volume, ε , and tortuosity factor, τ . Generally, an accurate solution may be obtained with ten terms ($n=10$) or less depending on the time frame of the extraction. The results in the following experiments were fitted with 13 terms. However, the fits for 5 and 10 terms usually generated similar values for pseudo- r^2 , which is defined as

$$\text{pseudo-}r^2 = (1 - \text{residual sum of squares} / \text{total corrected sum of squares}) \quad (3.41)$$

using the NLIN procedure (see Appendix C) within Statistical Analysis System (SAS, 1985).

CHAPTER IV

METHOD DEVELOPMENT

This research examined a bioprocess that included growth of a filamentous fungi and production of fungal lipids, harvesting and concentration of fungi from fermentation broth and supercritical extraction of fungal lipids. The supercritical extraction was divided into two types of experiments, equilibrium and kinetic experiments.

4.1 Fungal Biomass Cultivation and Preparation

Pythium irregulare was maintained on Corn Meal Agar (Difco Laboratories) and transferred every 3 months to new agar slants. Domsch and Gams (1972) noted that the optimum temperature for *Pythium* species was 20 to 28 °C. with the minimum being 5 to 6 °C and the maximum being 36 to 37 °C. They also noted that glucose, fructose and mannose were of equal value for growth. Cultivation of *Pythium irregulare* was achieved in a 2% glucose medium supplemented with 0.5% yeast extract (Difco Laboratories, Detroit, MI) and 0.1% KPO₄ with pH adjusted to 6.5. The cultivation was accomplished aerobically using 2.0 or 3.0 L shaker flasks in either a New Brunswick orbital shaker (NBS) at 200 rpm or a flask placed in a constant temperature water bath operated in airlift mode (Wang and McNeil, 1995). The fungi were cultivated at two temperatures (19 and 24 °C) and monitored for fatty acid

production and glucose utilization. The fatty acid production was determined by gas chromatography (GC) as described in the Lipid Analysis section (Section 4.4). The glucose concentration was determined by a Dionex (Model DX300) high-performance-liquid chromatograph (HPLC) equipped with a Dionex CarboPac PA100 anion-exchange carbohydrate column (4x250 mm). The mobile phase solvent was 100 mM sodium hydroxide at a flow rate of 1.0 mL /min. The quantification was accomplished using a Dionex pulsed amperometric detector (PAD) and Dionex AI-450 software for data processing.

Harvesting the cell mass was accomplished by vacuum filtration using either Whatman #1 filter paper or an AG Technology hollow-fiber microfiltration filter attached to a All Flo Diaphragm pump set to 10 L/min. This membrane cartridge would typically concentrate the 10 L biomass suspension by more than 10x over a 90 min. filtration period. An example of the filtration results plotting the filtration flux and energy consumption verses time is shown in Figure A.3 of Appendix A (Liao et al., 1997; Cui, 1993).

The cell mass was then concentrated to 10% moisture content (wet basis) by lyophilization and crushed with a mortar and pestle. Water activity, measured with a AquaLab water activity meter, was 0.48 at 25 °C for the fungi with a 10% moisture content. Average particle sizes were obtained using separate sieves of 1, 0.5 and 0.3 mm. Particles that passed through the 0.5 mm sieve were then mixed for 20 s in a Tekmar analytical mill for further cell mastication. These particles were then separated with the 0.3 mm sieve. The two particle size distributions used for the experiments had

average particle sizes of 0.25 and 0.15 mm (radius). A typical particle with the smallest radius was photomicrographed with a 10X objective lens on a phase-contrast microscope with attached video processing is shown in Figure 4.1. This particle shows the fragmented and dehydrated fungi, which were clumped together. For comparison, Figure 4.2 shows the fungi from an inoculum culture plate where the whole mycelium (tubular object with intracellular vesicles) and sporangium (ellipsoid object, center) were intact. *P. irregulare* gets its name from the morphological feature of irregular distribution of protrusions seen on the sporangium.

Distilled water was later added to two samples to obtain moisture contents of 20 and 30%, respectively. The following relationship determined the amount of moisture required to achieve the desired moisture content.

$$M_{added} = \frac{MC_{desired}M_{dm}}{(1-MC_{desired})M_{present}} \quad (4.1)$$

where

- M_{added} = mass of moisture added
- $MC_{desired}$ = desired moisture content (wet basis)
- M_{dm} = mass of dry matter
- $M_{present}$ = mass of moisture present

Moisture contents of the biomass were verified by drying in a vacuum oven under reduced pressure at 80 °C overnight or until no change in weight occurred (AOAC, 1990). The water activities for the fungi with 20 and 30% moisture contents were 0.76 and 0.87 at 25 °C, respectively. The dry biomass (10% MCwb) was then stored under nitrogen at -20 °C. The biomass having either 20 or 30% moisture was

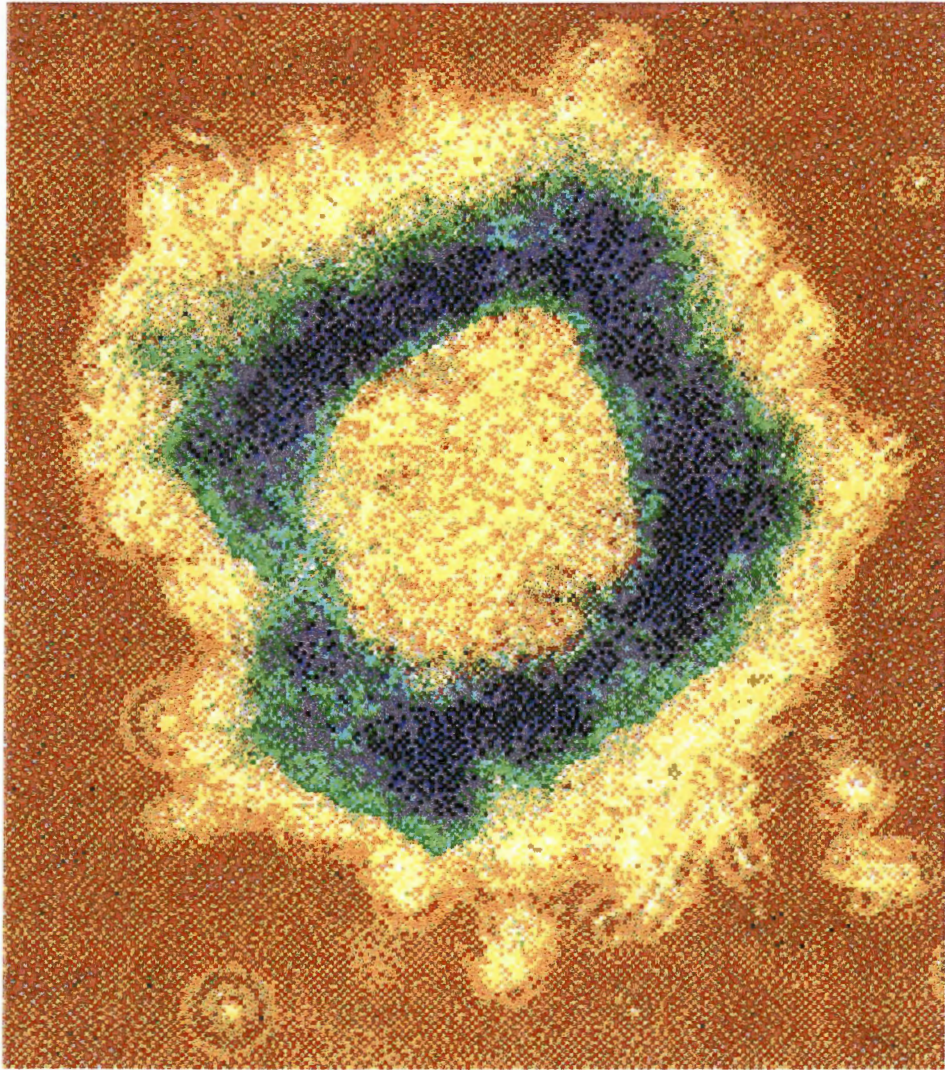


Figure 4.1. Photomicrograph (10X) of *P. irregulare* particle (0.15 mm radius) after cell mastication.

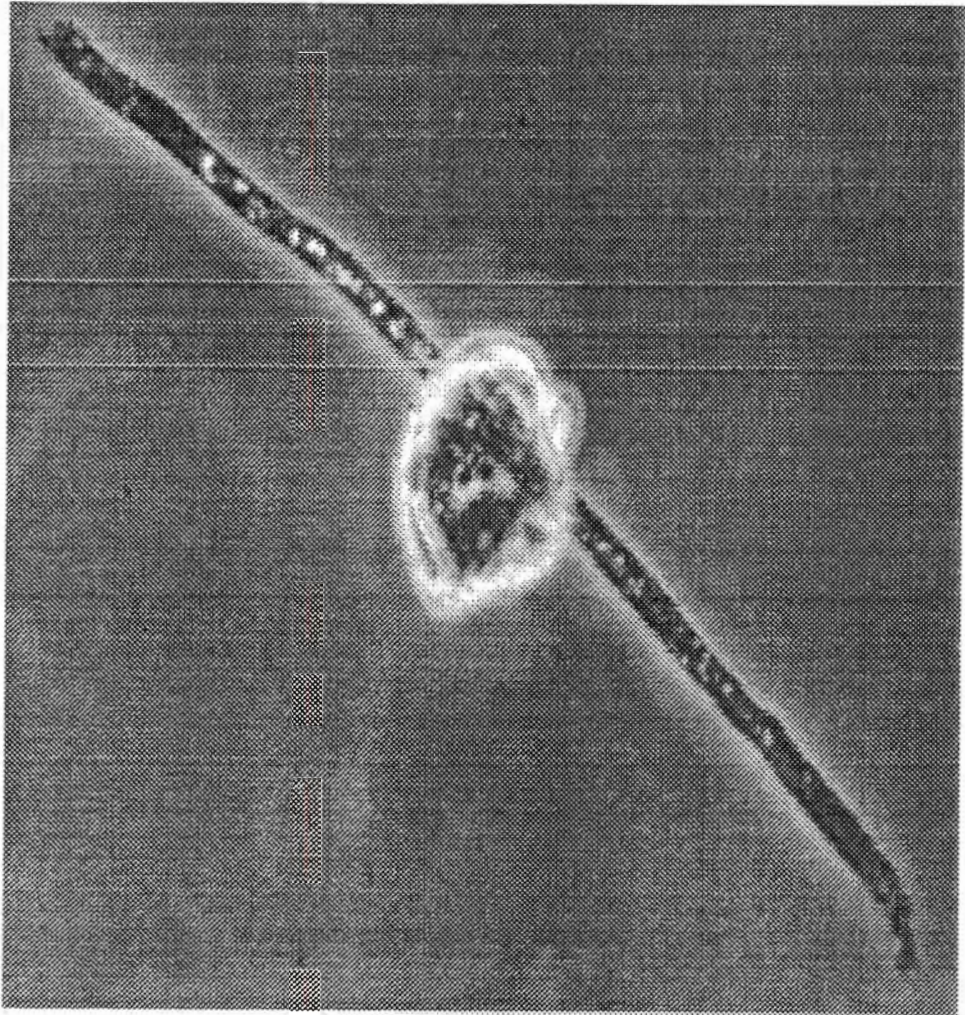


Figure 4.2. Photomicrograph (40X) of intact *P. irregulare* mycelium and sporangium

prepared a day before the experiment and allowed to equilibrate overnight in a closed glass container at 4 °C.

The CO₂-soluble surfactant used in this study was Krytox 157FSL (DuPont Chemicals), CF₃O[CF₂CF(CF₃)O]₃CF₂CO₂-NH₄, which is the ammonium salt of a perfluoropolyether (PFPE) carboxylic acid (average MW: 2500). A spatula was used to vigorously mix this surfactant with a high-moisture (95% MCwb) preparation of fungi to make a surfactant suspension of 10% w/w. The tubing and extraction column were later cleaned with Vertrel MCA (DuPont Chemicals) solvent.

4.2 CO₂ Extraction Apparatus

The apparatus (see Figure 4.3) was a single-pass flow system that was modified from the system described by Kaiser (1988), Barber et al. (1991). This system was based on a flow apparatus developed by Lin et al. (1985). The main advantage of the single-pass flow apparatus for determining the phase equilibria is the low residence time, especially at elevated temperatures (Lin et al., 1995). This is particularly important for biomaterials that are chemically unstable or susceptible to thermal degradation such as PUFA's.

Other advantages of this system include:

1. accurate sampling in systems with limited solubility
2. sampling has minimal effect on equilibrium
3. the apparatus is easily adapted to solid-fluid system
4. short-time exposure is possible which is conducive to sensitive compounds.

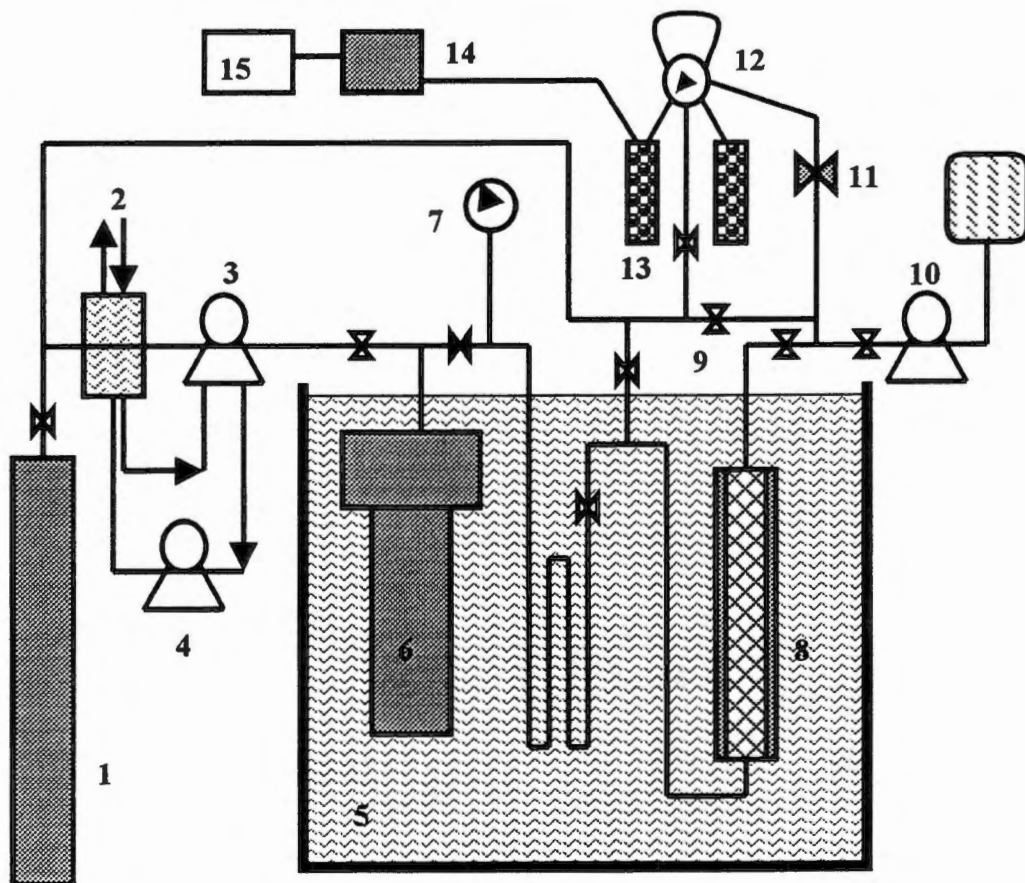


Figure 4.3. Schematic of continuous-flow supercritical CO₂ system.

1. CO₂ tank
2. refrigerated circulator
3. high pressure liquid pump
4. cooling pump
5. heated water bath
6. CO₂ pulse dampener
7. pressure display
8. extraction cell
9. CO₂ purge valves
10. liquid solvent pump
11. Metering valve
12. 6-way sampling valve
13. bubblers
14. mass flommeter
15. flow totalizer and display

The main components of the system include two high-pressure liquid feed pumps (Waters Assoc. and SpectraPhysics), a 300-cm³ pulse damper, a 19.3-cm³ extraction column and constant temperature water bath. The connecting stainless-steel tubing had outside and inside diameters of 3.2 mm and 1.6 mm, respectively. An equilibrium view cell was used only for viewing CO₂ phase changes and was not present for the extraction and equilibrium experiments.

The Waters pump was used to pump liquid CO₂ into the system. It was necessary to cool the pump heads with a propylene glycol-water (80:20 v:v) solution to avoid expansion of CO₂ in the pump heads. The SpectraPhysics pump was used to pump hexane through the sample loop to wash any fungal oil that accumulated on the tubing walls during expansion of CO₂ to atmospheric pressure. The pulse damper was used to reduce the oscillations (caused by the piston pump strokes) in the flow of CO₂ through the column that may disrupt equilibrium measurements. The height of the extraction column (Autoclave Engineering, Inc., Erie, PA) was 15.2 cm and the inside diameter was 1.3 cm. The equilibrium view cell (14 cm height and 1.3 cm inside diameter) containing two (2.54 cm diameter) sapphire windows is a modified version described by Lin et al. (1985). This cell was not used during the equilibrium and mass transfer experiments, but only for viewing phase behavior of CO₂. A Rheodyne six-way valve was insulated and maintained at 3 to 5 °C above the operating temperature with heating tape. This valve was only used to maintain constant flow during the sampling process for the flow-rate extraction experiments and was later removed to combine the periodic and cumulative samples. The flow rate through the column was

controlled with a high-pressure Autoclave Engineering valve. The water bath was maintained at constant temperature (± 0.1 °C) with a Haake (Model D8) submersion heater.

The flow rate and total volume of CO₂ were monitored by a Hastings-Teledyne Model 40 digital CO₂ mass-flow meter and a Model TR-1 totalizer, respectively. The pressure was monitored by a Heise digital pressure indicator and maintained within a precision of ± 0.035 MPa. Temperature was monitored with an Omega Engineering digital thermistor thermometer that had a precision of ± 0.1 °C. An Omega Engineering data acquisition system (WB-AAI interface card installed into an IBM PC) was adapted to the final extraction run to show the typical control parameters of bath, bubbler and heating tape temperatures and system pressure (see Figures A.1 and A.2. in Appendix A).

4.3 Extraction Procedure

Before each kinetic or equilibria test, the six-way valve (when present) and the tubing after the extraction cell were flushed with approximately 50 mL of hexane-isopropanol, HIP (3:2 v/v), solution to clean the system of any residual oil from the previous test. The HIP rinse was then followed by 30 mL of pure hexane, which could be removed with greater ease because of the greater volatility of pure hexane. Carbon dioxide was then flushed through the tubing to remove residual hexane. The extraction cell was cleaned with a cloth saturated with HIP and allowed to air dry. The extraction cell was then loaded with 1 to 2 g fungal biomass (dry weight) mixed with 5 mm (approximately 25 beads) and 1 mm glass beads (approximately 5 g) and packed

between glass wool (see Figure 4.4). This packing helped to insure good mixing and prevent channeling and entrainment in the extraction cell. The extraction cell was then assembled, placed in the constant temperature water bath, flushed with CO₂ and pressurized.

4.3.1 Flow-rate Kinetic Tests

The kinetic experiments were divided into two categories. The first category included flow-rate kinetic tests where four constant flow rates were compared to determine the effect of velocity on extraction rates. The second category included single-flow kinetic tests where the flow rate was held constant at 100 standard cm³/min.

For the flow-rate kinetic tests, the 6-way sample valve was periodically switched to isolate the sample loop and a sample was withdrawn by depressurization and rinsing with 20 mL hexane collected into a bubbler. The bubbler was a glass tube submersed in an ice bath (6 °C) containing approximately 15 mL of hexane that trapped any extracted oil. Two additional bubblers (including a backup bubbler at room temperature that also served as a visual aid for setting the flow rate) in series were used to collect the cumulative fractions from the 6-way sampling valve. The sample loop was pressurized and depressurized twice before the beginning of an extraction test to eliminate the void volume (containing only pure CO₂) in the tubing between the column and sample loop. After complete depressurization the sample loop was then flushed with 20 mL hexane to remove any oil remaining on the tubing walls.

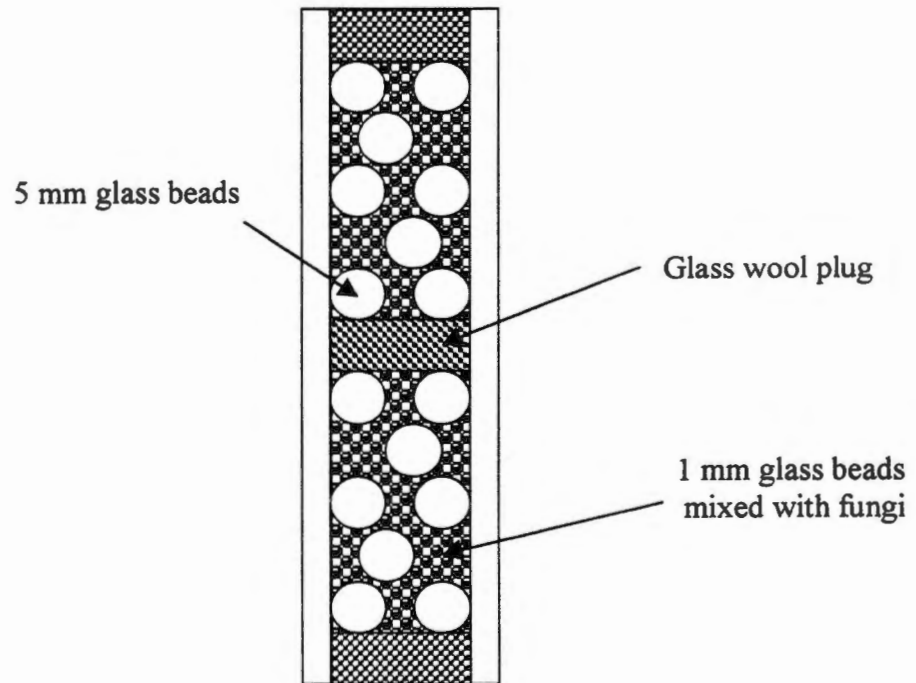


Figure 4.4. Extraction column packing.

Typically about 90% of total sample oil would collect on the tubing walls immediately following the sample loop, because the CO₂ depressurization took place mostly in that tubing section. The residual hexane was then purged with CO₂ and the valve was then switched back to repressurize the sample loop. A constant flow rate of CO₂ was then maintained through the sample loop until the next sample was taken. The flow rate of CO₂ remained constant to the cumulative bubbler until the completion of the kinetic test.

The expanded CO₂ escaped to the flow meter and totalizer to determine the total volume of CO₂ that passed through the column. The sample volume (constant at constant temperature and pressure) and cumulative volume were recorded for each time interval after each sample was taken. The total volume of CO₂ was recorded at atmospheric pressure and converted to moles using ideal gas relation,

$$n_i = \frac{PV}{RT} \quad (4.2)$$

4.3.2 Single-flow Kinetic Tests

The same procedure was followed for single-flow kinetic tests except the system did not contain the six-way valve. Only a cumulative sample bubbler and backup bubbler (room temperature) were present. Therefore the flow was temporarily blocked (approximately 5 minutes) at the valve immediately following the extraction column before taking each sample. The loop was slowly depressurized with the micro-metering valve, rinsed with hexane, repressurized and a constant flow rate resumed for taking the next sample.

Upon completion of all flow-rate and single-flow kinetic tests, the effluent was depressurized into the cumulative sample bubbler and rinsed with hexane. The extraction column was then removed and the tubing between the column and sampling valve was rinsed with 20 mL hexane, which was then combined with the hexane in the cumulative bubblers to obtain the residual oil. The biomass was then removed from the extraction column and separated from the glass beads into two fractions (the fraction between the top (column exit) and center glass wool plugs and the fraction between the center and bottom (column entrance) plugs). The biomass was tested for moisture content and residual oil for all extraction experiments. Residual oil and moisture were not measured for the phase-equilibrium experiments, which typically ran for only 90 to 120 minutes. Instead, the column was depressurized and cleaned for the next experiment.

4.3.3 Equilibrium Tests

The phase equilibrium tests were conducted in a similar manner to the single-flow kinetic tests. In experiments aimed at measuring the equilibrium distribution of oils between biomass and the supercritical fluid phase, the superficial velocity of the fluid phase was systematically reduced until the concentration of the oils in the fluid phase was observed to be constant, independent of fluid-phase velocity. Flow rates of 20 standard mL/min or lower provided stable equilibrium results when a small sample loop (0.25 mL) was used and at least two volumes of CO₂ were passed through the sample loop before sampling. Higher flow rates would result in slightly lower oil concentration in the fluid phase, which indicated that mass transfer limited the oil

concentration at flow rates of 50 standard mL/min and above. The equilibrium tests were usually stopped after two hours because significant depletion of the fungal lipids would possibly lead to mass-transfer limitation of lipids contacting the fluid phase at the surface of the fungal particles due to the transition to a regime limited by diffusion in the fungal matrix.

4.4 Lipid Analysis

After samples were taken during the extraction, the hexane was evaporated in a rotoevaporator (Yamato, Inc.) or placed in a water bath (40 °C) and flushed with a gentle stream of nitrogen. The samples were resuspended in 1 or 2 mL of hexane before methylation. Either 50 µL of pentadecanoic acid methyl ester or 20 µL of heptadecanoic acid methyl ester served as the internal standard for quantification. Both internal standards were supplied by Sigma Chemical Company. A mixture of 37 fatty acid methyl esters (FAME) was supplied by Supelco, Inc. for qualitative identification of the FAME present. This standard could also be used for quantitative purposes. The quantification FAME were accomplished with the internal standard method as follows:

$$C_s = \frac{C_{is} A_s R R_f D_f}{A_{is}} \quad (4.3)$$

where

C_s	=	concentration of sample
C_{is}	=	concentration of internal standard
A_s	=	area of sample
A_{is}	=	area of internal standard

RR_f = relative response area (shown in Appendix C)
 D_f = dilution factor (typically 1.0)

A modified rapid transmethylation procedure recommended by Christie (1982) was then implemented to convert the triglycerides to fatty acid methyl esters. For a 1 mL sample volume, the procedure first called for the addition of 20 μ L methyl acetate to suppress any competing hydrolysis reactions. The procedure then called for the addition of 20 μ L sodium methoxide (1M in dry methanol) that acted as a base-catalyst in the rapid transmethylation reaction of triacylglycerols with methanol. The mixture was then vortexed and allowed to react for 5 min. The final addition of 30 μ L acetic acid (1 M in dry methanol) stopped the reaction. A 0.5 mL aliquot of sample was placed in a 2 mL vial and taken directly to the GC for analysis. All reagents used in the rapid transmethylation procedure were supplied by Fisher Scientific.

The samples were then flushed with nitrogen and taken directly for analysis. The fatty acid methyl ester profile containing EPA and ARA methyl esters were determined with a Hewlett Packard 6890 capillary gas chromatograph equipped with an FID detector and a 30 m x 0.25 mm ChromPac CPwax-52 capillary column. The injection volume was 1 μ L. Temperature programming was 130 °C for 2 min, 10 °C/min to 180 °C, 2 °C/min to 215 °C, 10 °C/min to 230 °C and held for 2 min. The resulting areas were integrated and analyzed with HP Chemstation software. All samples were then stored at -20°C.

Lipids from the initial biomass and residual lipids remaining in the extracted biomass were determined to complete the mass balance. An extraction procedure similar to Hara and Radin (1978) required the addition of 14 mL of hexane and isopropanol (HIP: 3:2 v/v) to approximately 0.1 g of lyophilized biomass. The cell mass in HIP was then masticated with a Kinematics Polytron homogenizer for 1 min. The fatty acid content was then determined in a manner similar to the SFE extracts. Lipids from the initial biomass and residual lipids remaining in the extracted biomass were determined to complete the mass balance. The cell mass in HIP was then masticated with a Kinematics Polytron homogenizer for 1 min.

Thin-layer chromatography (TLC) was applied for one extraction run to determine the fraction of nonpolar lipids at different times during the extraction process. Samples obtained at the beginning, middle and end of the extraction were concentrated by flushing with nitrogen at 40°C. Five μL were then applied to Supelco silica plates (0.25 mm thick). Heptadecanoic acid and triheptadecanoic acid served as standards for free fatty acids and triglycerides, respectively. The plates were developed in petroleum ether, diethyl ether and acetic acid (80:20:2, v/v/v) and sprayed with 2',7'-dichlorofluorescein (Sigma Chemical Co.) and viewed under ultraviolet light.

CHAPTER V

RESULTS AND DISCUSSION

5.1 Fungal Production

Pythium irregulare, which is a member of the mastigomycetes (or oomycetes) class, produces considerable amounts of EPA at lower temperatures; however, the growth rates are expected to decrease at lower temperatures. The fungal cultures grown at 19 and 24 °C produced variable amounts of the desired PUFA.

Table 5.1 presents the results obtained for cultures grown at each temperature in several types of bioreactors. Typically, cultures grown at 24 °C produced less fungal oil with a smaller percentage of EPA than cultures grown at 19 °C. Because the lower temperature was initially expected to produce less biomass, the fermentation was allowed to continue for 10 d compared to 6 and 8 d for the higher temperature. After 8 days, however, the growth of fungi at 19 °C was greater than at 24 °C suggesting that the lower temperature may be near the optimum for this strain. Domsch and Gams (1972) also noted that the optimum temperature for many *Pythium* species was 20 °C. After 10 d, the glucose was almost completely utilized in all lower-temperature bioreactors as opposed to the higher-temperature reactors, which averaged only 61% glucose utilization after 8 d. Also, EPA production was higher at 19 °C with an average of 97.5 mg/L opposed to 50 mg/L for the 24 °C bioreactors.

Table 5.1. Growth of *P. irregulare* and production of fungal oil.

Bioreactor Type-Volume	Temperature (°C) /days (d)	Biomass Production (g/L)	Glucose Utilization (%)	Fungal Oil Production (mg/L)	EPA Production (mg/L)	Final pH
DT-2L ¹	24/6	6.5	97.3 ⁴	241.1	30.1	5.6
DT-2L	24/8	3.4	66.9	43.2	8.8	6.5
DT-2L	24/8	3.6	61.2	90.7	14.8	7.0
NBS-2L ²	24/8	3.9	42.4	478.5	19.5	5.7
NBS-2L	24/8	3.8	42.2	110.2	12.9	5.9
NBS-1L	24/8	7.1	58.3	677.3	213.0	5.8
DT-2L	19/10	9.9	90.6	642.5	124.8	5.3
NBS-2L	19/10	3.5	83.2	279.0	30.1	5.5
NBS-3L	19/10	3.5	88.2	295.8	28.0	5.7
NBS-0.5L ³	19/10	12.7	100.0	1491.0	208.3	7.0

1. DT-draft-tube airlift bioreactor design 2. New Brunswick shaker flasks 3. Three 250 mL erlenmeyer flasks combined to make 0.5 L 4. Simple sucrose (store grade) used instead of glucose

Production of ARA was greater than EPA at 24 °C; however, at the lower temperature EPA fractions were greater than ARA fractions, suggesting that different desaturase enzymes that convert lower-chain fatty acids to ARA and EPA are activated at the lower temperature. This phenomena has been documented by investigators including Kendrick and Ratledge (1992) and Shimizu et al. (1988). Table 5.2 shows the average distribution of fatty acids (converted to the respective methyl esters for GC analysis) for the fungi after lyophilization and homogenation. A sample chromatogram is shown in Figure 5.1. Saturated fatty acids account for about 38% of the total fatty acids. The rest were either mono- or polyunsaturated with EPA, which made up approximately 11% of the total fatty acids and about 30% of the PUFA. It should be noted that a small amount (1.2%) of GLA, another high-value product, was also produced.

Table 5.2. Typical fatty acid methyl ester distribution in *P. irregularis*.

Fatty Acid Methyl Ester (FAME)	Carbon # : Deg. Unsat. ¹	Molecular Weight	% of Total FAMES
Myristic acid	C14:0	242.40	16.8
Myristoleic acid	C14:1	240.38	0.4
Palmitic acid	C16:0	270.45	18.6
Palmitoleic acid	C16:1	268.43	4.1
Stearic acid	C18:0	298.51	1.1
Oleic acid	C18:1 ω 9 <i>cis</i>	296.49	17.3
Linoleic acid (LNA)	C18:2 ω 6 <i>cis</i>	294.48	16.0
γ -Linolenic acid (GLA)	C18:3 ω 6	292.46	1.2
Arachidic acid	C20:0	326.56	1.6
<i>cis</i> -11-Eicosenoic acid	C20:1 ω 9	324.54	1.8
Arachidonic acid (ARA)	C20:4 ω 6	318.50	8.2
<i>cis</i> -5,8,11,14,17-Eicosapentaenoic acid (EPA)	C20:5 ω 3	316.48	10.5
unknowns			2.4

1. Degree of Unsaturation

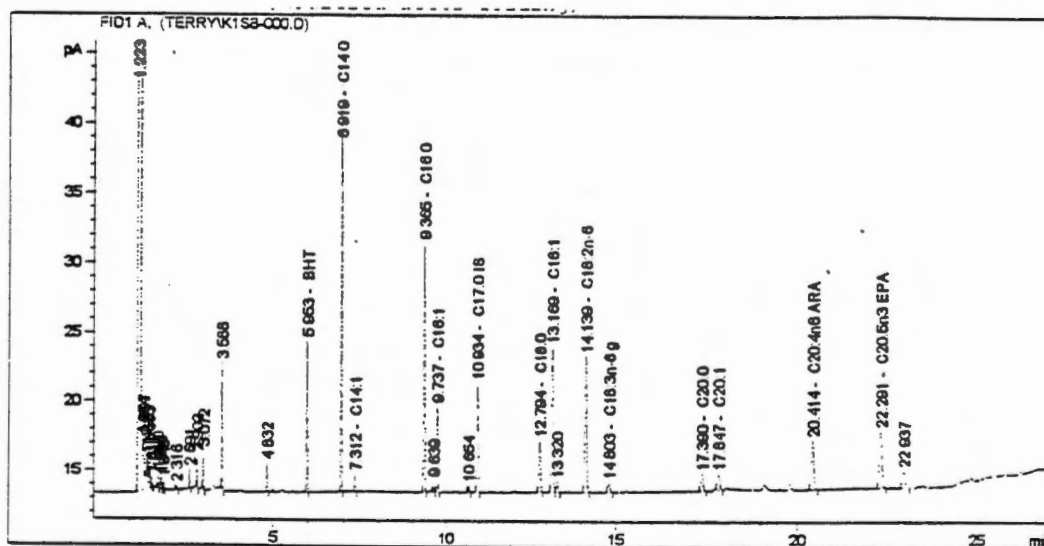


Figure 5.1. Sample chromatogram of fatty acid methyl ester distribution in *P. irregularis*.

The type of bioreactor was the other main variable studied in the production of fungi. The larger volume reactors appeared to negatively influence the production of fungi and EPA. Because the inoculum amounts were nearly the same in all reactors, greater fermentation time was required for substrate utilization in the larger-volume reactors. Another explanation may include a lower aeration rate per unit volume that may result from the lower surface area for oxygen diffusion from the air to the fermentation broth in the larger flasks. In most cases the airlift reactor contributed to greater growth and EPA production compared to the same size NBS shaker flask (2 L). The airlift reactor distributed oxygen at the base of the flask causing both circulation and greater oxygen transfer. The smallest flasks (250 mL) gave the best results for growth of fungi and production of EPA. Glucose was 100% utilized and the pH became neutral, possibly because of the decay of organisms contributing to the production of ammonia. In most other bioreactors, the pH averaged 5.7 at the end of the fermentation period. The low pH was possibly caused by acid production during the logarithmic and stationary phases of growth.

5.2 Equilibrium Results

Figure 5.2 shows solubility data obtained for pure naphthalene at 40 °C compared to literature values (Mendes et al., 1995; McHugh and Krukoni, 1994) to verify the accuracy of the system apparatus and to test our implementation of the compressed-gas model. The data compared reasonably well with literature values with an estimated AAD of about 7.0%. The compressed-gas model fit well with an AAD of

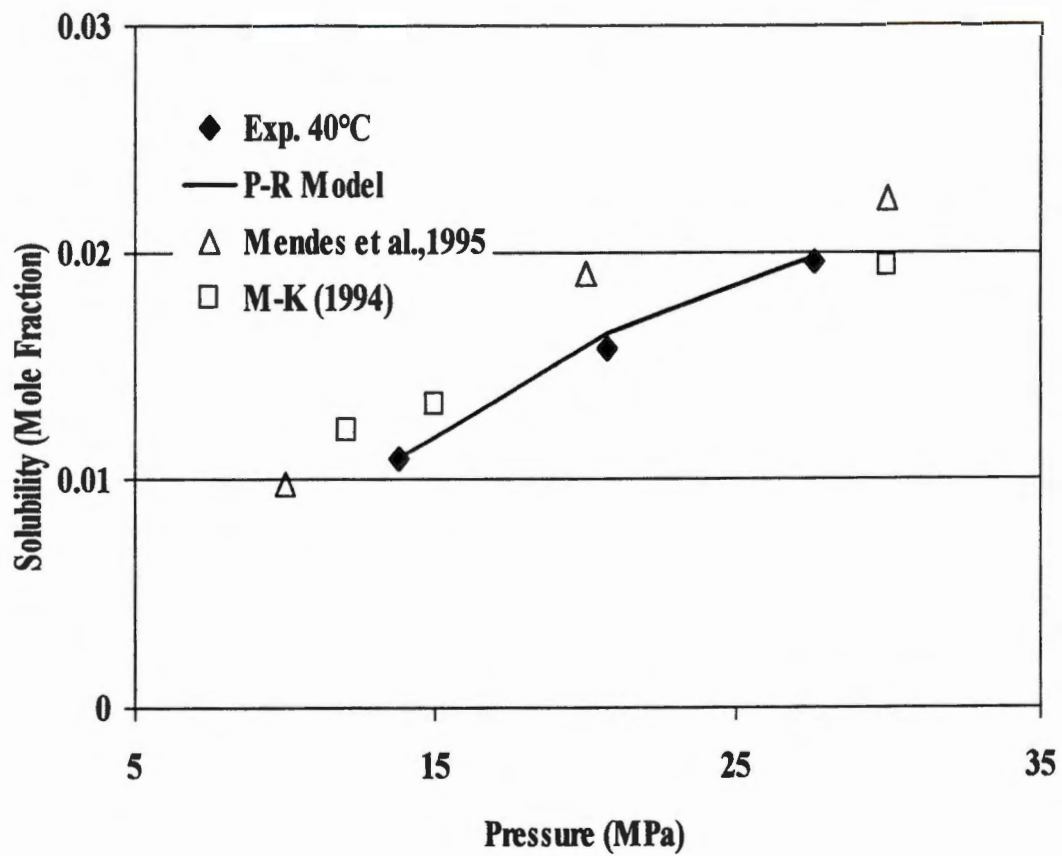


Figure 5.2. Experimental and literature solubility values for naphthalene at 40 °C. P-R Model is the fitted values from the compressed-gas model. M-K (1994) is McHugh and Krukonis (1994).

1.06%. The fitted binary interaction parameter, k_{ij} , was 0.152, which was similar to that obtained by Mendes et al. (1995).

Figures 5.3 and 5.4 show solubility data at three pressures for fungal oil at 40 and 60 °C, respectively. Data in the first 30 minutes of sampling, however, were generally disregarded for averaging the solubility values, because equilibrium values were not achieved during the startup of the process as can be seen by lower solubility values. Two hours were usually adequate for obtaining enough data to average for solubility readings. Depending on the solubility of the oil, data beyond two to three hours may result in lower values because of depletion of the surface oil. The average solubility data obtained from Figures 5.3 and 5.4 are shown in Figure 5.5.

Table 5.3 shows the solubilities of the fungal lipids in weight % compared to literature values of linoleic acid (C18:2), a ternary system of CO₂-oleic acid (C18:1)-triolein and fungal oil from *Saprolegnia parasitica*, which is another filamentous mold. The solubility of the triolein in the ternary system was similar to the solubility of oil from both filamentous molds. The free fatty acids had much higher solubilities than the triglycerides, particularly at higher pressures. The evidence of retrograde condensation, where solubility decreases with increasing temperature, was seen for all constituents within the temperature-pressure range shown. Nilsson and Hudson (1993) noted that this behavior typically diminishes at higher pressures (310 bar) for CO₂-triolein systems. They also noted that a decrease in the melting point for saturated triglycerides under pressure was observed in a Jerguson gauge, used for visual observation of phase equilibria.

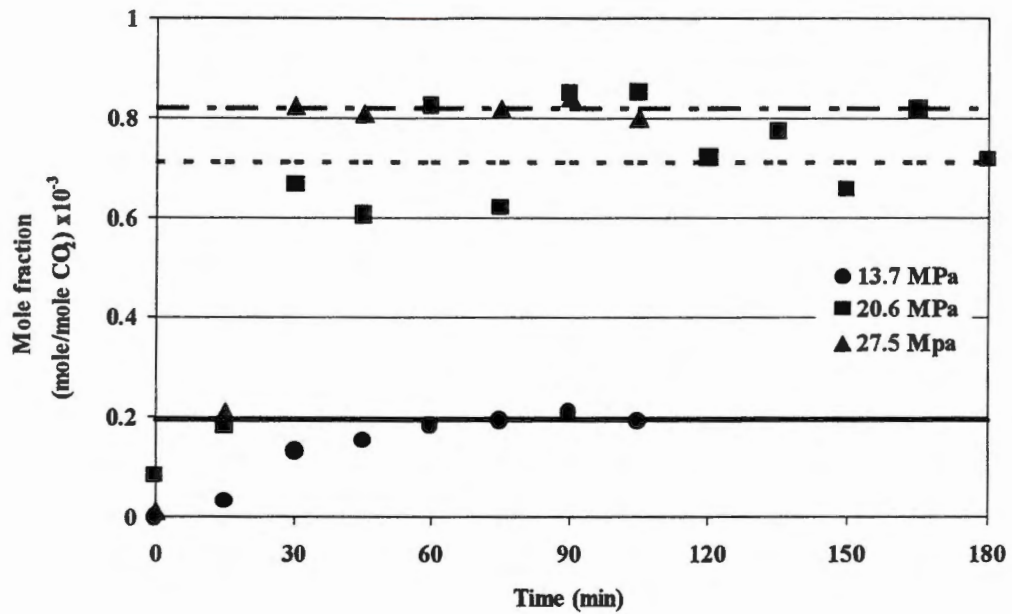


Figure 5.3. Equilibrium data of fungal oil at 40 °C. The dehydrated fungi had a 0.15 mm particle radius and 10% moisture content.

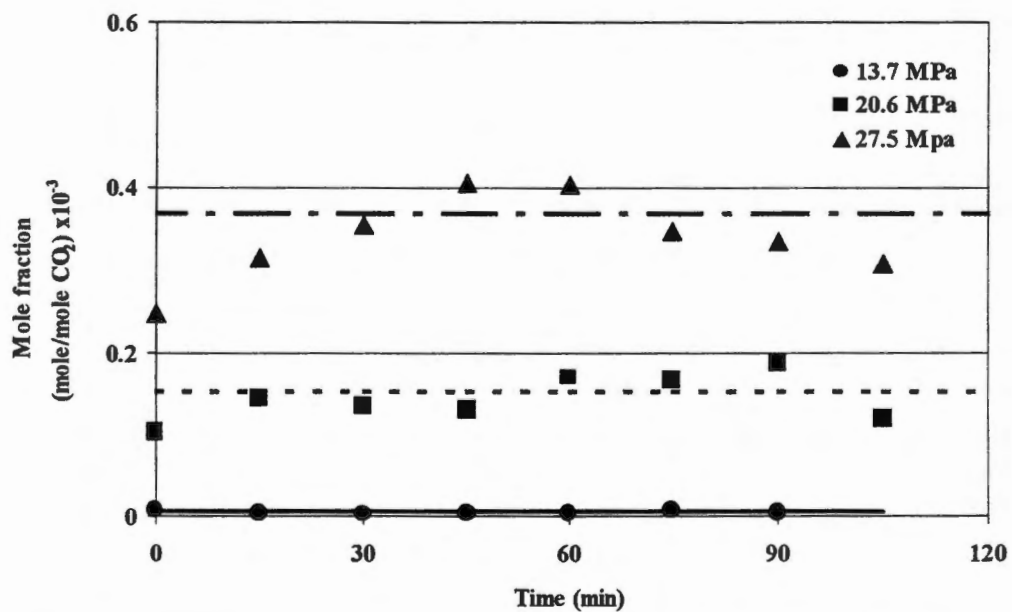


Figure 5.4. Equilibrium data of fungal oil at 60 °C. The dehydrated fungi had a 0.15 mm particle radius and 10% moisture content.

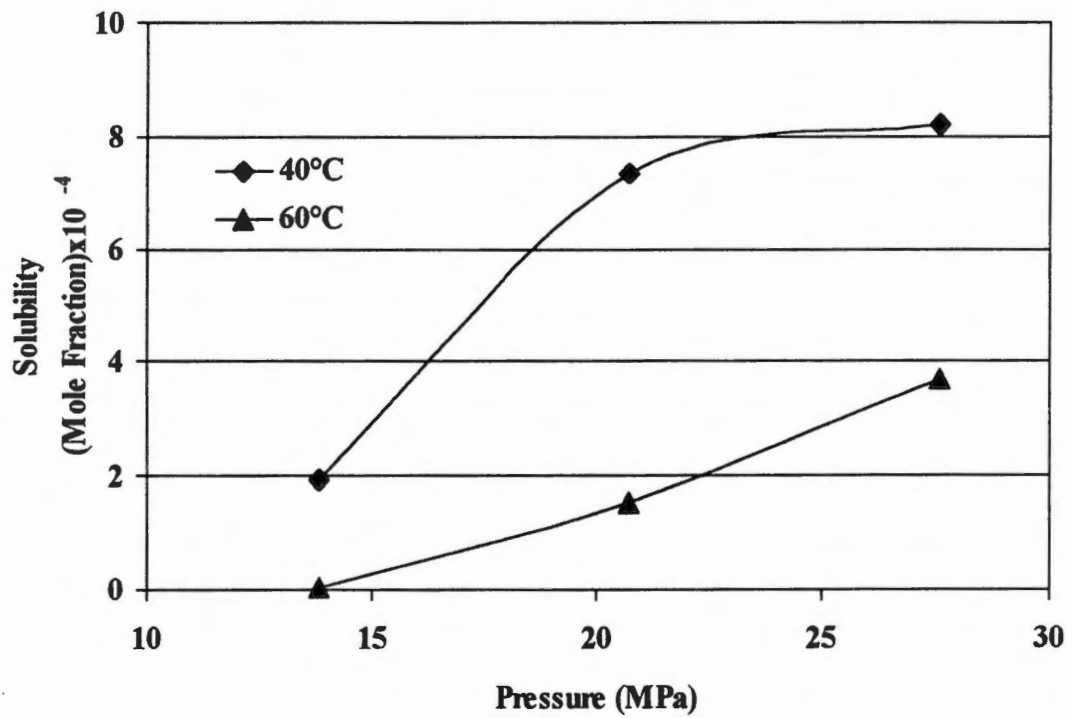


Figure 5.5. Equilibrium data for fungal oil extracted from dehydrated fungi with 10% moisture content and 0.15 mm particle radius.

Table 5.3. Comparison of solubilities (wt%) of *P. irregulare* oil with selected literature values.

Temperature (°C)	Pressure (Mpa)	<i>P. irregulare</i> oil	Linoleic Acid ¹	Oleic Acid ²	Triolein ²	<i>S. Parsiticus</i> Oil ³
40	13.8	0.12	0.45			
40	20.7	0.43	2.2	2.9	0.4	
40	27.6	0.52	2.6	1	0.6	
60	13.8	0.0028	0.11			
60	20.7	0.1	1.8	0.5	0.1	0.18
60	27.6	0.23	1.9	1	0.4	0.2

1. values from Maheshwari et al.(1992)

2. values from Bharath et al., (1992) from ternary mixture with CO₂

3. values from Cygnarowicz-Provost et al. (1992).

A complex relationship between the oil solubility and pressure existed at each temperature. This relationship can be better explained in Figure 5.6, which shows the density of pure CO₂ as a function of pressure for several isotherms. This plot indicates the large change in the density of CO₂ near the critical point that eventually tapers off at higher pressures depending on the temperature. For the critical temperature isotherm the effect was most noticeable, however at higher temperatures (near 150 °C) the increase in density became almost linear with increasing pressure. In other words, a small decrease in temperature at lower pressures resulted in a large increase in the density; however, at higher pressures a small change in temperature had less effect on the density.

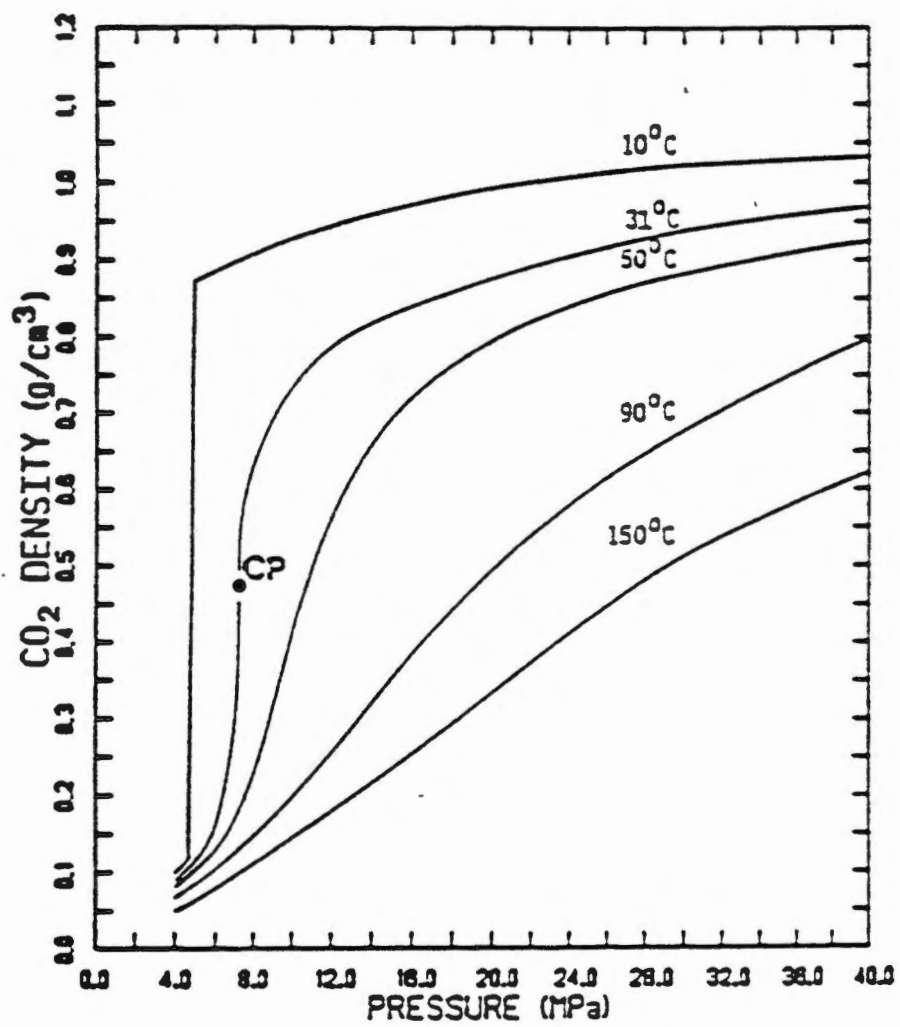


Figure 5.6. Density of carbon dioxide as a function of pressure for several isotherms.

Source: Fattori et al. (1988)

On the other hand, the vapor pressure of the oil increases exponentially with increasing temperature as can be seen by the predicted values in Table 3.1. At lower pressures near the critical pressure of CO₂ in the binary mixture, an increase in temperature will increase the vapor pressure of the oil, but will also greatly decrease the CO₂ density and, in turn, has the effect of decreasing the oil solubility. The pressure range in this study showed this effect of retrograde behavior. However, at higher pressures (beyond the pressures in this study) an increase in temperature continues to have a large effect on the vapor pressure of the oil, but does not substantially increase the CO₂ density; therefore, the solubility of the oil increases at higher temperatures.

5.2.1 Application of the Compressed-Gas Model

Table 5.4 shows the attempts to fit the data in Figure 5.5 by using the physical properties from the representative pseudo-compounds. The physical properties of tetradecane appeared to be the most reliable, although the vapor pressure was reduced greatly from its actual predicted vapor pressure shown in Table 3.1. The large reduction in vapor pressure values were necessary to obtain a solution that met convergence criteria. The fatty acid pseudo-components required even larger reduction in the vapor pressure values to obtain a solution. The AAD values indicate the lack of fit to the model; therefore, the physical properties for these components were not capable of accurately representing the lipid solubility possibly due to the complexity of the lipid mixture.

Table 5.4. Peng-Robinson EOS parameters estimated for fungal lipids.

Temp (°C)	Pseudo comp. ¹	T_c	P_c	ω	p^{sat} (bar) ²	k_{ij}	%AAD
40	OA	781.0	13.9	1.187	2.0E ⁻¹⁶	-0.46	29.7
40	PA	776.0	15.1	1.083	3.0E ⁻¹⁸	-0.44	53.2
40	TD	693.0	14.4	0.581	7.0E ⁻¹³	-0.43	25.8
40	HC	600.0*	15.0*	0.8*	3.0E ⁻¹¹	-0.32	26.7
40	HC	700.0*	10.0*	0.8*	3.1E ⁻¹⁵	-0.45	8.2
60	OA	781	13.9	1.187	1.0E ⁻¹³	-0.41	52.2
60	PA	776.0	15.1	1.083	1.0E ⁻¹⁵	-0.42	55.2
60	TD	693.0	14.4	0.581	5.0E ⁻¹¹	-0.36	33.1
60	HC	600.0*	15.0*	0.8*	1.7E ⁻⁹	-0.32	23.3
60	HC	700.0*	10.0*	0.8*	5.24E ⁻¹³	-0.4	39.1

1. physical properties of oleic acid (OA), palmitic acid (PA), tetradecane (TD) and a hypothetical compound (HC) chosen to represent the pseudo-component of the binary system.

2. all vapor pressure values were regressed with k_{ij} to obtain a solution.

* represents a hypothetical physical property

The application of the compressed-gas model using the optimum hypothetical physical properties, however, fitted the solubility data with reasonable accuracy where the AAD values were 8.2 and 23.3% for the 40 and 60 °C isotherms, respectively. When the same hypothetical values were used for both isotherms, however, the fit was not as accurate, which again suggested that a single pseudo-component applied to the model was not an adequate representation of the data.

Because the system contained a complex mixture of free fatty acids and triglycerides, it was reasonable to assume that the physical properties of the fungal lipids might not be accurately approximated by the properties of only one constituent. The need for a multicomponent application was evident from the relatively poor fit

and the large discrepancy in the vapor pressure. The complexity of the model, however, increases substantially if the physical properties of all components are considered by using multicomponent mixing rules.

Many of the physical properties for triglycerides are unknown, but could be estimated. Also, very little vapor pressure data exists for triglycerides in the temperature range of interest. Because triglycerides are much larger molecules than the constituent fatty acids, the vapor pressure for a mixture of triglycerides (e.g. palm oil vapor pressure is 1.73×10^{-9} bar @250 °C; Andersen, 1962) may be less than the vapor pressure for oleic acid (6.7×10^{-9} bar @40 °C from Table 3.1). However, the reactive acidic group on the fatty acid molecules also tends to decrease the vapor pressure of the compound. The order of magnitude was unknown, therefore the model essentially becomes a reasonably accurate curve-fitting tool for the present system, but cannot be used directly for other similar systems.

5.3 Mass Transfer Results

Figure 5.8 shows the raw data obtained from the sample loop, expressed in terms of mole fraction. Initially unstable readings were evident possibly due to free lipids on the surface of the fungi that may show the effect of forced-convective mass transfer in a heterogeneous matrix. The data for the 20 mL/min flow rate was fairly constant at the beginning of the extraction and slightly greater than data for the higher flow rates.

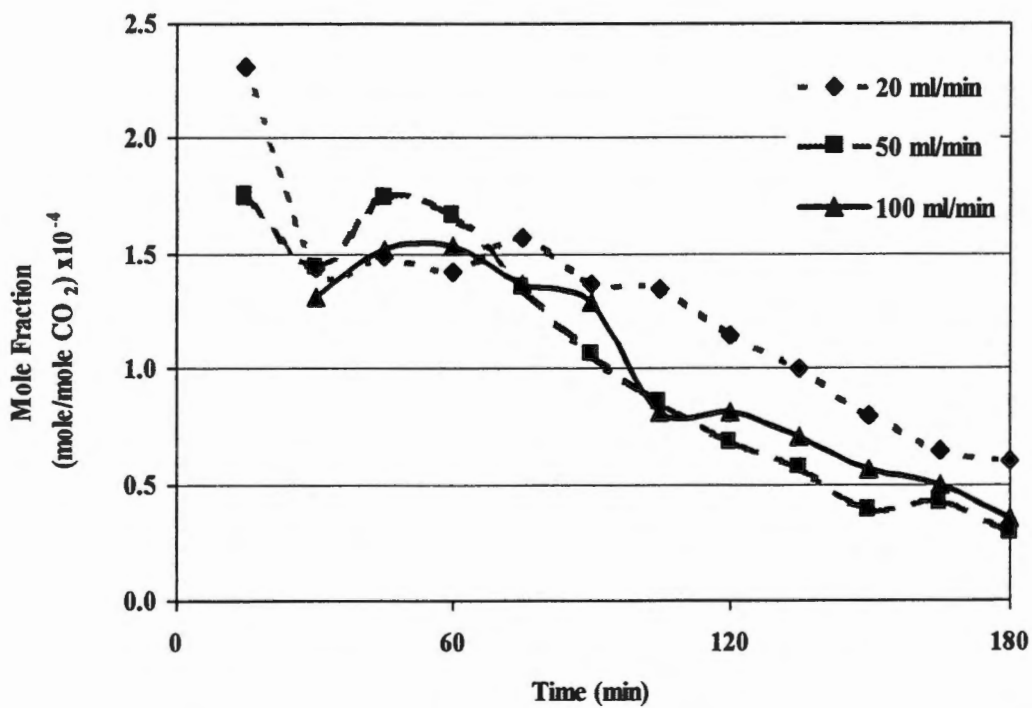


Figure 5.8. Sample-loop mole fractions of fungal oil at 50 °C, 20.7 MPa, 10% moisture content and 0.15 mm particle radius.

Figure 5.9 shows the effect of flow rate on the mass transfer of lipids in fungi with a 10% moisture content (wb) and 0.15 mm particle size at 50 °C. The average effective diffusivity was 1.6×10^{-9} cm²/s predicted with an average 0.94 pseudo- r^2 (shown in Table 5.5). The flow rate appeared to affect the extraction rate initially; therefore, diffusion of oil within the fungal matrix did not appear to be the main form of resistance to mass transfer for lipid removal up to 40 to 50% of the total lipids. The lipids were assumed to be available at the surface of the fungal particles and the resistance to mass transfer occurred primarily in the surface film. The extraction rates significantly decreased after 40 to 50% of the lipids were removed, which indicate a diffusion-controlled regime may exist. Therefore, only the later part of the extraction was modeled using the analytical solution to Fick's second law (equation 3.40) for the 60 and 100 cm³/min runs, where unsteady-state conditions also prevailed. The initial linear portion of the curve shows the brief pseudo-steady-state conditions in the extraction.

The effect of particle size and moisture content is shown in Figure 5.10 for the extraction of fungal oil at 40 °C and 20.6 MPa. Two particle sizes (0.15 and 0.25 mm radius) for the 10% moisture fungi were compared and the effective diffusivity for the later portion of the extraction curve was estimated using Fick's 2nd Law. Again, the initial portion of the curve was assumed to represent surface-film mass transfer and was not included in the diffusion model. The effective diffusion coefficients for both (see Table 5.5). The effective diffusivities for both particle sizes were nearly equal

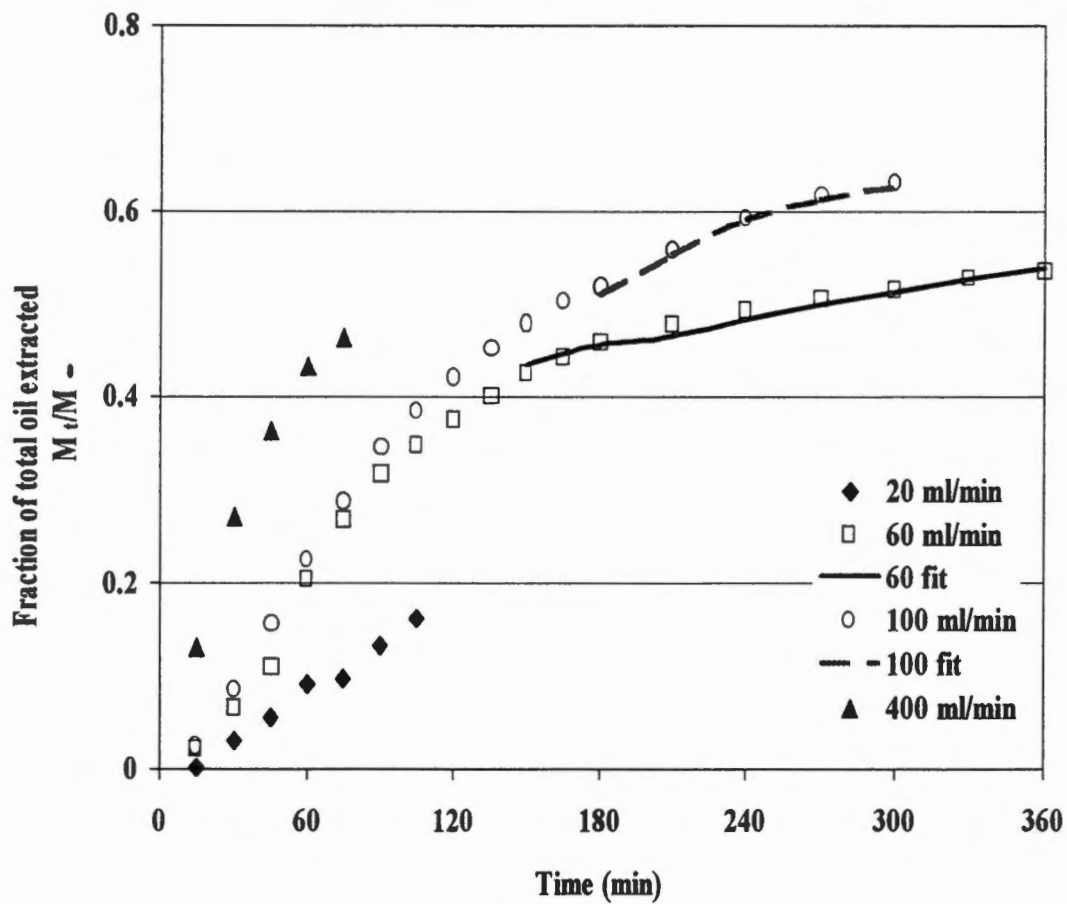


Figure 5.9. Effect of flow rate on the extraction rate of fungal oil at 50 °C, 20.6 MPa, 10% moisture content and 0.15 mm particle radius.

Table 5.5. Effective diffusivities for *P. irregulare* obtained from Equation 32 at 20.6 Mpa.

Temperature (°C)	Flow Rate (cm ³ /min)	Particle Size (mm)	D x 10 ⁻⁹ (cm ² /s)	Pseudo-r ²
40	100	0.15	1.15	0.96
40	100	0.25	2.05	0.92
50	60	0.15	4.60	0.95
50	100	0.15	4.01	0.93

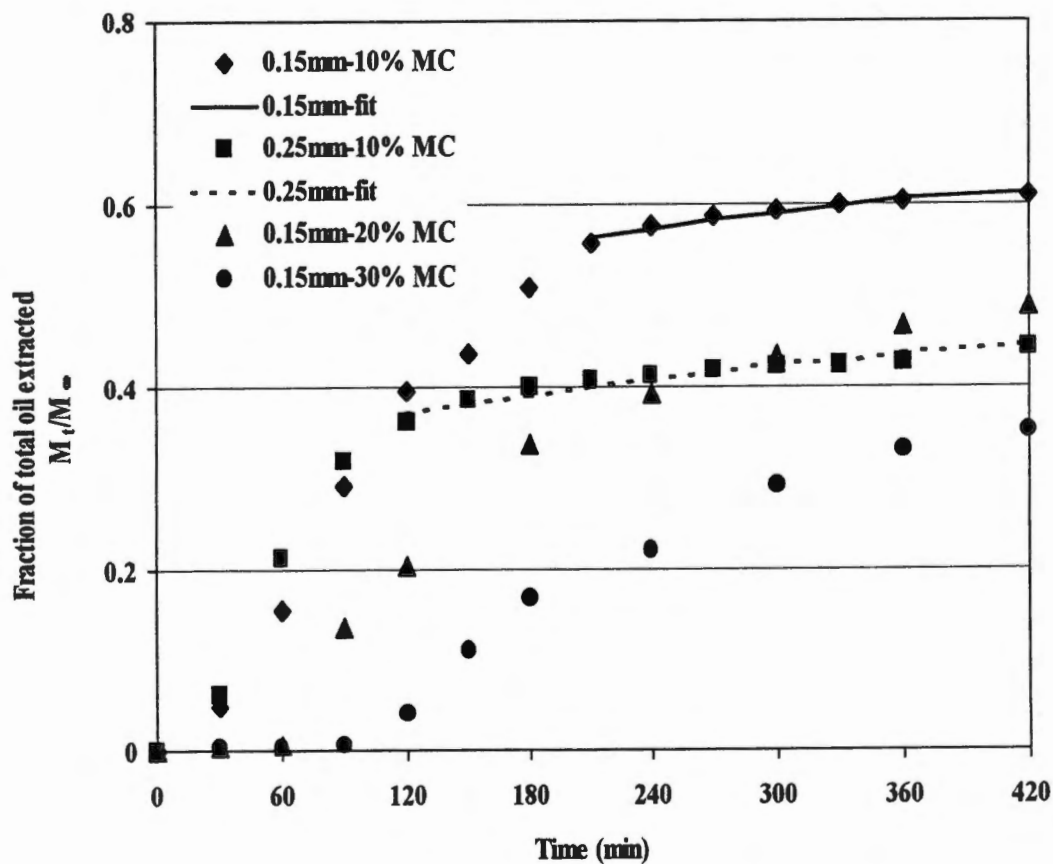


Figure 5.10. Effect of moisture content and particle size on the extraction rate of fungal oil at 40 °C and 20.6 Mpa.

indicating that the model reasonably explains the phenomena for the range of data representing the later part of the extraction. The low effective diffusivity value indicates that the diffusion of oil in the fungal matrix was an extremely slow process compared to the mass transfer observed at the beginning of the extraction. The fungi with 10% moisture content typically lost approximately 20 to 30% of the total moisture by the end of the process. The remaining moisture, however, may present a significant barrier to diffusion of oil embedded within the crushed mycelial structure.

The initial mass transfer rates were decreased considerably for the fungi at higher moisture contents. The lower observed rates occurred for longer periods as the initial moisture content increased. Figure 5.10 shows an initial lag in the extraction rate that lasted about 90 min for the 30% moisture fungi and only about 60 min for the 20% fungi. After the initial lag period, the mass transfer rate increased substantially to nearly the rate of the 10% moisture fungi. Significant drying was observed during the process as nearly 30 to 50% of the initial moisture in the higher moisture samples was removed by the end of the process. These results suggest that the initial water was readily available for coextraction with the fungal oil and was substantially removed, which then provides greater access of the surface oil to the surrounding fluid phase.

An increase in temperatures resulted in a slight increase in the effective diffusion coefficient of the fungal oil (average effective diffusivity of 4.3×10^{-9} cm²/min at 50 °C). Because the solubility decreased in this temperature range due to retrograde behavior, the mass-transfer driving force would decrease as a result. However, the effect of greater molecular movement with increased temperature was

probably more significant. This would explain the greater diffusion through the cellular material at higher temperatures.

Figure 5.11 shows the percent of total lipids extracted verses the total moles of CO₂. The similarity in the slopes for the 20 and 50 standard mL/min flow rates confirm that equilibrium conditions prevailed initially at the 20 mL/min flow rate. The slopes decreased significantly for the higher flow rates toward the end of the extraction, which shows further indication that intraparticle diffusion resistance was important (Goto et al., 1993).

The effect of moisture content on the extraction of lipids from fungi with a 0.15 mm particle size is shown in Figure 5.12. Nearly 50% of the lipids were extracted in three hours for the 10% moisture tests. The extraction rate for the fungi with 30% moisture content was initially much less than the rate for the fungi with 10% moisture content. This showed the significant effect of moisture on the reduction of extraction rates of lipids with supercritical CO₂ in biological materials. This figure suggests that surface moisture presented a barrier to mass transfer in the 30% moisture sample and after about 45 min this surface-moisture barrier was removed leaving surface oil exposed for extraction. The final moisture content of the fungi after extraction was 20%, indicating that moisture removal was significant during the extraction.

Figures 5.13 and 5.14 show the distribution of fatty acid methyl esters for the extracts from fungi with 10 and 30% moisture plotted against time, respectively. The results were obtained by GC quantification for the 14:0 (myristic acid), 16:0 (palmitic acid), 18:2 (LNA), ARA and EPA fractions. The results showed differences in the

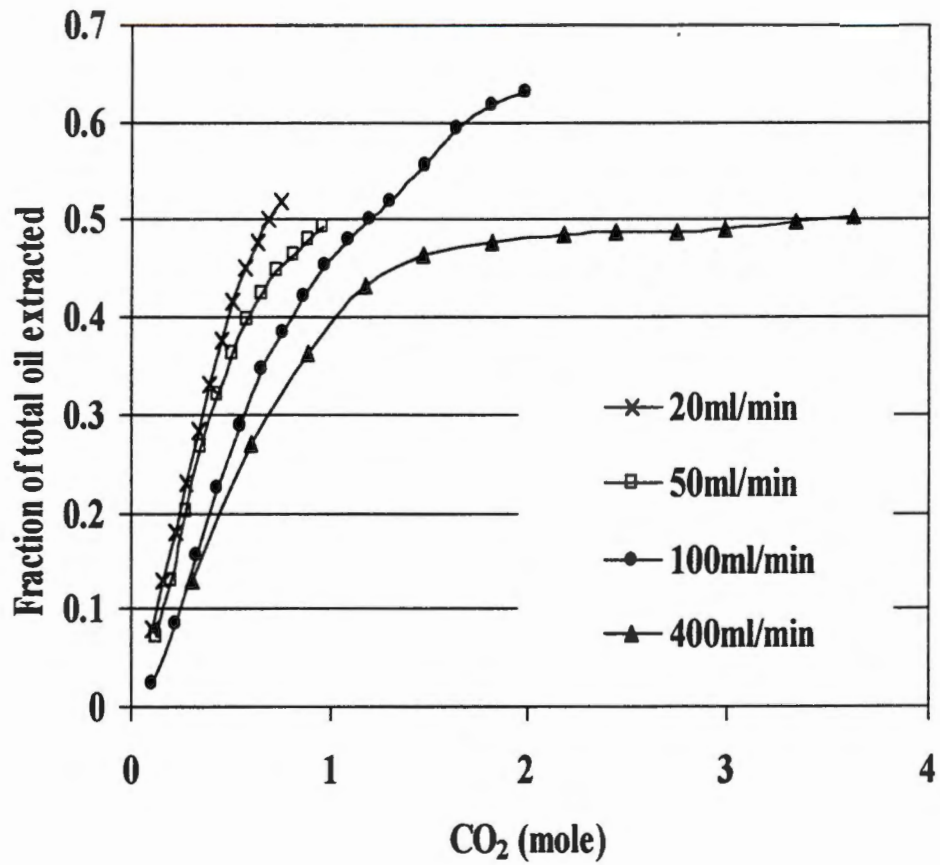


Figure 5.11. Extraction of lipids at selected flow rates from fungi with a particle size of 0.15 mm versus total moles of CO₂ consumed.

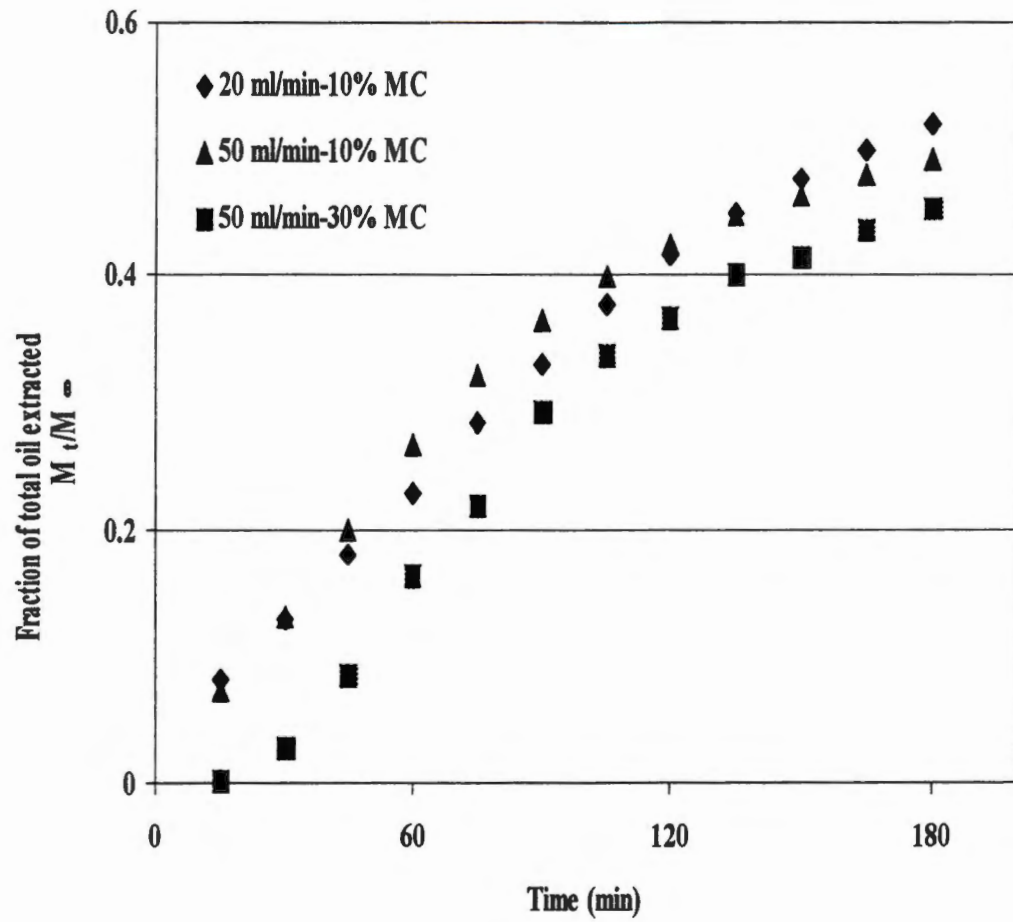


Figure 5.12. Effect of flow rate and moisture content on the extraction rate of fungal oil at 50 °C and 20.6 MPa.

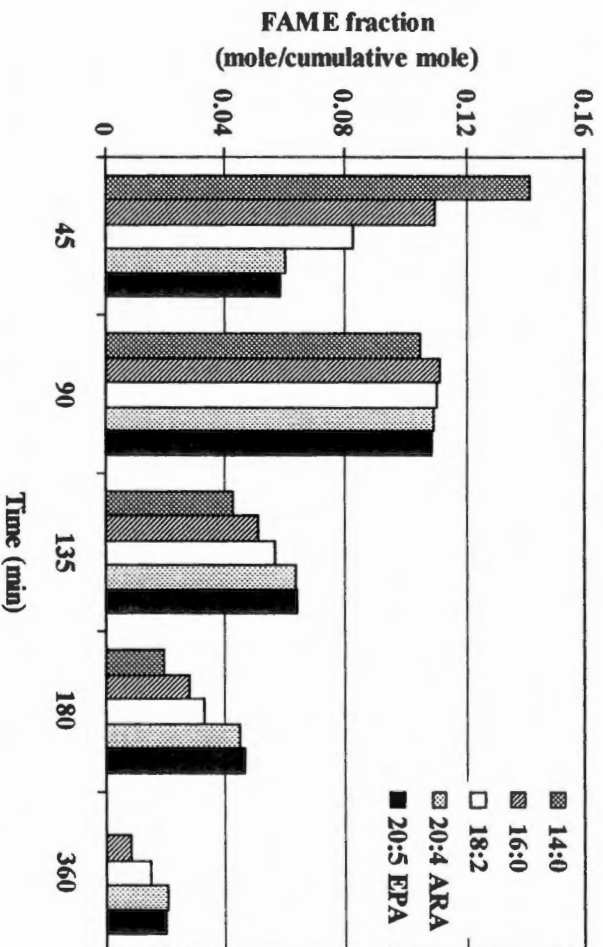


Figure 5.13. Fatty acid methyl ester fraction for fungi with a 10% MCwb extracted at 50 °C and 20.6 MPa.

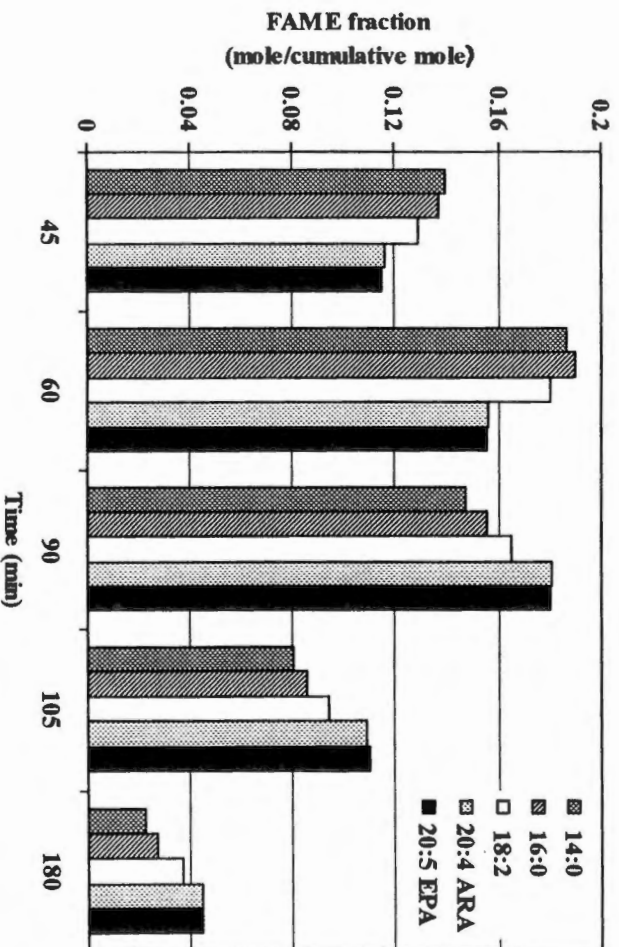


Figure 5.14. Fatty acid methyl ester distribution 30% MCwb extracted at 50 °C and 20.6 MPa.

affinity of supercritical CO₂ for lower molecular weight, saturated compounds versus higher molecular weight unsaturated compounds. The degree of unsaturation does not affect the solubility of fatty acids or fatty acid methyl esters, except for highly unsaturated compounds such as EPA, where greater solubility is favored (McHugh and Krukonis, 1994).

The higher solubility of lower-molecular weight compounds was evident for fungi at both moisture contents. The 14:0 and 16:0 fractions were extracted rapidly at the beginning of the process and were nearly depleted toward the end of the extraction. Higher molecular weight components such as EPA appeared in greater amounts toward the end of the extraction process. The fractions, however, were obtained from neutral triglycerides where the EPA and ARA typically occupy the second (middle) position of the triacylglycerol molecule, and may share the other two positions with lower molecular weight compounds.

O'Brien et al. (1993) noted that approximately 83% of the lipids in *P. irregulare* were in the neutral triglyceride fraction. About 10% of the lipids were in the polar (e.g. phospholipid) fraction. Quantification of the triglyceride fractions would be interesting for further study with fungi containing higher molecular weight components.

Thin-layer chromatography results showed that up to seven main classes of lipid compounds were present including neutral triglycerides, free fatty acids, and polar-lipid material. Evidence of all fractions were present throughout the extraction process, however Mendes et al. (1993) noted that the neutral triglyceride fraction in

freeze-dried algae was typically depleted before the other fractions toward the end of extraction.

Figure 5.15 shows that very little extraction takes place for fungi with 95% moisture content that would be typical for fermentation broth filtered with continuous microfiltration membranes or vacuum filter presses. However, with the addition of 10% w/w PFPE surfactant resulted in an order of magnitude increase in extraction of total lipids over 60 min. These results show significant potential for the use of surfactants where the resistance to mass transfer was high because of the aqueous barrier.

In all tests where the moisture content was greater than 10%, the moisture initially presented the greatest resistance to mass transfer followed by the resistance in the surface film that was probably evident only after considerable moisture removal. The size of the micelles were unknown, but were thought to form a limited microdispersion because of the simple mixing technique used. More complete extraction of fungal oil would be expected if much greater mixing were accomplished to obtain a very fine microdispersion. This might create greater micellar surface area resulting in more intimate contact of the micelles with the fluid phase.

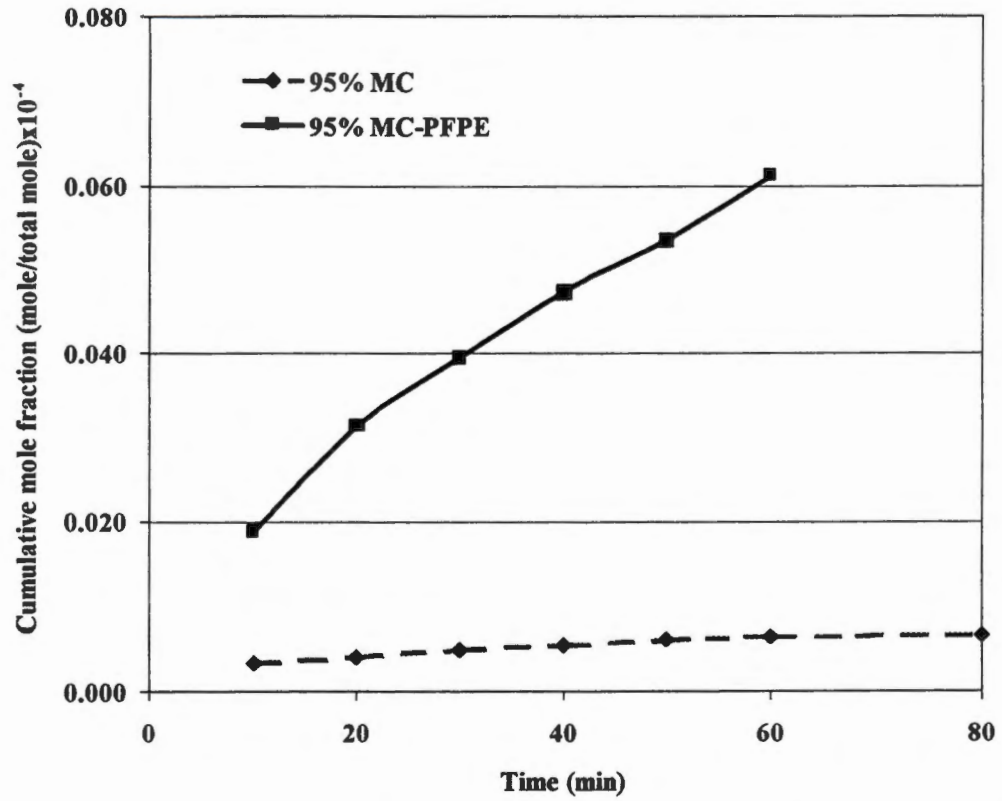


Figure 5.15. Effect of surfactant (10% w/w PFPE) on diffusion of fungal oil in *P. irregulare* with a 95% moisture content.

CHAPTER VI

CONCLUSIONS AND RECOMMENDATIONS

A series of experiments was performed to determine the solubility and mass-transfer characteristics of the extraction of oil from the lower fungi, *P. irregulare* by supercritical CO₂. Solubility data were obtained for 40 and 60 °C isotherms in a flow-through apparatus that achieved equilibrium at a low flow rate of 20 standard ml/min. The solubility of fungal oil in the pressure range of this experiment showed retrograde behavior. The compressed-gas model that utilizes the Peng-Robinson equation of state was applied to model the solubility isotherms for the naphthalene to test the system at 40 °C and the fungal oil for both isotherms. Because of the lack of vapor-pressure data for triglycerides in the literature, the physical properties for several model oil pseudocomponents were used to approximate the system. The pseudocomponent vapor pressure data were not sufficient for modeling the system. The vapor pressure was estimated to be several orders of magnitude less than that of oleic acid, for example, and may approximate the vapor pressures of the larger triglyceride molecules. Physical properties of a hypothetical compound were then applied to the model. The model fit the data fairly well (AAD as low as 8%), but cannot be extended to other similar systems. These results indicated that a simplified binary representation was not adequate for modeling the fungal lipid solubility. However, a detailed multicomponent application of the model using the available fatty acid data would possibly provide a reasonable fit.

Experiments were conducted to determine the effect of flow rate and particle size on the mass transfer of the supercritical extraction system at 20.6 MPa and 40 or 50°C containing fungi at different moisture levels. The purpose of testing flow rate and particle size was to establish the necessary flow conditions for determining equilibrium data and to determine the limiting mass transfer resistance. A diffusion-controlled regime that shows intraparticle diffusion as the main resistance to mass transfer may be determined if the effect of flow rate is negligible. The mass transfer experiments using variable flow rates indicated that flow rate did indeed affect the extraction rate during the initial part of the extraction; therefore, the external-film appeared to contribute as the main resistance to mass transfer. Another model addressing this rate-limiting step in the surface film would be necessary to depict the mass transfer in the initial period. The later part of the extraction process showed significant decline in the extraction rate for all flow-rate tests indicating a transition to a diffusion-controlled regime that could be modeled using Fick's Second Law. Tests that extended for periods of 6 h were modeled for the later part of the extraction to determine the effective diffusivity for fungal oil in the biomass matrix with an initial moisture content of 10%. Two particle sizes (0.15 and 0.25 mm radius) were also tested to verify the effective diffusivity values at 40 °C. The effective diffusivity was regressed from the nonlinear analytical solution to Fick's Second Law for spherical geometry. The effective diffusivities were approximately 1.6 and 4.3×10^{-9} cm²/s for the 40 and 50 °C tests, respectively, indicating an increase in effective diffusivity with temperature.

The extraction rate decreased significantly with increasing moisture content and was very low for the 95% moisture content. Evidence suggested that moisture removal from the high-moisture samples during the initial extraction appeared to significantly increase the extraction rate to nearly the rate achieved for the 10% moisture samples before the transition to the diffusion regime. The addition of the PFPE surfactant to the 95% moisture sample demonstrated a potential use for extraction of oils under extremely adverse conditions where the water to surfactant ratio is important for decreasing the aqueous barrier. The extraction rate was increased by an order of magnitude. A significant savings in the drying costs might be realized. Further exploration of the use of surfactants to aid extraction from biomass with high moisture content is recommended.

Other recommendations include:

1. conducting tests for the initial period of the mass-transfer experiments to characterize the conditions of possible surface-film mass transfer and determine the appropriate model for both the initial and transition regions of the extraction process.
2. acquiring more solubility data for the two isotherms previously mentioned and for 50 °C over a wider pressure range (including near critical pressure and 34.5 Mpa). Taking data at higher pressures would require the replacement of some fittings in the apparatus that are rated for only 41.3 Mpa.

3. obtaining a better estimation for the vapor pressure of triglycerides by conducting vapor pressure experiments with pure triglycerides containing fatty acids that are also present in the fungal oil. This may be done for a narrow temperature range utilizing the GC method (Mishra et al., 1994) with the appropriate triglyceride chromatography column. Other methods would be required for estimations outside the temperature range used for GC analysis.

REFERENCES

- Anderson, A.J.C. 1962. *Refining of Oils and Fats for Edible Purposes*, 2nd ed., ed. P.N. Williams. Pergamon Press, The MacMillan Co.: New York.
- AOAC. 1990. *Official Methods of Analysis*, 15th ed. Association of Official Analytical Chemists, Washington, DC.
- Bajpai, P. and P.K. Bajpai. 1993. Eicosapentaenoic acid (EPA) production from microorganisms: a review. *J. Biotechnol.* **30**: 161-183.
- Barber, T.A., P.R. Bienkowski, and H.D. Cochran. 1991. Solubility of solid CCl₄ in supercritical CF₄. *J. Chem. Eng. Data.* **36**: 99.
- Beckman, E.J. 1996. Carbon Dioxide Extraction of Biomolecules. *Science.* **271**: 613.
- Bharath, R., H. Inomata, T. Adschiri and K. Arai. 1992. Phase equilibrium study for the separation and fractionation of fatty oil components using supercritical carbon dioxide. *Fluid Phase Equilib.* **81**: 307-320.
- Bird, R.B., W.E. Stewart and E.N. Lightfoot. 1960. *Transport Phenomena*. New York: John Wiley and Sons.
- Boersma, L.L. and 21 other authors. 1995. Waste management and utilization in food production and processing. Council for Agricultural Science and Technology task force report #124, ISSN 0194-4088.
- Chrastil, J. 1982. Solubility of solids and liquids in supercritical gases. *J. Phys. Chem.* **86**: 3016-3021.
- CRC Handbook of Chemistry and Physics*. 1990. 1st Student edition, Weast, R.C., Ed. Boca Raton, FL: CRC Press.
- Chang, P.S., J.S. Rhee and J. Kim. 1991. Continuous glycerolysis of olive oil by *Chromobacterium viscosum* Lipase immobilized on liposome in reversed micelles. *Biotechnol. Bioeng.* **38**: 1159-1165.
- Chittofrati, A., D. Lenti, A. Sanguineti, M. Visca, C.M.C. Gambi, D. Senatra and Z. Zhou. 1989. Perfluoropolyether microemulsions. *Progr. Colloid Polym. Sci.* **79**: 218-225.
- Choi, K.J., Z. Nakhost, V.J. Krukonis and M. Karel. 1987. Supercritical fluid extraction and characterization of lipids from algae *Scenedesmus obliquus*. *Food Biotechnol.* **1(2)**: 263-281.

- Christie, W.W. 1982. A simple procedure for rapid transmethylation of glycerolipids and cholesteryl esters. *J. Lipid Res.* **23**: 1072-1075.
- Cochran, H.D., L.L. Lee and D.M. Pfund. 1987. Application of the Kirkwood-Buff theory of solutions to dilute supercritical mixtures. *Fluid Phase Equilib.* **34**: 219.
- Cochran, H.D., E. Johnson and L.L. Lee. 1990. Molecular theory of ternary supercritical solutions. I. Theory and methods of calculations. *J. Supercritical Fluids.* **3**: 157.
- Crank, J. 1956. *The Mathematics of Diffusion*. Oxford Press: London.
- Cui, Z. 1993. Experimental investigation on enhancement of crossflow ultrafiltration with air sparging. In *Effective Membrane Processes-New Perspectives*. ed. R. Paterson, 237-245. London: Mechanical Engineering.
- Cygnarowicz, M.L. and W.D. Seider. 1989. Effect of retrograde solubility on the design optimization of supercritical extraction processes. *Ind. Eng. Chem. Res.* **28**: 1497-1503.
- Cygnarowicz-Provost, M., D.J. O'Brien, R.J. Maxwell and J.W. Hampson. 1992. Supercritical-Fluid Extraction of fungal lipids using mixed solvents: Experiment and modeling. *J. Supercritical Fluids.* **5**: 24-30.
- Daubert, T.E. and R.P. Danner. 1993. *Physical & Thermodynamic Properties of Pure Chemicals: Data Compilation*. Design Institute for Physical Property Data, AIChE, Washington, D.C.: Taylor and Francis.
- DeSimone, J. M., E. E. Maury, J. R. Combes, and Y. Z. Menceloglu. 1993. Heterogeneous Polymerizations in Supercritical Carbon Dioxide Continuous Phases. *PMSE Preprints*, 68.
- Dickinson, N.L. and J.M. Meyers. 1952. Solexol fractionation of menhaden oil. *J. Am. Oil Chem. Soc.* **29**: 235.
- Domsch, K.H. and W. Gams. 1972. *Fungi in Agricultural Soils*. Halsted Press Div., John Wiley & Sons Inc., New York.
- D'Souza R. and A.S. Teja. 1987. The prediction of the vapor pressures of carboxylic acids. *Chem. Eng. Comm.* **61**: 13-22.

- Dunstan, G.A., J.K. Volkman, S.M. Barrett and C.D. Garland. 1993. Changes in the lipid composition and maximization of the polyunsaturated fatty acid content of three microalgae grown in mass culture. *J. Appl. Phycology*. **5**: 71-83.
- Eggers, R. and U. Sievers. 1989. Processing of oilseed with supercritical carbon dioxide. *J. Chem. Eng. of Japan*. **22**: 641-649.
- Eisenbach, W. 1984. Supercritical fluid extraction: A film demonstration. *Ber. Bunsenges Phys. Chem.* **88**: 882.
- Eldridge, A.C., J.P. Friedrich, K. Warner, and W.F. Kwolek. 1986. Preparation and evaluation of supercritical carbon dioxide defatted soybean flakes. *J. Food Sci.* **51**: 584.
- Erickson, J.C., P. Schyns and C.L. Cooney. 1990. Effect of pressure on an enzymatic reaction in a supercritical fluid. *Am. Inst. Chem. Eng. J.* **36(2)**: 299-301.
- Eubank, P.T., C.H. Wu, J.F.J. Alvarado, A. Forero and M.K. Beladi. 1994. Measurement and prediction of three-phase water/hydrocarbon equilibria. *Fluid Phase Equilib.* **102**: 181-203.
- Fattori, M., N.R. Bulley and A. Meisen. 1988. Carbon dioxide extraction of canola seed: oil solubility and effect of seed treatment. *J. Am. Oil Chem. Soc.* **65(6)**: 968-974.
- Flatt, J.T., T.A. Cooper, D.C. Cameron, and E.N. Lightfoot. 1988. Utilization of dairy waste: microbial production of galactose-containing polysaccharides. Paper 105c presented at the AIChE 1988 Annual Meeting, Washington, D.C.
- Friedrich, J.P. and E.H. Pryde. 1984. Supercritical CO₂ extraction of lipid-bearing materials and characterization of the products. *J. Am. Oil Chem. Soc.* **61(2)**: 223-228.
- Fulton, J.L., D.M. Pfund, J.B. McClain, T.J. Romack, E.E. Maury, J.R. Combes, E.T. Samulski, J.M. DeSimone, and M. Capel. 1995. Aggregation of Amphiphilic Molecules in Supercritical Carbon Dioxide: A Small Angle X-ray Scattering Study. *Langmuir*. **11**: 4241.
- Ghandi, S.R. and J.D. Weete. 1991. Production of the polyunsaturated fatty acids arachidonic acid and eicosapentaenoic acid by the fungus *Pythium ultimum*. *J. Gen Microbiol.* **137**: 1825-1830.

- Giovenco S., F. Verheggen and C. Laane. 1987. Purification of intracellular enzymes from whole bacterial cells using reversed micelles. *Enzyme Microb. Technol.* **9**: 470-473.
- Goodrum, J.W. and M.A. Eiteman. 1996. Physical properties of low molecular weight triglycerides for the development of bio-diesel fuel models. *Bioresource Technol.* **56**: 55-60.
- Goto, M., M. Sato and T. Hirose. 1993. Extraction of peppermint oil by supercritical carbon dioxide. *J. Chem. Eng. Japan.* **26(4)**: 401-407.
- Grima, E.M., J.A. Sánchez Pérez, F.García Camacho, J.L. García Sánchez, D.López Alonso. 1993. n-3 PUFA productivity in chemostat cultures of microalgae. *Appl. Microbiol biotechnol.* **38**: 599-605.
- Guan, Z. and J.M. DeSimone. 1994. Fluorocarbon Based Heterophase Polymeric Materials: Blockcopolymer Surfactants for CO₂ Applications. *Macromolecules.* **27**: 5527.
- Handbook of Physical Properties of Organic Chemicals.* 1997. Eds. P.H. Howard and W.M. Meylan. Boca Raton, FL: CRC Press.
- Hara, A. and N.S. Radin. 1978. Lipid extraction of tissues with a low-toxicity solvent. *Anal. Biochem.* **90**: 420-426.
- Hardardottir, I. and J.E. Kinsella. 1988. Extraction of lipid and cholesterol from fish muscle with supercritical fluids. *J. Food Sci.* **53(6)**: 1656-1661.
- Harrison, K., J. Goveas, K.P. Johnston and E.A. O'Rear III. 1994. Water-in-carbon dioxide microemulsions with a fluorocarbon-hydrocarbon hybrid surfactant. *Langmuir.* **10**: 3536-3541.
- Hedrick, J. and L.T. Taylor. 1989. Quantitative supercritical fluid extraction/supercritical fluid chromatography of a phosphonate from aqueous media. *Anal. Chem.* **61**: 1986-1988.
- Hendy, N.A., C.R. Wilke, and H.W. Blanch. 1984. *Enzyme Microbiol. Technol.* **6**: 73-77.
- Hoefling, T.A., R.M. Enick and E.J. Beckman. 1991. Microemulsions in near-critical and supercritical CO₂. *J. Phys. Chem.* **95**: 7127-7129.

- Hoefling, T.A., R.R. Beitle, R.M. Enick and E.J. Beckman. 1993. Design and synthesis of highly CO₂-Soluble surfactants and chelating agents. *Fluid Phase Equilib.* **83**: 203-212.
- Ikushima, Y., N. Saito, K. Hatakeda and O. Sato. 1996. Promotion of a lipase-catalyzed esterification in supercritical carbon dioxide in the near-critical region. *Chem. Eng. Sci.* **51(11)**: 2817-2822.
- Ikushima, Y., N. Saito and T. Goto. 1989. Selective extraction of oleic, linoleic, and linolenic acid methyl esters from their mixture with supercritical carbon dioxide-entrainer systems and a correlation of the extraction efficiency with a solubility parameter. *Ind. Eng. Chem. Res.* **28**: 1364-1369.
- Johnston, K.P., K.L. Harrison, M.J. Clarke, S.M. Howdle, M.p. Heitz, F.V. Bright, C. Carlier and T.W. Randolph. 1996. Water-in-carbon dioxide microemulsions: an environment for hydrophiles including proteins. *Science.* **271**: 624-626.
- Jonah, D.A. and H.D. Cochran. 1994. Chemical potentials in dilute, multicomponent solutions. *Fluid Phase Equilib.* **92**: 107-137.
- Kaiser, J.A. 1988. Supercritical fluid extraction of 2,3 butanediol with CO₂: the construction of equipment. Thesis at the University of Tennessee, Knoxville.
- Kaler, E.W., J.F. Billman, J.L. Fulton and R.D. Smith. 1991. A small-angle neutron scattering study of intermicellar interactions in microemulsions of AOT, water, and near-critical propane. *J. Phys. Chem.* **95**: 458-462.
- Katz, S.N., J.E. Spence, M.J. O'Brien, R.H. Skiff, G.J. Vogel, , and R. Prasad 1990. Method for decaffeinating coffee with a supercritical fluid. U.S. Patent 4,911,941, March 27.
- Kendrick, A. and C. Ratledge. 1992. Lipids of selected molds grown for production of n-3 and n-6 polyunsaturated fatty acids. *Lipids.* **27(1)**: 15-20.
- King, J.W. 1993. Analysis of fats and oils by SFE and SFC. *Inform.* **4(9)**: 1089-1098.
- Kirk, T.K. 1976. Ch. 11. In *The Filamentous Fungi. Vol. 4: Fungal Technology.* eds. J.E. Smith, D.R. Berry, and B.Kristiansen, London: Edward Arnold Ltd.
- Ko, M., V. Shah, P.R. Bienkowski, and H.D. Cochran. 1991. Solubility of the antibiotic penicillin v using supercritical CO₂. *J. Supercrit. Fluids.* **4**: 32-39.

- Laio, W.C., G.J. Hulbert and T.H. Walker. Use of injected gas to increase flux in cross-flow filtration processes. ASAE Paper No. St. Joseph, MI: ASAE.
- Lambert, P.W. 1983. Ch. 9. In *The Filamentous Fungi. Vol. 4: Fungal Technology*. eds. J.E. Smith, D.R. Berry, and B.Kristiansen,. London: Edward Arnold Ltd.
- Lee, A.K.K., N.R. Bulley, M. Fattori and A. Meisen. 1986. Modelling of supercritical carbon dioxide extraction of canola oilseed in fixed beds. *J. Am. Oil Chem. Soc.* **63(7)**: 921-925.
- Lin, H.M., H. Kim, W.A. Leet and K.C. Chao. 1985. New vapor-liquid equilibrium apparatus for elevated temperatures and pressures. *Ind. Eng. Chem. Fundam.* **24**: 260.
- Lin, H.M., R.J. Lee and M.J. Lee. 1995. High-temperature vapor-liquid equilibria of helium + 1-methylnaphthalene and helium + n-hexadecane. *Fluid Phase Equilib.* **111**: 89-99.
- Londono, J.D., H.D. Cochran, P.R. Bienkowski, and V.M. Shah. 1993a. Cryogenic apparatus for scattering and phase equilibrium studies. *Rev. Sci. Instrum.* **64**: 200-202.
- Londono, J.D., V.M. Shah, G.D. Wignall, H.D. Cochran, and P.R. Bienkowski. 1993b. Small angle neutron scattering (SANS) studies of dilute supercritical solutions: 1. Pure supercritical neon. *J. Chem. Phys.* **99**: 466-470.
- Maury, E.E., H.J. Batten, S.K. Killia, Y.Z. Menciloglu, J.R. Combes, and J.M. DeSimone. 1993. Graft Copolymer Surfactants for Supercritical Carbon Dioxide Applications. *Polymer Preprints*, **34**: 664.
- Mehr, C.B., R.N. Biswal, H.D. Cochran, and J.L. Collins. 1996. Supercritical carbon dioxide extraction of caffeine from guaraná. *J. Supercritical Fluids.* **9**: 185-191
- McHugh M. and V. Krukoniš 1994. *Supercritical Fluid Extraction: Principles and Practices*. 2nd ed., Boston: Butterworth-Heinemann.
- Mendes R.L., H.L. Fernandes, M. Cygnarawicz-Provost, J.M.S. Cabral, J.M. Novais and A.F. Palavra. 1994a. Supercritical CO₂ extraction of lipids from microalgae. Proceedings of the "3rd International Symposium on SCF", Paris, France, 477.
- Mendes R.L., H.L. Fernandes, J.A.P. Coelho, J.M.S. Cabral, A.M.F. Palavra and J.M. Novais . 1994b. Supercritical Carbon dioxide extraction of hydrocarbons from the microalgae *Botryococcus braunii*. *J. Appl. Phycol.* **6**: 289-293.

- Mendes R.L., J.A.P. Coelho, H.L. Fernandes. 1995. Applications of supercritical CO₂ extraction to microalgae and plants. *J Chem. Tech. Biotechnol.* **62**: 53-59.
- Mishra, V.K., F. Temelli and B. Ooraikul. 1993. Extraction and purification of ω -3 fatty acids with an emphasis on supercritical fluid extraction-A review. *Food Research International.* **26**: 217-226.
- Mishra, V.K, F. Temelli and B. Ooraikul. 1994. Vapor pressure of fatty acid esters: Correlation and estimation. *J. Food Eng.* **23**: 467-480.
- Mühlbauer, A.L. and J.D. Raal. 1995. Computation and thermodynamic interpretation of high-pressure vapour-liquid equilibrium- A review. *Chem. Eng. J.* **60**: 1-29.
- Nilsson, W.B., E.J. Gauglitz Jr., J.K. Hudson, V.F. Stout and J. Spinelli. 1988. Fractionation of Menhaden oil ethyl esters using supercritical fluid CO₂. *J. Am. Oil Chem. Soc.* **65(1)**: 109-117.
- Nilsson, W.B. and J.B. Hudson. 1993. Solubility of simple and mixed triacylglycerols in supercritical CO₂. *J. Am. Oil Chem. Soc.* **70(8)**: 749-753.
- O'Brien, D.J., M.J. Kurantz and R. Kwoczak. 1993. Production of eicosapentaenoic acid by the filamentous fungus *Pythium irregulare*. *Appl. Microbiol. Biotechnol.* **40**: 211-214.
- Pabai, F., S. Kermasha and A. Morin. 1995. Lipase from *Pseudomonas fragi* CRDA 323: Partial purification, characterization and interesterification of butter fat. *Appl. Microbiol. Biotechnol.* **43**: 42-51.
- Panagiotopoulos, A.Z. and R.C. Reid. 1985. *Am. Chem. Soc. Div. Fuel Chem., Preprints.* **30**: 46.
- Pariser, E.R., M.B. Wallerstein, C.J. Corkery and N.L. Brown. 1978. *Fish Protein Concentrate: Panacea for World Malnutrition*. Cambridge, MA: MIT Press.
- Peker, H., M.P. Srinivasan, J.M. Smith and B.J. McCoy. 1992. Caffeine extraction rates from coffee beans with supercritical carbon dioxide. *AIChE J.* **38(5)**: 761-770.
- Peng, D. Y. and D. B. Robinson. 1976. A new two-constant equation of state. *Ind. Eng. Chem. Fund.* **15(1)**: 59.

- Polak, J.T., M. Balaban, A. Peplow and A.J. Philips. 1989. Supercritical fluid extraction of lipids from algae. Ch.12. Washington D.C.: ACS symposium series.
- Prausnitz, J. M., R. N. Lichtenthaler, and E. G. de Azevedo. 1986. *Molecular Thermodynamics of Fluid-phase Equilib.* 2nd ed., Englewood Cliffs, N. J.: Prentice-Hall Inc.
- Prazeres, D.M.F., F.A.P. Farcia and J.M.S. Cabral. 1993. An ultrafiltration membrane bioreactor for the lipolysis of olive oil in reversed micellar media. *Biotechnol. Bioeng.* **41**: 761-770.
- Radmer, R.J. and B.C. Parker. 1994. Commercial applications of algae: opportunities and constraints. *J. Appl. Phycology.* **6**: 93-98.
- Radwan, S.S. 1991. Sources of C-20-polyunsaturated fatty acids for biotechnological use. *Appl. Microbiol. Biotechnol.* **35**: 421-430.
- Ratledge, C. 1993. Single cell oils - Have they a biotechnological future? *Tibtech.* **11(7)**: 278-284.
- Reid, R.C., J.M. Prausnitz and B.E. Poling. 1987. *The Properties of Gases and Liquids.* 4th ed. New York: McGraw Hill Inc.
- Reverchon, E. and L.Sesti Osséo. 1994. Comparison of processes for the supercritical carbon dioxide extraction of oil from soybean seeds. *J. Am. Oil Chem. Soc.* **71(9)**: 1007-1012.
- Rizvi, S. S. H., A. L. Benado, J. A. Zollweg, and J. A. Daniels. 1986a. Supercritical fluid extracton: Fundamental principles and modeling methods. *Food Technol.* **6**: 55-64.
- Rizvi, S. S. H., A. L. Benado, J. A. Zollweg, and J. A. Daniels. 1986b. Supercritical fluid extracton: Operating principles and food applications. *Food Technol.* **7**: 57-64.
- SAS, 1985. *SAS User's Guide: Statistics, version 5th Edition.* Cary, NC.: SAS Institute Inc.
- Sebastião, M.J., J.M.S. Cabral and M.R. Aires-Barros. 1993. Synthesis of fatty acid esters by a recombinant cutinase in reversed micelles. *Biotechnol. Bioeng.* **42**: 326-332.

- Sakaki, K., T. Yokochi, O. Suzuki and T. Hakuta. 1990. Supercritical fluid extraction of fungal oil using CO₂, N₂O, ChF₃ and SF₆. *J. Am. Oil Chem. Soc.* **67(9)**: 553-557.
- Schaeffer, S.T., L.H. Zalkow and A.S. Teja. 1989. Modelling of the supercritical fluid extraction of monocrotaline from *Crotalaria spectabilis*. *J. Super. Fluids* **65(9)**: 1455-1459.
- Shah, V.M., P.R. Bienkowski and H.D. Cochran. 1994. Generalized quartic equation of state for pure nonpolar fluids. *AIChE J.* **40(1)**: 152-159.
- Shah, V.M., Y.L. Lin, P.R. Bienkowski and H.D. Cochran. 1996. Generalized quartic equation of state. *Fluid Phase Equilib.* **116**: 87-93.
- Shamala, T.R. and K.R. Sreekantiah. 1987. Successive cultivation of selected cellulolytic fungi on rice straw and wheat bran for economic production of cellulases and D-xylanase. *Enzyme Microb. Technol.* **9**: 97-101.
- Shimizu, S., H. Kawashima, Y. Shinmen, K. Akimoto and H. Yamada. 1988. Production of eicosapentaenoic acid by *Mortierella* fungi. *J. Am. Oil Chem. Soc.* **65(9)**: 1455-1459.
- Shimizu, S., H. Kawashima, K. Akimoto, Y. Shinmen, and H. Yamada. 1989a. Microbial conversion of an oil containing γ -linolenic acid to an oil containing eicosapentaenoic acid. *J. Am. Oil Chem. Soc.* **66(3)**: 342-347.
- Shimizu, S., H. Kawashima, K. Akimoto, Y. Shinmen and H. Yamada. 1989b. Conversion of linseed oil to an eicosapentaenoic acid-containing oil by *Mortierella alpina* 1S-4 at low temperature. *Appl. Microbiol. Biotechnol.* **32**: 1-4.
- Shinmen Y., H. Kawashima, S. Shimizu, and H. Yamada. 1992. Concentration of eicosapentaenoic acid and docosahexaenoic acid in an arachidonic acid-producing fungus, *Mortierella alpina* 1S-4, grown on fish oil. *Appl. Microbiol. Biotechnol.* **38**: 301-304.
- Simopoulos, A.P. 1989. Summary of the NATO advanced research workshop on dietary ω -3 and ω -6 fatty acids: biological effects and nutritional essentiality. *J. Nutrition* **119**: 521-528.
- Shishikura, A., K. Fujimoto, T. Suzuki and K. Arai. 1994. Improved lipase-catalyzed incorporation of long-chain fatty acids into medium-chain triglycerides assisted by supercritical carbon dioxide extraction. *J. Am. Oil Chem. Soc.* **71(9)**: 961-967.

- Shuler, M.L. and F. Kargi. 1992. *Bioprocess Engineering: Basic Concepts*. Englewood Cliffs, N.J., Prentice Hall.
- Staby, A., T. Forskov and J. Mollerup. 1993. Phase equilibria of fish oil fatty acid ethyl esters and sub- and supercritical CO₂. *Fluid Phase Equilib.* **87**: 309-340.
- Stamatis, H., A. Xenakis, M. Provelegiou and F.N. Kolisis. 1993. Esterification reactions catalyzed by lipases in microemulsions: The role of enzyme localization in relation to its selectivity. *Biotechnol. Bioeng.* **42**: 103-110.
- Steytler, D.C., P.S. Moulson and J. Reynolds. 1991. Biotransformations in near-critical carbon dioxide. *Enzyme Microb. Technol.* **13**: 221-226.
- Svensson I., E. Wehtje, P. Adlercreutz and B. Mattiasson. 1994. Effects of water activity on reaction rates and equilibrium positions in enzymatic esterifications. *Biotechnol. Bioeng.* **44**: 549-556.
- Temelli, F. 1992. Extraction of triglycerides and phospholipids from canola with supercritical carbon dioxide and ethanol. *J. Food Sci.* **57(2)**: 440-442.
- Turker, M. and F. Mavituna. 1987. Production of cellulase by freely suspended and immobilized cells of *Trichoderma reesei*. *Enzyme Microb. Technol.* **9**:739-743.
- Van Der Wende, L.A. 1988. Omega-3 fatty acids: Algal and fish fatty acids could net \$790 million, but market needs backing of medical industry. *In: Biomarkets: 33 Market Forecasts for Key Product Areas*, pp. 199-203. New Jersey: Technical Insights, Inc.
- Vermuë, M.H., J. Tramper, J.P.J. de Jong and W.H.M. Oostrom. 1992. Enzymic transesterification in near-critical carbon dioxide: Effect of pressure, Hildebrand solubility parameter and water content. *Enzyme Microb. Technol.* **14**: 649-655.
- Wang, Y. and B. McNeil. 1995. Production of the fungal exopolysaccharide scleroglucan by cultivation of *Sclerotium gluconicum* in an airlift reactor with an external loop. *J. Chem. Tech. Biotechnol.* **63**: 215-222.
- Wessinger, E.W., D.J. O'Brien, and M.J. Kurantz. 1990. Identification of fungi for sweet whey permeate utilization and eicosapentaenoic acid production. *J. Ind. Microbiol.* **6**:191-197.
- Yamada, H., S. Shimizu and Y. Shinmen. 1987. Production of arachidonic acid by *Mortierella elongata* 1S-5. *Agric. Biol. Chem.* **51(3)**:785-790.

- Yokochi, T., M.T. Usita, Y. Kamisaka, T. Nakahara and O. Suzuki. 1990. Increase in the γ -linolenic acid content by solvent winterization of fungal oil extracted from *Mortierella* genus. *JAOCS*. 67(11):846-851.
- Zall, R.R. 1984. Trends in whey fractionation and utilization, a global perspective. *J. Dairy Sci.* 67: 2621-2624.
- Zosel, K. 1978. Separation with supercritical gases: Practical applications. *Angew. Chem. Int. Ed. Engl.* 17: 702.

APPENDIXES

APPENDIX A

PROCESS CONTROL AND FILTRATION DATA

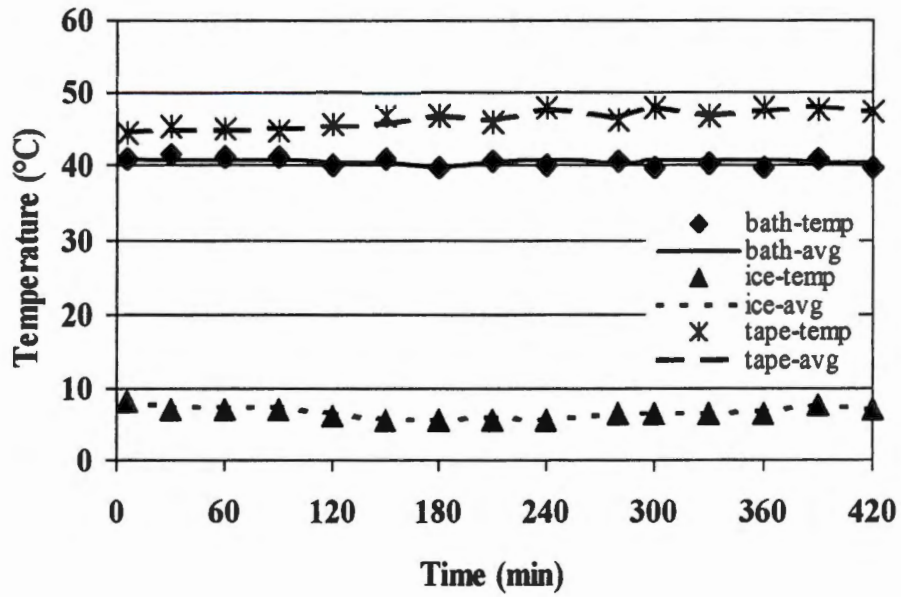


Figure A.1. Temperature data taken for experiment K1 (40 °C and 20.7 MPa) for the bath, cold trap and heating tape.

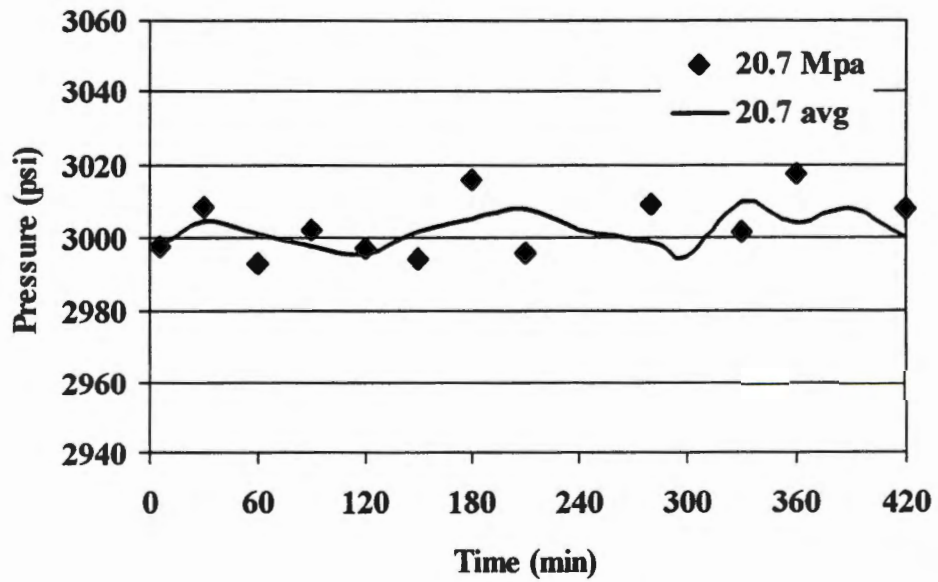


Figure A.2. Pressure data taken for experiment K1 (40 °C and 20.7 MPa) for the bath, cold trap and heating tape.

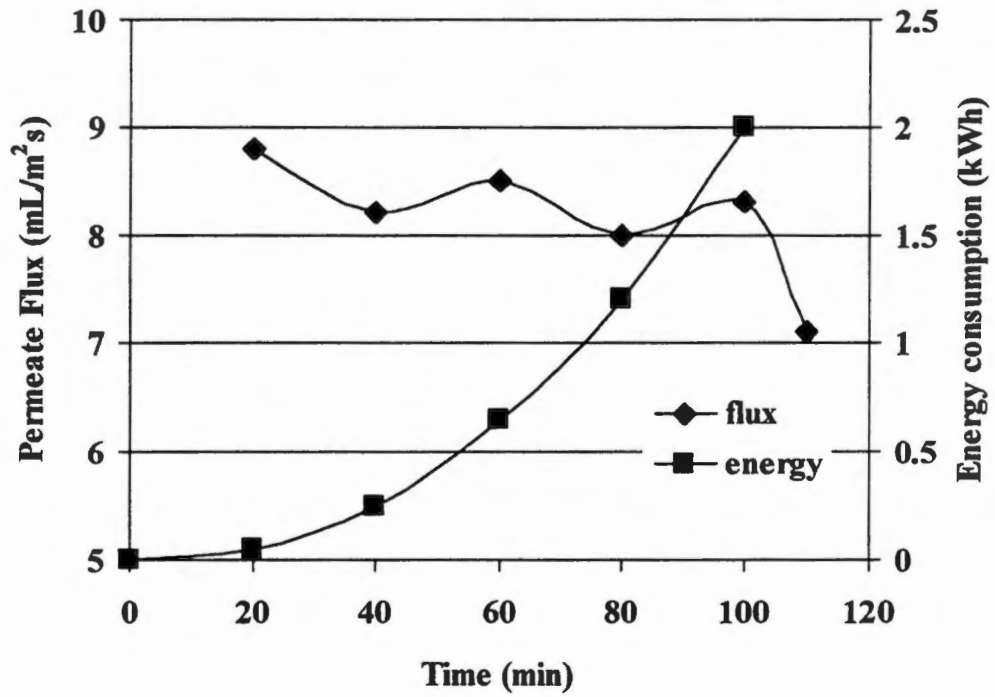


Figure A.3. Filtration flux and energy consumption as a function of time for the fungal biomass.

APPENDIX B

KINETIC AND EQUILIBRIUM DATA

Table B.1. Raw data for flow-rate kinetic experiments

Test Sample	Time min	FR ¹ CO ₂ mole min scfm	Mole FAME/mole CO ₂ × 10 ⁻⁵												FRF	
			FR ¹ 14:0	14:1	16:0	16:1	18:0	18:1	18:2	GLA 20:0	20:1	ARA 20:1	EPA 20:1	TFA ²		
			FR ¹ 14:0	14:1	16:0	16:1	18:0	18:1	18:2	GLA 20:0	20:1	ARA 20:1	EPA 20:1	TFA ²		
f1	s1	20	0.058	0.09	0	0.12	0.06	0.14	0.09	0.13	0.16	0	0	0	0.18	0.961
f1	s2	20	0.058	0.33	0	1.27	0.73	3.14	1.58	1.65	3.43	2.6	0	0.82	2.5	18.04
f1	s3	45	0.058	0.82	0	0.96	0.49	2.52	1.17	1.26	2.77	1.61	0	1.11	1.31	14.01
f1	s4	60	0.058	1.6	0	3.02	0.19	2.51	1.52	2.29	3.36	2.46	0	1.38	2.68	21.01
f1	s5	75	0.058	0.06	0	0.08	0.04	0.13	0.07	0.1	0.15	1.45	0	1	0.14	3.227
f1	s6	90	0.058	1.55	0	3.42	1.2	0.72	1.81	2.78	2.86	2	0	1.74	2.76	20.86
f1	s7	105	0.058	1.42	0.17	3.02	0.19	1.37	1.77	2.77	2.35	1.63	0.56	1.19	1.4	17.85
f1	c1	120	0.185	1.89	0.11	2.51	1.3	0.48	1.79	2.87	0.44	0.13	0	1.62	2.87	16
f1	Total		0.590	7.76	0.28	14.4	4.2	11	9.8	13.9	15.5	11.9	0.56	8.86	13.8	112
f2	s1	60	0.086	1.14	0.09	1.35	0.15	0.19	0.95	1.56	0.27	0	0	0.75	1.16	7.621
f2	s2	60	0.088	2.06	0.13	2.48	0.27	0.32	1.83	2.97	0.48	0.08	0.14	1.51	2.52	14.8
f2	s3	60	0.093	2.29	0.15	2.58	0.28	0.27	1.61	2.61	0.42	0	0.1	1.12	1.84	13.26
f2	s4	60	0.083	4.07	0.26	5.44	0.56	0.78	4.34	7.07	1.07	0.24	0.44	3.74	6.37	34.39
f2	s5	60	0.094	0.04	0	0.04	0.07	0	0.11	0.22	0.04	0.01	0	0.11	0.17	0.8
f2	s6	60	0.085	1.69	0.1	2.61	0.25	0.41	2.16	3.48	0.53	0.14	0.22	2.03	3.41	17.05
f2	s7	60	0.084	1.1	0.07	1.73	0.17	0.27	1.42	2.34	0.4	0	0.12	1.37	2.33	11.32
f2	s8	60	0.088	0.83	0.05	1.35	0.13	0.22	1.1	1.86	0.3	0	0.11	1.15	1.9	8.989
f2	s9	60	0.085	0.69	0.04	1.21	0.11	0.21	1.06	1.78	0.28	0	0.12	1.18	2.02	8.701
f2	s10	60	0.087	0.59	0.04	1.08	0.56	0.19	0.95	1.63	0.26	0	0.11	1.13	1.95	8.485
f2	s11	60	0.086	0.39	0.01	0.77	0.07	0.15	0.7	1.21	0.19	0	0.09	0.9	1.57	6.043
f2	s12	60	0.083	0.32	0	0.66	0.06	0.12	0.64	1.05	0.16	0.03	0.08	0.84	1.47	5.434

Table B.1. continued

Test Sample	Time	FR ¹	CO ₂	min	scm	mole	Mole FAME/mole CO ₂ × 10 ⁻⁵	GLA	18:2	18:1	18:0	16:1	16:0	14:1	14:0	CO ₂	min	scm	mole	FR ¹	Time	Test Sample
F2	s13	210	60	0.121	0.37	0.01	0.63	0.34	0.1	0.55	0.9	0.14	0	0	0.59	0.95	4.559					
F2	s14	240	60	0.128	0.27	0	0.48	0.26	0.08	0.44	0.74	0.11	0	0	0.53	0.88	3.796					
F2	s15	270	60	0.116	0.2	0	0.39	0.2	0.07	0.36	0.61	0.1	0	0	0.45	0.75	3.126					
F2	s16	300	60	0.118	0.14	0	0.28	0.14	0.03	0.26	0.45	0.07	0	0	0.34	0.58	2.297					
F2	s17	330	60	0.120	0	0	0.26	0.13	0.05	0.33	0.59	0	0	0	0.55	0.96	2.867					
F2	s18	360	60	0.118	0	0	0.19	0.07	0.04	0.23	0.49	0	0	0	0.39	0.63	2.037					
F2	c1	180	60	0.614	2.96	0.42	4.03	2.12	0.64	3.23	4.97	0.68	0.18	0.51	2.7	3.86	26.31					
F2	c2	360	60	0.574	0	0	0.03	0.01	0.19	0.03	0.04	0	0	0	0.02	0.03	0.348					
F2	c2-r	360	60	0.391	0.2	0.01	0.43	0.22	0.07	0.38	0.63	0.09	0.03	0.05	0.41	0.67	3.18					
F2	Total			3.339	19.3	1.4	28	6.16	4.41	22.7	37.2	5.59	0.7	2.09	21.8	36	185.4					
F3	s1	15	400	0.302	1.85	0.12	2.19	1.45	0.23	1.5	2.42	0.39	0	0.08	0.92	1.47	12.63					
F3	s2	30	400	0.296	1.5	0.1	2.18	1.17	0.37	1.65	2.67	0.4	0.09	0.14	1.47	2.43	14.16					
F3	s3	45	400	0.286	0.95	0.06	1.47	0.83	0.22	1.14	1.89	0.3	0	0.09	0.97	1.61	9.529					
F3	s4	60	400	0.295	0.57	0.04	0.91	0.51	0.16	0.79	1.33	0.21	0	0.09	0.9	1.54	7.024					
F3	s5	75	400	0.292	0.23	0	0.39	0.21	0.07	0.34	0.6	0.09	0	0	0.43	0.72	3.071					
F3	s6	90	400	0.354	0.08	0	0.14	0.07	0	0.12	0.22	0	0	0	0.17	0.28	1.08					
F3	s7	105	400	0.351	0.05	0	0.09	0.04	0	0.08	0.14	0	0	0	0.1	0.16	0.657					
F3	s8	120	400	0.275	0.04	0	0.07	0	0	0.05	0.09	0	0	0	0.03	0.05	0.339					
F3	s9	135	400	0.307	0	0	0.04	0	0	0	0	0	0	0	0	0	0.042					
F3	s10	150	400	0.239	0.02	0	0.03	0.01	0	0.02	0.04	0	0	0.09	0.02	0.03	0.252					
F3	s11	165	400	0.346	0.07	0	0.11	0.06	0	0.08	0.14	0	0	0	0.09	0.15	0.702					
F3	s12	180	400	0.287	0.05	0	0.09	0.04	0	0.07	0.12	0	0	0	0.08	0.14	0.581					
F3	c1	180	400	3.505	0.28	0.02	0.39	0.22	0.06	0.31	0.5	0.08	0.02	0.03	0.28	0.47	2.651					
F3	Total			7.133	5.68	0.33	8.1	4.61	1.11	6.16	10.2	1.47	0.11	0.52	5.44	9.05	52.71					

Table B.1. continued

Test Sample	Time	FR ¹	CO ₂	min	scm	mole	Mole FAME/mole CO ₂ × 10 ⁻⁵	GLA	18:2	18:1	18:0	16:1	16:0	14:1	14:0	FR ¹	CO ₂	min	scm	mole	FR ²	EPA	ARA	20:1	ARA	EPA	TFA ²						
f4	s1	100	0.111	0.64	0.04	0.8	0.5	0.12	0.66	0.99	0.19	0.03	0.05	0.48	0.75	5.25	f4	s2	100	0.110	1.57	0.1	1.94	1.23	0.27	1.61	2.5	0.42	0.08	0.13	1.25	2	13.11
f4	s3	100	0.109	1.85	0.12	2.29	1.45	0.31	1.84	2.87	0.45	0.09	0.14	1.46	2.31	15.2	f4	s4	100	0.107	1.79	0.12	2.32	1.44	0.32	1.89	2.93	0.46	0.1	0.16	1.49	2.38	15.38
f4	s5	100	0.108	1.48	0.09	2.12	1.27	0.3	1.74	2.72	0.43	0.07	0.13	1.28	2.09	13.73	f4	s6	100	0.107	1.17	0.07	1.78	1.03	0.29	1.58	2.48	0.38	0.1	0.16	1.46	2.38	12.88
f4	s7	100	0.109	0.7	0.04	1.11	0.62	0.19	0.99	1.57	0.24	0.07	0.11	0.96	1.58	8.167	f4	s8	100	0.107	0.66	0.04	1.08	0.6	0.19	0.98	1.57	0.24	0.07	0.11	0.98	1.6	8.109
f4	s9	100	0.108	0.56	0.03	0.94	0.52	0.16	0.84	1.36	0.21	0.06	0.09	0.86	1.42	7.067	f4	s10	100	0.110	0.43	0.03	0.73	0.4	0.13	0.67	1.09	0.17	0	0.07	0.7	1.2	5.631
f4	s11	100	0.109	0.35	0	0.63	0.34	0.12	0.59	0.97	0.15	0	0.07	0.67	1.13	5.001	f4	s12	180	0.109	0.27	0.02	0.47	0.25	0.08	0.41	0.66	0.1	0.03	0.04	0.44	0.73	3.506
f4	s13	100	0.174	0.53	0.06	0.81	0.43	0.13	0.68	1.06	0.14	0	0	0.54	0.85	5.234	f4	s14	100	0.165	0.45	0	0.71	0.41	0.11	0.63	1.01	0.16	0	0	0.63	1.04	5.145
f4	s15	100	0.175	0.24	0	0.42	0.24	0.07	0.4	0.65	0.1	0	0	0.44	0.72	3.272	f4	s16	100	0.171	0.13	0	0.25	0.13	0.04	0.24	0.4	0.06	0	0	0.3	0.49	2.042
f4	c1	180	0.926	0.57	0.04	0.77	0.51	0.11	0.71	1.19	0.19	0.03	0.06	0.71	1.08	5.957	f4	c2	100	0.664	0.23	0.01	0.33	0.19	0.05	0.27	0.43	0.06	0.02	0.03	0.24	0.4	2.268
f4	Total	300	3.577	13.6	0.82	19.5	11.6	3.01	16.7	26.4	4.16	0.74	1.36	14.9	24.1	137	f5-f6	RRF	0.89	0.90	0.96	0.94	1.08	1.03	1.05	1.11	1.12	1.23	1.12	1.29	1.39		
f5	s0	20	0.045	1.2	0.07	1.53	0.76	0.33	1.71	1.08	0.24	0.1	0.16	0.72	0.64	8.524	f5	s1	20	0.059	2.87	0.18	3.83	1.92	0.91	4.72	2.95	0.44	0.32	0.59	2.34	2.04	23.11
f5	s2	30	0.058	3.2	0.2	3	1.59	0.44	2.46	1.54	0.24	0	0.17	0.84	0.71	14.39	f5	s3	45	0.059	2.11	0.13	2.55	1.33	0.55	2.97	1.87	0.28	0.19	0.34	1.41	1.22	14.94

Table B.1. continued

Test Sample	Time	FR	CO ₂	min	sccm	mole	Mole FAME/mole CO ₂ x10 ⁵									
							18:0	18:1	18:2	GLA	20:0	20:1	ARA	EPA	TFA ²	
F5	s4	20	0.059	1.97	0.12	2.43	1.28	0.52	2.84	1.79	0.26	0.17	0.36	1.31	14.2	
F5	s5	20	0.059	2.36	0.15	2.77	1.47	0.56	3.11	1.96	0.27	0.17	0.3	1.38	15.72	
F5	s6	20	0.058	1.8	0.11	2.35	1.22	0.51	2.8	1.75	0.24	0.17	0.29	1.31	13.67	
F5	s7	20	0.058	1.64	0.1	2.23	1.14	0.51	2.78	1.74	0.23	0.18	0.36	1.39	13.48	
F5	s8	20	0.058	1.59	0.1	2.11	1.08	0.43	2.34	1.47	0.2	0.12	0.23	0.99	11.45	
F5	s9	20	0.060	1.49	0.09	2.37	1.17	0.59	3.13	1.97	0.26	0.19	0.31	1.42	10	
F5	s10	20	0.059	1.15	0.07	1.89	0.93	0.53	2.72	1.72	0.22	0.23	0.46	1.67	8	
F5	s11	20	0.058	1.07	0.04	1.28	0.66	0.23	1.28	0.83	0	0	0.58	0.48	6.452	
F5	s12	20	0.058	0.52	0.03	0.88	0.43	0.25	1.28	0.82	0.1	0.12	0.16	0.77	6.038	
F5	c1	20	0.298	1.02	0.06	1.19	0.61	0.25	1.36	0.86	0.12	0.09	0.17	0.66	6.998	
F5	Total		1.045	24	1.48	30.4	15.6	6.61	35.5	22.3	3.08	2.05	3.91	16.8	167	
F6	s0	50	0.045	1.24	0.08	1.35	0.75	0.28	1.6	1.04	0.17	0.18	0.15	0.72	8.18	
F6	s1	50	0.079	3.62	0.24	3.38	1.97	0.5	3.08	1.94	0.28	0.11	0.22	1.18	17.52	
F6	s2	50	0.076	2.37	0.15	2.68	1.49	0.48	2.86	1.77	0.24	0.2	0.21	1.12	14.47	
F6	s3	50	0.077	2.66	0.17	3.38	1.82	0.6	3.54	2.18	0.31	0.14	0.25	1.31	17.48	
F6	s4	50	0.076	1.86	0.12	2.61	1.35	0.65	3.51	2.18	0.28	0.25	0.49	1.84	16.69	
F6	s5	50	0.077	1.47	0.09	2.14	1.09	0.54	2.86	1.73	0.23	0.21	0.37	1.51	13.53	
F6	s6	50	0.077	1.46	0.09	1.9	0.99	0.4	2.2	1.37	0.18	0.03	0.21	0.95	10.65	
F6	s7	50	0.076	0.78	0.05	1.25	0.63	0.36	1.87	1.14	0.15	0.16	0.24	1.05	8.598	
F6	s8	50	0.076	0.79	0.05	1.1	0.57	0.27	1.41	0.88	0.11	0.03	0.18	0.83	6.884	
F6	s9	50	0.076	0.46	0.03	0.79	0.4	0.24	1.37	0.75	0.1	0.11	0.16	0.72	5.734	
F6	s10	50	0.075	0.39	0.02	0.64	0.32	0.17	0.89	0.56	0.02	0.02	0.09	0.42	3.923	
F6	s11	50	0.076	0.35	0.02	0.62	0.31	0.19	0.98	0.61	0.02	0.02	0.12	0.56	4.313	
F6	s12	50	0.078	0.23	0.02	0.42	0.22	0.13	0.66	0.42	0.02	0.02	0.08	0.36	2.915	

Table B.1. continued

Test	Sample	Time	FR ¹	CO ₂	14:0	14:1	16:0	16:1	18:0	18:1	18:2	GLA	20:0	20:1	ARA	EPA	TFA ²
		min	sccm	mole	Mole FAME/mole CO ₂ x10 ⁻⁵												
f6	c1	180	50	0.539	0.69	0.04	0.89	0.48	0.21	1.18	0.74	0.1	0.08	0.15	0.61	0.5	5.663
f6	Total			1.503	18.36	1.17	23.16	12.39	5.01	28.00	17.30	2.21	1.56	2.91	13.18	11.31	136.6

1. FR – flow rate; sccm (standard cm³/min)

2. TFA – total fatty acid methyl esters

Table B.2. Raw data for moisture-content kinetic experiments

Test Sample	Time	MC ¹	CO ₂	CO ₂	14:0	14:1	16:0	16:1	18:0	18:1	18:2	GLA	20:0	20:1	ARA	EPA	TFA ²
			min	%	Mole FAME/mole CO ₂ x10 ⁻⁵												
m1	s1	30	0.084	0.05	0.00	0.00	0.00	0.00	0.00	0.00	0.00	0.18	0.00	0.00	0.00	0.00	0.23
m1	s2	30	0.083	0.51	0.00	0.69	0.41	0.12	0.63	1.12	0.32	0.00	0.00	0.00	0.85	1.74	6.38
m1	s3	30	0.082	1.05	0.06	1.49	0.90	0.23	1.37	2.45	0.50	0.00	0.09	1.71	3.43	13.29	
m1	s4	30	0.085	1.40	0.08	2.07	1.26	0.30	1.86	3.40	0.65	0.00	0.13	2.28	4.63	18.08	
m1	s5	30	0.086	1.12	0.07	1.47	0.92	0.20	1.21	2.22	0.41	0.00	0.00	1.56	3.18	12.34	
m1	s6	30	0.082	1.11	0.06	1.69	1.04	0.29	1.73	3.12	0.54	0.00	0.16	2.65	5.38	17.77	
m1	s7	30	0.083	0.61	0.00	0.94	0.57	0.16	0.99	1.79	0.30	0.00	0.00	1.60	3.30	10.25	
m1	s8	30	0.083	0.48	0.00	0.72	0.46	0.11	0.71	1.28	0.22	0.00	0.00	1.04	2.12	7.12	
m1	s9	30	0.080	0.46	0.00	0.73	0.48	0.13	0.80	1.45	0.24	0.00	0.00	1.27	2.59	8.16	
m1	s10	30	0.083	0.37	0.00	0.44	0.31	0.00	0.32	0.61	0.00	0.00	0.00	0.35	0.70	3.10	
m1	s11	30	0.104	0.21	0.00	0.36	0.24	0.00	0.45	0.80	0.13	0.00	0.00	0.71	1.45	4.34	
m1	s12	30	0.083	0.17	0.00	0.30	0.21	0.00	0.39	0.70	0.11	0.00	0.00	0.66	1.34	3.87	
m1	c1	180	0.600	0.57	0.04	0.71	0.44	0.11	0.59	0.88	0.17	0.03	0.04	0.37	2.95	6.89	
m1	Total		1.618	8.10	0.32	11.59	7.23	1.64	11.04	19.82	3.77	0.03	0.43	15.05	32.81	111.8	
m2	s0	95	0.000	0.32	0.00	0.37	0.00	0.00	0.00	0.00	0.00	0.00	0.00	0.00	0.00	0.00	0.69
m2	s1	95	0.045	0.02	0.00	0.03	0.00	0.00	0.03	0.00	0.00	0.00	0.00	0.00	0.00	0.00	0.09
m2	s2	95	0.061	0.04	0.00	0.04	0.00	0.00	0.03	0.00	0.00	0.00	0.00	0.00	0.00	0.00	0.11
m2	s3	95	0.059	0.03	0.00	0.04	0.01	0.00	0.03	0.04	0.00	0.00	0.00	0.00	0.00	0.00	0.15
m2	s4	95	0.065	0.02	0.00	0.04	0.00	0.00	0.03	0.00	0.00	0.00	0.00	0.00	0.00	0.00	0.10
m2	s5	95	0.064	0.02	0.00	0.03	0.01	0.00	0.03	0.02	0.00	0.00	0.00	0.00	0.00	0.00	0.10
m2	s6	95	0.062	0.02	0.00	0.03	0.00	0.00	0.00	0.00	0.00	0.00	0.00	0.00	0.00	0.00	0.05
m2	s8	95	0.078	0.01	0.00	0.02	0.00	0.00	0.00	0.00	0.00	0.00	0.00	0.00	0.00	0.00	0.02

Table B.2. continued

Test Sample	Time	MC ¹	CO ₂	Mole FAME/mole CO ₂ × 10 ⁻⁵									
	min	%	mole	18:0	18:1	18:2	GLA	20:0	20:1	ARA	EPA	TFA ²	
m2	s12	95	0.066	0.00	0.00	0.00	0.00	0.00	0.00	0.00	0.00	0.00	
m2	c1	95	0.064	0.00	0.00	0.00	0.00	0.00	0.00	0.00	0.00	0.00	
m2	Total		0.330	0.48	0.00	0.59	0.03	0.00	0.16	0.06	0.00	1.30	
m3	s0	95-s ³	0.893	0.22	0.03	0.26	0.12	0.06	0.29	0.20	0.00	1.26	
m3	s1	95-s	0.000	0.38	0.02	0.42	0.22	0.09	0.45	0.24	0.00	2.21	
m3	s2	95-s	0.045	0.36	0.02	0.37	0.19	0.08	0.36	0.19	0.00	1.84	
m3	s3	95-s	0.065	0.41	0.06	0.32	0.17	0.00	0.27	0.15	0.00	1.39	
m3	s4	95-s	0.072	0.23	0.04	0.25	0.13	0.05	0.26	0.14	0.00	1.29	
m3	s5	95-s	0.064	0.21	0.04	0.23	0.11	0.04	0.20	0.12	0.00	1.03	
m3	s6	95-s	0.066	0.19	0.04	0.24	0.12	0.06	0.27	0.15	0.00	1.29	
m3	c1	95-s	0.064	0.04	0.02	0.03	0.02	0.00	0.04	0.00	0.00	0.15	
m3	Total		0.062	2.05	0.27	2.12	1.08	0.39	2.14	1.20	0.00	10.45	
k1	s0	0	0.03	0.91	0.04	0.74	0.31	0.13	0.54	0.53	0.13	3.73	
k1	s1	30	0.15	5.29	0.28	2.31	1.18	0.34	1.51	1.68	0.17	14.40	
k1	s2	60	0.12	9.22	0.44	7.12	3.21	1.58	6.11	6.59	0.59	42.92	
k1	s3	90	0.13	0.09	0.06	0.07	0.04	0.02	0.09	0.13	0.01	50.00	
k1	s4	120	0.12	5.79	0.26	6.18	2.50	1.79	6.57	6.91	0.61	41.05	
k1	s5	150	0.12	5.14	0.21	3.38	1.27	0.57	1.99	2.06	0.18	17.00	
k1	s6	180	0.12	4.01	0.15	5.34	1.72	1.67	4.87	4.89	0.40	29.78	
k1	s7	210	0.13	3.04	0.12	3.30	1.09	0.93	2.71	2.74	0.22	18.01	
k1	s8	240	0.12	1.55	0.07	1.26	0.44	0.34	1.00	1.04	0.08	7.28	
k1	s9	270	0.12	0.86	0.04	0.80	0.29	0.18	0.58	0.62	0.05	4.17	
	RRF		0.96	0.96	1.02	1.01	1.01	1.01	1.04	1.16	1.03	1.36	
											1	1.25	

Table B.2. continued

Test Sample	Time	MC ¹	CO ₂	14:0	14:1	16:0	16:1	18:0	18:1	18:2	GLA	20:0	20:1	ARA	EPA	TFA ²	Mole FAME/mole CO ₂ x10 ⁵
K1	s10	300	10	0.11	0.76	0.00	0.57	0.21	0.10	0.33	0.42	0.00	0.00	0.00	0.16	2.72	
K1	s11	330	10	0.12	0.73	0.04	0.46	0.18	0.07	0.23	0.27	0.03	0.03	0.04	0.10	2.30	
K1	s12	360	10	0.12	0.38	0.02	0.31	0.12	0.06	0.19	0.21	0.01	0.02	0.02	0.09	1.56	
K1	s13	r ⁴	10	0.3	0.09	0.00	0.33	0.19	0.14	0.22	0.19	0.04	0.01	0.00	0.03	1.25	
K1	Total			1.81	37.8	1.71	32.2	12.7	7.91	26.9	28.3	2.51	2.63	2.55	13.1	236.2	
K2	s0	0	10	0.05	0.88	0.05	0.81	0.35	0.15	0.62	0.66	0.03	0.05	0.05	0.21	4.20	
K2	s1	30	10	0.15	3.50	0.18	3.23	1.54	0.64	2.74	3.09	0.34	0.13	0.05	1.48	19.34	
K2	s2	60	10	0.14	16.35	0.81	9.65	4.44	1.34	5.60	6.14	0.63	0.28	0.31	3.41	51.09	
K2	s3	90	10	0.12	12.86	0.61	7.96	3.35	1.25	4.81	5.15	0.49	0.27	0.30	1.95	42.24	
K2	s4	120	10	0.12	3.95	0.17	3.46	1.35	0.63	2.24	2.40	0.24	0.16	0.03	0.95	17.05	
K2	s5	150	10	0.13	1.86	0.08	1.79	0.71	0.33	1.18	1.27	0.13	0.08	0.09	0.48	8.71	
K2	s6	180	10	0.13	1.25	0.06	1.08	0.44	0.17	0.65	0.72	0.07	0.04	0.04	0.27	5.20	
K2	s7	210	10	0.13	0.84	0.04	0.68	0.28	0.10	0.39	0.43	0.04	0.02	0.03	0.16	3.24	
K2	s8	240	10	0.13	0.39	0.02	0.34	0.14	0.05	0.21	0.24	0.02	0.01	0.01	0.10	1.67	
K2	s9	270	10	0.15	0.57	0.03	0.34	0.15	0.04	0.18	0.20	0.02	0.01	0.01	0.06	1.71	
K2	s10	300	10	0.12	0.45	0.02	0.32	0.14	0.04	0.16	0.18	0.01	0.00	0.01	0.05	1.46	
K2	s11	330	10	0.13	0.27	0.01	0.24	0.11	0.03	0.14	0.16	0.01	0.00	0.01	0.02	1.00	
K2	s12	360	10	0.13	0.37	0.02	0.26	0.12	0.03	0.13	0.15	0.01	0.00	0.00	0.05	1.21	
K2	s13	425	10	0.31	0.78	0.05	0.44	0.27	0.05	0.29	0.32	0.03	0.01	0.01	0.12	2.56	
K2	s14	r ⁴	10	0.57	0.10	0.01	0.06	0.03	0.01	0.04	0.04	0.00	0.00	0.02	0.02	0.34	
K2	Total			2.5	44.4	2.16	30.7	13.4	4.86	19.4	21.1	2.07	1.07	0.94	8.03	161	
K3	s0	0	30	0.04	1.13	0.06	0.57	0.24	0.08	0.35	0.35	0.03	0.01	0.02	0.07	3.05	
K3	s1	30	30	0.15	0.02	0.01	0.01	0.01	0.00	0.02	0.08	0.00	0.00	0.00	0.02	0.23	

Table B.2. continued

Test Sample	Time	MC ¹	CO ₂	14:0	14:1	16:0	16:1	18:0	18:1	18:2	GLA	20:0	20:1	ARA	EPA	TFA ²
			min	%	Mole FAME/mole CO ₂ x10 ⁵											
K3	s2	60	30	0.14	0.02	0.01	0.01	0.00	0.03	0.08	0.00	0.00	0.00	0.00	0.03	0.04
K3	s3	90	30	0.15	0.04	0.01	0.03	0.02	0.01	0.06	0.10	0.00	0.00	0.00	0.02	0.06
K3	s4	120	30	0.09	4.08	0.18	2.58	1.08	0.58	2.15	2.27	0.19	0.20	0.17	1.14	1.42
K3	s5	150	30	0.13	3.80	0.16	3.22	1.29	0.81	2.95	3.07	0.25	0.25	0.31	1.55	1.96
K3	s6	180	30	0.12	5.44	0.24	3.45	1.42	0.70	2.59	2.74	0.23	0.20	0.21	1.26	1.58
K3	s7	240	30	0.24	1.52	0.06	1.47	0.58	0.37	1.35	1.41	0.12	0.10	0.12	0.65	0.80
K3	s8	300	30	0.25	1.74	0.08	1.43	0.60	0.40	1.47	1.53	0.12	0.15	0.23	0.89	1.12
K3	s9	360	30	0.24	0.83	0.04	0.79	0.33	0.21	0.80	0.84	0.07	0.07	0.08	0.45	0.57
K3	s10	420	30	0.24	0.72	0.03	0.56	0.23	0.14	0.52	0.55	0.04	0.05	0.05	0.30	0.38
K3	s11	r ⁴	30	0.24	0.24	0.03	0.27	0.00	0.09	0.39	0.40	0.01	0.03	0.05	0.27	0.31
K3	Total			2.03	19.6	0.92	14.4	5.81	3.4	12.7	13.4	1.07	1.06	1.24	6.67	8.44
K4	s0	0	20	0.03	1.24	0.06	0.93	0.44	0.19	0.77	0.79	0.09	0.04	0.04	0.29	0.36
K4	s1	30	20	0.16	0.03	0.01	0.02	0.04	0.01	0.03	0.02	0.00	0.00	0.01	0.01	0.17
K4	s2	60	20	0.13	0.03	0.02	0.02	0.01	0.01	0.04	0.07	0.01	0.00	0.01	0.03	0.28
K4	s3	90	20	0.14	5.81	0.26	5.55	2.31	1.62	5.97	6.27	0.52	0.54	0.61	3.36	4.49
K4	s4	120	20	0.13	3.13	0.14	3.09	1.22	0.91	3.18	3.32	0.28	0.32	0.33	1.79	2.36
K4	s5	180	20	0.29	5.92	0.27	3.97	1.66	0.76	2.85	3.02	0.26	0.27	0.15	1.13	1.46
K4	s6	240	20	0.27	2.47	0.11	1.65	0.71	0.36	1.35	1.43	0.12	0.11	0.11	0.66	0.85
K4	s7	300	20	0.26	2.07	0.10	1.26	0.56	0.26	0.99	1.06	0.09	0.08	0.08	0.50	0.65
K4	s8	360	20	0.27	1.07	0.05	0.96	0.41	0.21	0.80	0.85	0.07	0.05	0.05	0.34	0.43
K4	s9	420	20	0.25	1.17	0.05	0.79	0.35	0.14	0.57	0.61	0.05	0.03	0.04	0.25	0.33
K4	s10	rc	20	0.24	0.01	0.00	0.01	0.01	0.00	0.02	0.02	0.00	0.00	0.00	0.02	0.12
K4	s11	rv	20	0.24	0.33	0.02	0.25	0.11	0.04	0.18	0.19	0.02	0.00	0.00	0.07	0.09
K4	Total			2.41	23.29	1.08	18.51	7.82	4.50	16.73	17.64	1.49	1.44	1.42	8.45	11.09

1. MCwb - Moisture content (wet basis) 2. TFA - total fatty acid methyl esters 3. 95-s - 95 % moisture content (wet basis) + 10 % w/w PFPE surfactant 4. r - decompress extraction cell and rinse lines

Table B.3. Raw data from equilibrium experiments.

Test Sample	P ¹ MPa	T ² °C	CO ₂ mole	14:0	14:1	16:0	16:1	18:0	18:1	18:2	GLA	20:0	20:1	ARA	EPA	TFA
Mole FAME/mole CO ₂ × 10 ⁵																
e2	15	13.8	40	0.038	2.37	0.00	0.81	0.00	0.00	0.00	0.00	0.00	0.00	0.00	0.00	3.18
e2	30	13.8	40	0.038	5.75	0.31	2.37	1.20	0.32	1.31	1.44	0.00	0.00	0.00	0.77	0.00
e2	45	13.8	40	0.038	2.95	0.15	2.41	1.15	0.53	2.01	2.27	0.88	0.63	0.10	0.88	1.08
e2	60	13.8	40	0.037	6.37	0.35	3.41	1.74	0.46	1.94	2.24	0.22	0.06	0.07	0.62	0.83
e2	75	13.8	40	0.037	6.27	0.34	3.26	1.67	0.55	2.16	2.52	0.24	0.12	0.13	0.95	1.29
e2	90	13.8	40	0.038	7.26	0.38	2.08	1.86	0.64	2.77	3.00	0.29	0.13	0.14	1.03	1.38
e2	105	13.8	40	0.039	6.80	0.36	3.41	1.75	0.45	1.84	2.19	0.21	0.10	0.10	0.63	1.12
e3	0	20.7	40	0.014	2.48	0.43	1.42	0.51	0.00	1.07	1.01	0.00	0.00	0.00	1.29	0.00
e3	15	20.7	40	0.028	6.75	0.37	2.99	1.48	0.51	2.02	2.15	0.00	0.00	0.00	0.78	1.09
e3	30	20.7	40	0.029	24.67	1.28	11.18	5.53	1.72	6.93	7.51	0.70	0.33	0.37	2.55	3.62
e3	45	20.7	40	0.030	25.21	1.33	10.29	5.15	1.37	5.64	6.25	0.59	0.00	0.00	1.97	2.88
e3	60	20.7	40	0.029	33.22	1.72	14.38	7.08	1.90	7.87	8.60	0.83	0.31	0.35	2.57	3.67
e3	75	20.7	40	0.033	19.14	0.97	10.77	5.16	1.87	7.38	7.95	0.74	0.42	0.47	2.91	4.14
e3	90	20.7	40	0.030	35.77	1.90	13.77	6.98	1.90	7.80	8.52	0.82	0.23	0.34	2.84	4.01
e3	105	20.7	40	0.032	33.99	1.75	14.87	7.43	1.96	8.15	8.89	0.86	0.33	0.38	2.66	3.82
e3	120	20.7	40	0.030	24.34	1.23	13.29	6.46	1.96	8.03	8.73	0.83	0.34	0.41	2.69	3.79
e3	135	20.7	40	0.032	29.72	1.52	13.76	6.84	1.84	7.71	8.43	0.80	0.28	0.33	2.51	3.43
e3	150	20.7	40	0.029	15.48	0.75	11.83	5.43	2.36	9.20	9.80	0.90	0.53	0.49	3.62	5.09
e3	165	20.7	40	0.032	30.13	1.50	14.32	6.90	2.13	8.54	9.23	0.87	0.38	0.41	3.01	4.34
e3	180	20.7	40	0.037	22.79	1.08	13.70	6.30	2.07	8.33	8.96	0.84	0.35	0.43	2.73	3.80
e4	0	27.6	40	0.015	0.39	0.00	0.33	0.13	0.00	0.23	0.25	0.00	0.00	0.00	0.00	1.33
e4	15	27.6	40	0.043	6.00	0.30	3.98	1.81	0.69	2.63	2.78	0.31	0.16	0.13	0.86	1.21
e4	30	27.6	40	0.032	28.35	1.41	15.28	7.12	2.34	9.11	9.82	0.92	0.43	0.48	3.00	4.18
e4	45	27.6	40	0.032	24.16	1.20	14.70	6.78	2.60	9.93	10.71	1.01	0.53	0.60	3.67	5.17
e4	60	27.6	40	0.031	45.18	2.29	18.90	9.08	2.93	11.34	12.34	1.16	0.65	0.67	4.46	6.32
e4	75	27.6	40	0.033	11.78	0.55	11.94	4.95	3.86	13.05	13.72	1.19	1.39	1.49	7.31	10.56
e4	90	27.6	40	0.034	22.42	1.06	15.75	6.80	3.06	11.03	11.71	1.07	0.66	0.82	4.12	5.76

Table B.3. continued

Test Sample	P ¹	T ²	CO ₂	CO ₂ mole	Mole FAME/mole CO ₂ × 10 ⁵	GLA	20:0	20:1	ARA	EPA	TFA						
e4	105	27.6	40	0.032	12.10	0.57	11.84	4.93	3.81	12.66	13.27	1.13	1.42	1.47	6.97	9.93	80.10
e4	120	27.6	40	0.029	0.56	0.03	0.49	0.29	0.15	0.68	1.05	0.09	0.96	0.05	0.67	0.96	6.01
e4	120	27.6	40	0.281	0.01	0.00	0.01	0.00	0.00	0.01	0.00	0.00	0.00	0.00	0.00	0.00	0.04
e5	15	20.7	60	0.032	3.72	0.20	1.75	0.96	0.27	1.19	1.23	0.11	0.00	0.01	0.37	0.47	10.28
e5	30	20.7	60	0.036	2.69	0.14	2.09	1.05	0.57	2.31	2.36	0.22	0.18	0.27	1.09	1.42	14.39
e5	45	20.7	60	0.035	2.33	0.12	1.87	0.94	0.57	2.24	2.28	0.20	0.19	0.20	1.14	1.46	13.54
e5	60	20.7	60	0.037	2.51	0.13	1.94	0.98	0.59	2.15	2.19	0.20	0.15	0.15	0.92	1.20	13.10
e5	75	20.7	60	0.034	2.98	0.15	2.46	1.21	0.72	2.80	2.85	0.25	0.23	0.24	1.34	1.76	16.98
e5	90	20.7	60	0.037	5.19	0.26	2.85	1.50	0.46	2.00	2.10	0.19	0.09	0.54	0.64	0.83	16.65
e5	150	20.7	60	0.075	7.51	0.38	3.20	1.73	0.43	1.93	2.06	0.18	0.01	0.01	0.57	0.76	18.78
e5	180	20.7	60	0.049	2.00	0.10	1.67	0.83	0.51	2.02	2.07	0.18	0.20	0.03	1.04	1.36	12.00
e6	15	13.8	60	0.031	0.15	0.01	0.12	0.05	0.04	0.13	0.13	0.01	0.00	0.00	0.09	0.07	0.81
e6	30	13.8	60	0.030	0.10	0.00	0.06	0.03	0.05	0.04	0.00	0.00	0.00	0.02	0.02	0.02	0.32
e6	45	13.8	60	0.031	0.16	0.00	0.07	0.04	0.00	0.00	0.00	0.00	0.00	0.00	0.00	0.00	0.27
e6	60	13.8	60	0.030	0.13	0.01	0.06	0.04	0.00	0.05	0.00	0.00	0.00	0.01	0.02	0.40	
e6	75	13.8	60	0.030	0.08	0.01	0.05	0.03	0.01	0.06	0.00	0.00	0.00	0.01	0.01	0.33	
e6	90	13.8	60	0.032	0.14	0.01	0.10	0.06	0.02	0.11	0.11	0.00	0.00	0.04	0.05	0.65	
e6	120	13.8	60	0.050	0.12	0.01	0.09	0.04	0.02	0.07	0.07	0.00	0.00	0.02	0.02	0.47	
e7	15	27.6	60	0.038	4.62	0.21	4.17	1.86	1.07	3.95	4.12	0.36	0.28	1.64	2.09	24.67	
e7	30	27.6	60	0.035	4.34	0.20	4.52	1.94	1.57	5.39	5.53	0.46	0.60	2.90	3.84	31.39	
e7	45	27.6	60	0.038	9.38	0.44	6.37	2.93	1.28	4.82	5.08	0.45	0.29	1.79	2.35	35.49	
e7	60	27.6	60	0.036	6.52	0.30	6.10	2.62	1.95	6.67	6.87	0.57	0.71	3.46	4.61	40.49	
e7	75	27.6	60	0.037	11.55	0.53	7.34	3.30	1.40	5.17	5.46	0.49	0.32	1.92	2.58	40.40	
e7	90	27.6	60	0.040	4.23	0.19	4.81	1.95	1.85	5.99	6.13	0.50	0.78	3.50	4.69	34.74	
e7	120	27.6	60	0.051	5.24	0.23	5.28	2.15	1.69	5.55	5.73	0.48	0.56	2.74	3.65	33.38	

Table B.3. continued

Test	Sample	P ¹ MPa	T ² °C	CO ₂ mole	14:0	14:1	16:0	16:1	18:0	18:1	18:2	GLA	20:0	20:1	ARA	EPA	TFA
Mole FAME/mole CO ₂ x10 ⁻⁵																	
e7	180	27.6	60	0.088	3.26	0.14	4.06	1.56	1.68	5.14	5.34	0.44	0.76	0.81	3.27	4.34	30.79
e7	240	27.6	60	0.077	3.01	0.13	3.72	1.42	1.60	4.77	4.87	0.40	1.65	0.76	2.99	0.64	25.97

1. P – Pressure

2. T – Temperature

APPENDIX C

COMPUTER PROGRAMS

Program A. Compressed-Gas Model

```
REM*****
REM *          PENG-ROB.BAS *
REM * *
REM * This program executes the compressed-gas model for determining *
REM * the solubility of a solute in the fluid phase by utilizing the *
REM * Peng-Robinson equation of state in terms of the compressibility *
REM * factor, Z. Vapor pressure and accentric factor of the solute is also *
REM * predicted. The roots to the cubic equation of state are determined *
REM * in the subroutine, CUBIC. The program will ask for a range of kij *
REM * values and a step size to reduce the run time. *
REM * Applying this program to other compounds at various temperatures *
REM * is relatively easy by forming the appropriate data files: *p.txt for *
REM * the physical properties data and *(temp).txt for the isotherm data. *
REM * The *p.txt file should contain "compound",nz,T,MW,Tc,Pc,Vc,Vm,w,Tm,*
REM * Tb,psat,A,B,C,D,E. If any values are not available, then use 0. *
REM * The *(temp).txt file should contain P,CO2den,Y data in row form. *
REM * Some modifications would be necessary for systems larger than binary. *
REM * The output data file contains the predicted solubility for each *
REM * pressure in an isotherm, the enhancement factor, the value for kij, *
REM * the % AAD and predicted vapor pressure. *
REM *
REM *****
```

```
DIM tc(2), pc(2), omega(2), atc(2), om(2), tr(2), alp(2), ai(2)
DIM y(2), bepk(2, 2)
DIM co2mol(10), ystar(10), so(10), vskf(10), scfden(10)
DIM a(4), R1(2), R2(2), R3(2), cr(3), ypc(10), ep(10)
DIM eemf(10), bi(2), aa(2, 2), fugcf(2), fugf(2), z(10)
```

CLS

```
REM -----
REM DEFINE PHYSICAL PROPERTIES FOR BINARY SYSTEM
```

```
REM INPUT "Enter Input parameter filename: (ex. pirrp.txt) "; o$
o$ = "palmp.txt"
n$ = "pirr40.txt"
```

```
OPEN o$ FOR INPUT AS #1
INPUT #1, sys$, nz1, t, famw, tc(1), pc(1), vc(1), pmv, omega(1)
INPUT #1, tm, tb, psat3, vpa, vpb, vpc, vpd, et
```

```

PRINT "The parameters are: sys$, nz1, t, famw, tc(1), pc(1), vc(1)"
PRINT "The parameters are: "; sys$, nz1, t, famw, tc(1), pc(1), vc(1)
PRINT "pmv, omega(1), tm, tb, psat3"
PRINT pmv, omega(1), tm, tb, psat3
PRINT vpa, vpb, vpc, vpd, et
CLOSE

```

```

GOSUB 5000: REM OBTAIN OMEGA(1)
IF omega(1) = 0 THEN omega(1) = omega1
PRINT "OMEGA1="; omega(1), omega1

```

```
t = t + 273.15
```

```

REM INPUT "Enter Input data filename: (ex. pirr40.txt) "; n$
OPEN n$ FOR INPUT AS #2
  FOR i = 1 TO nz1
    INPUT #2, ep(i), scfden(i), eemf(i)
    PRINT "Read from file: "; ep(i), scfden(i), eemf(i)
  NEXT i
CLOSE

```

```
REM INPUT "Enter Output filename"; m$
```

```

REM -----
REM Obtain the estimated vapor pressure
REM -----

```

```

GOSUB 4000
REM INPUT "vapor pressure of solute"; psat#
  psat# = fugsb
PRINT "the vapor pressure is "; psat#

```

```
REM -----
```

```

nz = nz1
tc(2) = 304.1
pc(2) = 73.8
omega(2) = .225
R = 83.14: REM gas constant (cm3*bar/mol*K)
tol = .001
aadmin = 100
n = 0

```

```
REM FOR tc = 600 TO 800 STEP 50
```

```

REM FOR pc = 10 TO 20 STEP 5
REM FOR omega = .6 TO 1.2 STEP .2
REM tc(1) = tc
REM pc(1) = pc
REM omega(1) = omega

REM -----
REM CALCULATE P-R PARAMETERS AT THE CRITICAL POINT
FOR i = 1 TO 2
  atc(i) = .45724 * R ^ 2 * (tc(i)) ^ 2 / pc(i)
  om(i) = .37464 + 1.54226 * omega(i) - .26992 * (omega(i)) ^ 2
  tr(i) = t / tc(i)
  alp(i) = (1 + om(i) * (1 - SQR(tr(i)))) ^ 2
  ai(i) = atc(i) * alp(i)
  bi(i) = .0778 * R * tc(i) / pc(i)
NEXT i
FOR i = 1 TO 2
  FOR j = 1 TO 2
    aa(i, j) = SQR(ai(i) * ai(j))
    bepk(i, j) = 0
  NEXT j
NEXT i

REM -----
101 REM BEGINNING OF MAIN LOOP
REM INPUT "input kij range and step size"; kij1, kij2, step1
REM FOR bep = kij1 TO kij2 STEP step1
  FOR bep = -.5 TO -.3 STEP .02
    bep1 = bep
    bepk(1, 2) = bep1
    bepk(2, 1) = bepk(1, 2)
  REM -----
  REM BEGINNING OF 2ND MAIN LOOP
  FOR j = 1 TO nz
    l = 0
    REM ESTABLISH AN INITIAL GUESS FOR Y(I) TO BEGIN ITERATION
    y(1) = .00001#
    100 y(2) = 1 - y(1)
    am = 0
    bm = 0
    FOR i = 1 TO 2
      FOR j1 = 1 TO 2

```

```

      am = am + y(i) * y(j1) * (1 - bepk(i, j1)) * aa(i, j1)
    NEXT j1
    bm = bm + y(i) * bi(i)
  NEXT i
  az = am * ep(j) / (R * t) ^ 2
  bz = bm * ep(j) / (R * t)
  a(1) = 1
  a(2) = bz - 1
  a(3) = az - 3 * bz ^ 2 - 2 * bz
  a(4) = bz ^ 3 + bz ^ 2 - az * bz
  REM FOR i = 1 TO 4
  REM PRINT "the coefficient a("; i; ") is "; a(i)
  REM NEXT i

  REM -----
  REM CALL SUBROUTINE CUBIC to obtain roots to P-R EOS in terms of Z
  GOSUB 1000

  IF ABS(rt1(2)) > 0 THEN rt1(1) = 0
  IF ABS(rt2(2)) > 0 THEN rt2(1) = 0
  IF ABS(rt3(2)) > 0 THEN rt3(1) = 0
  REM FIND THE MAXIMUM REAL ROOT
  IF rt1(1) >= rt2(1) AND rt3(1) THEN GOTO 71 ELSE
  IF rt2(1) >= rt1(1) AND rt3(1) THEN GOTO 72 ELSE
  IF rt3(1) >= rt1(1) AND rt2(1) THEN GOTO 73
  71 zzv = rt1(1): GOTO 75
  72 zzv = rt1(2): GOTO 75
  73 zzv = rt1(3): GOTO 75
  75 REM PRINT "the max root is"; zzv
  IF zzv > bz THEN GOTO 81 ELSE GOTO 82

  REM -----
  REM APPLY VAN DER WAALS MIXING RULE TO THE PR-EOS
  REM WRITTEN IN TERMS OF Z: Z^3+(B-1)Z^2+(A-3B^2-2B)Z+(B^3+B^2-
  AB)=0
  REM THEN OBTAIN THE FUGACITY COEFFICIENTS
  REM -----

  81 vmix1 = y(1) * aa(1, 1) + y(2) * aa(1, 2) * (1 - bepk(1, 2))
  REM PRINT "aa"; aa(1, 1), aa(1, 2), bepk(1, 2)
  m = 1
  p1 = bi(m) * (zzv - 1) / bm
  p2 = LOG(zzv - bz)
  p3 = az * (2 * vmix1 / am - bi(m) / bm) / (2 * SQR(2) * bz)

```

```

p4 = LOG((zzv + 2.414 * bz) / (zzv - .414 * bz))
arg = p1 - p2 - (p3 * p4)
fugcf(m) = EXP(arg)
fugf1(m) = y(m) * fugcf(m) * ep(j)
poynt(j) = EXP(pmv * (ep(j) - psat#) / (R * t))
fugf2 = psat# * poynt(j)
enhan(j) = poynt(j) / fugcf(m)
q1 = fugf2 / fugf1(m)
yy = fugf2 / (ep(j) * fugcf(m))
ypc(j) = yy

REM PRINT "fcf,ff,yy,pf"; fugcf(m), fugf1(m), yy, poynt(j)

```

```

z(j) = zzv
kij1 = bepk(1, 2)

```

```

REM -----
REM Convergence criteria test

```

```

test = q1 - 1

```

```

IF ABS(test) < .01 THEN GOTO 50
l = l + 1
y(1) = yy
IF l > 100 THEN GOTO 82 ELSE GOTO 100
82 PRINT "Non-convergence or zzv<bz error"
REM PRINT "l,zzv,bz and old y(1) is"; l, zzv, bz, y(1)
INPUT "new y"; y(1)
REM psat# = psat# / 1.5
l = 0
GOTO 100

```

```

50 PRINT "y("; ep(j); ")="; ypc(j)
NEXT j
REM END OF 2NDARY LOOP -----

```

```

aad1 = 0
FOR j = 1 TO nz
    aad1 = aad1 + ABS((eemf(j) - ypc(j))) / eemf(j)
NEXT j
aad = aad1 * 100 / nz
REM IF vp = psat1# THEN END
IF aad < aadmin THEN aadmin = aad ELSE GOTO 200
kij = bepk(1, 2)

```

```

vp = psat#
pcl = pc
tcl = tc
omegal = omega
FOR j = 1 TO nz
ypred(j) = ypc(j)
enhanc(j) = enhan(j)
NEXT j

200 NEXT bep
REM end of main loop -----
PRINT "tc,pc,omega,vp"; tc, pc, omega, vp
PRINT "kij,ypred"; kij, ypc(j)
PRINT "aadmin"; aadmin

REM NEXT omega
REM NEXT pc
REM NEXT tc

m$ = "out"
OPEN m$ FOR OUTPUT AS #3
  WRITE #3, "System output for fatty acid ", sys$, "at Temp (K)", t
  WRITE #3, "kij, aad, psat", kij, aadmin, psat#
  WRITE #3, "pressure yexp ypred enhancement"
  FOR i = 1 TO nz
    WRITE #3, ep(i), eemf(i), ypred(i), enhanc(i)
  NEXT i
CLOSE

REM -----
REM Print results
REM -----

PRINT "System output for fatty acid "; sys$; "at Temp (K)"; t
PRINT "kij, zzv, psat,omega"; zzv, psat#, omega(1)
REM PRINT "tc,pc,omega,vp"; tcl, pcl, omegal, vp
PRINT "kij, aad"; kij, aadmin

PRINT "pressure    yexp(mf)    ypred(mf)    enhancement"
FOR i = 1 TO nz
PRINT ep(i), eemf(i), ypred(i), enhanc(i)
NEXT i
END

```

```

REM *****
1000 REM subroutine          CUBIC.BAS
REM *****

zero = tol / 10
IF ABS(a(1)) - zero > 0 THEN GOTO 12
GOSUB 2000
REM call subroutine quadrat to solve for quadratic roots
RETURN
12 noroot = 3
it = 0
FOR i = 2 TO 4
a(i) = a(i) / a(1)
NEXT i
a(1) = 1
IF ABS(a(2)) <= 0 THEN GOTO 2 ELSE
nda = 3
b(1) = 1
b(2) = -(a(2) * .333333)
GOSUB 3000
it = 1
GOTO 4
2 FOR i = 1 TO 4
c(i) = a(i)
NEXT i
4 x = (c(4) ^ 2) * .25 + (c(3) ^ 3) * .037037
REM PRINT c(3), c(4), x
IF x < 0 THEN GOTO 9
x = SQR(x)
y = -(c(4) * .5)
i = 1
rt1(i) = y + x
5 n = 0
IF rt1(i) < 0 THEN n = 1
IF ABS(rt1(i)) < zero GOTO 6
rt1(i) = EXP((LOG(ABS(rt1(i)))) * .333333)
IF n = 1 THEN rt1(i) = -rt1(i)
6 IF i = 2 THEN GOTO 8
i = 2
rt1(i) = y - x
GOTO 5
8 rt2(2) = ((rt1(1) - rt1(2)) * .5) * 1.73205
rt1(1) = rt1(1) + rt1(2)
rt1(2) = 0

```

```

rt2(1) = -rt1(1) * .5
rt3(1) = rt2(1)
rt3(2) = -rt2(2)
GOTO 11
9 zz = ABS(c(3))
x = -(c(4) * .5) / SQR((zz ^ 3) * .037037)
ang = 1.5708 / (1 + ATN(x))
y = 2 * (SQR(zz * .333333))
ang = ang * .333333
rt1(1) = y * COS(ang)
rt2(1) = y * COS(ang + 2.0944)
rt3(1) = y * COS(ang + 4.18879)
rt1(2) = 0
rt2(2) = 0
rt3(2) = 0
11 IF it = 0 THEN GOTO 1050 ELSE
rt1(1) = rt1(1) + b(2)
rt2(1) = rt2(1) + b(2)
rt3(1) = rt3(1) + b(2)
1050 REM PRINT "the root are "; rt1(1), rt2(1), rt3(1)
REM PRINT "the imag roots are "; rt1(2), rt2(2), rt3(2)
RETURN

```

```

REM *****
2000 REM subroutine quadrt a(1)x^2+a(2)x+a(3)
REM *****

```

```

DIM root1(2), root2(2)
zero = tol / 10
IF ABS(a(1)) - zero > 0 THEN GOTO 256 ELSE
IF ABS(a(2)) - zero > 0 THEN GOTO 258 ELSE
noroot = 0
PRINT "no roots found"
RETURN
256 noroot = 2
x = a(2) ^ 2 - 4 * a(1) * a(3)
y = 2 * a(1)
z = SQR(ABS(x)) / y
w = -a(2) / y
IF x < 0 THEN GOTO 257
root1(1) = w + z
root1(2) = 0
root2(1) = w - z
root2(2) = 0

```



```

RETURN
257 root1(1) = w
root1(2) = z
root2(1) = w
root2(2) = -z
RETURN
258 noroot = 1
root1(1) = -a(3) / a(2)
root1(2) = 0
RETURN

```

```

REM *****
3000 REM subroutine lincng
REM *****

```

```

b1pwr = 1
nl = nda + 1
FOR i = 1 TO nl
c(i) = a(i)
NEXT i
36 FOR i = 2 TO nl
c(i) = c(i) + c(i - 1) * b(2)
NEXT i
c(nl) = c(nl) * b1pwr
nl = nl - 1
b1pwr = b1pwr * b(1)
IF nl > 1 GOTO 36
c(1) = c(1) * b1pwr
RETURN

```

```

REM *****
4000 REM SUBROUTINE VAPPRE
REM *****

```

```

REM This subroutine uses the extended Clapeyron equation and other methods
REM to estimate the vapor pressure:
REM  $\ln(\text{psat}) = H^*(1 - 1/\text{Tr})$ 
REM  $H = \text{Tbr} * \ln(\text{Pc}/1.01325)/(1 - \text{Tbr})$ 
REM from Reid, Prausnitz and Poling (1987)
REM Sublimation pressure may be estimated from the following relationship
REM  $\ln(\text{fl}/\text{fs}) = dH/\text{RTt}(Tt/T - 1)$  where fs is the fugacity of the solid taken
REM to be equal to the sublimation pressure. (Teja et al., 1987)
tr = t / tc(1)
tbr = tb / tc(1)

```

```

h = (tbr * LOG(pc(1) / 1.01325)) / (1 - tbr)
psat1 = h * (1 - 1 / tr)
psat1 = EXP(psat1)
REM Lee-Kessler (Pitzer) relationship
f0 = 5.92714 - 6.09648 / tr - 1.28862 * LOG(tr) + .169347 * tr ^ 6
f1 = 15.2518 - 15.6875 / tr - 13.4721 * LOG(tr) + .43577 * tr ^ 6
psat2 = EXP(f0 * tr + omega(1) * f1 * tr)

```

```

REM Use vp equation below for naphthalene (Reid et al.,1987)
xt = 1 - t / tc(1)
REM pvp11 = pc(1) * EXP((1 - xt) ^ -1
REM pvp12 = (vpa * xt + vpb * xt ^ 1.5 + vpc * xt ^ 3 + vpd * xt ^ 6))
REM pvp1# = pvp11*pvp12
REM pvp3 = EXP(vpa - vpb / (t + vpc))
REM pvp2 = EXP(vpa - vpb / t + vpc * LOG(t) + vpd * pvp / t ^ 2)
REM use vp eq. for octadecane
pvp2# = EXP(vpa - vpb / (t + vpc))

```

```

REM Wagner equation for vp of carboxylic acids (D'Souza and Teja, 1987)
REM properties for oleic acid
REM t10 = 228 + 273.13
REM pc(1) = 1390
REM data for stearic acid
t10 = 228 + 273.13: REM oleic at 15 mm
REM t760 = 204.5462 + .02 * t10 ^ 1.61
t760 = tb
PRINT t760
ecn = -4.098 + (1.49306 * 10 ^ -6) * (t760 ^ 2.55)
ps = (.0789 + .0226 * (ecn - 1)) ^ 2
a = 16.538816# - 21.575171# * (ecn - 1) ^ .16
b = -120.993735# + 115.211079# * (ecn - 1) ^ .07
c = 48.389806# - 43.670484# * (ecn - 1) ^ .28
d = -10.895522# + 6.615897 * (ecn - 1)
REM pc for sat'd fa only
REM pc(1) = 7.5 * famw / ps
REM ts for unsat'd fa
ts = 1 / 4.054
REM ts for sat'd fa
REM ts = 1 / (1.82 + .138 * (ecn - 1))
tc1 = t760 * (1 + ts)
tr2 = t / tc1
pc1 = pc(1) * 1000 / 10: REM convert bar to kPa
pvp21 = a * (1 - tr) + b * (1 - tr) ^ 1.5
pvp22 = c * (1 - tr) ^ 3 + (d * (1 - tr) ^ 6) / tr

```

```

pvp2 = pc1 * EXP(pvp21 + pvp22)
pvp = pvp * 10 / 1000: REM convert from kPa to bar
REM pvp31 = a * (1 - tr2) + b * (1 - tr2) ^ 1.5 +
REM pvp32=c * (1 - tr2) ^ 3 + d * (1 - tr2) ^ 6) / tr2
REM pvp3 = pc(1) * EXP(pvp31 + pvp32)

REM Use Benson vp equation below for fatty acids (Pa) (Daubert and Danner,1993)
pvp0# = EXP(vpa + vpb / t + vpc * LOG(t) + vpd * t ^ et)

REM use sublimation pressure for saturated fatty acids near room temp.
pvpa = pvp * 1000000 / 10: REM convert bar to Pa
Tt = tm
REM dHf = 56586: REM J/mol, heat of fusion from CRC handbook for stearate
REM dHf = 45377: REM myristate
dHf = 42037: REM palmitic acid
R2 = 8.314: REM J/mol K
eterm = EXP((dHf / (R2 * Tt)) * (Tt / t - 1))
fugsubl = pvp0# / eterm
pvp0# = pvp0# * .00001: REM convert Pa to bar
fugsub = fugsubl * .00001
benvp = pvp0#
wagvp = pvp
PRINT "sublimation pressure"; fugsub, benvp, wagvp, eterm
RETURN

REM *****
5000 REM SUBROUTINE ACENT2 FOR CALCULATION OF ACENTRIC
FACTOR
REM *****
REM USING THE LEE-KESLER VAPOR PRESSURE RELATIONSHIP
tet = tb / tc(1)
tet1 = LOG(tet)
tet2 = tet ^ 6
w1 = -LOG(pc(1)) - 5.92714 + 6.09648 / tet + 1.28862 * tet1 - .169347 * tet2
w2 = 15.2518 - 15.6875 / tet - 13.4721 * tet1 + .43577 * tet2
omegal = w1 / w2

RETURN

```

Program B. Kinetic Model (Fick's Second Law)

*This program determines the diffusivity for spherical geometries
*using Crank's analytical solution to Fick's 2nd Law up to 13 terms
*of the infinite series solution.
* model $y = 1 - ((6/\pi_sq) * term1)$;
* $term1 = \exp(-dw*\pi_sq*min/a_sq)$;
* where y=dependent variable
* min= minutes converted to seconds
* dw=diffusivity (cm/s)
* $\pi_sq = \pi$ squared
* $a_sq =$ radius squared (cm)

OPTIONS LS=72;
DATA fungi;
INPUT TIME FR total;
MIN=time*60;
 $\pi_sq = 9.8696044$;
 $a_sq = .015$;

CARDS;
15 60 0.089508127
30 60 0.189925769
45 60 0.255278546
60 60 0.305544294
75 60 0.327389036
90 60 0.336633728
105 60 0.342193848
120 60 0.344432979
135 60 0.344723487
150 60 0.346246803
165 60 0.352052716
180 60 0.356109529

;
PROC SORT; BY FR;
*PROC PRINT;
*PROC GLM; *CLASS TEMP FR TIME REP;
*MODEL CAFX=TIME TEMP FR REP;
*LSMEANS TIME FR TEMP/PSTDERR;
*PROC GLM; *CLASS TEMP FR TIME;
*MODEL CAFX= TEMP FR TIME TIME*TEMP*FR;
*LSMEANS TEMP FR TIME*TEMP*FR/PDIFF;

```

*          Flowrate 60 sccm          *
*****
proc nlin;
  WHERE FR=60;
  parms dw = 1.0e-6;

  term1 = exp(-dw*pi_sq*min/a_sq);

  model total = 1 - ((6/pi_sq) * term1);

  title1 '1 term TRT=60';

*****

proc nlin;
  where FR=60;
  parms dw = 1.0e-6;

  term1 = exp(-dw*pi_sq*min/a_sq);
  term2 = (1/4)*exp(-dw*4*pi_sq*min/a_sq);

  model total = 1 - ((6/pi_sq) * (term1 + term2));

  title1 '2 terms, tmt 60';

*****

proc nlin;
  where FR=60;
  parms dw = 1.0e-6;

  term1 = exp(-dw*pi_sq*min/a_sq);
  term2 = (1/4)*exp(-dw*4*pi_sq*min/a_sq);
  term3 = (1/9)*exp(-dw*9*pi_sq*min/a_sq);
  term4 = (1/16)*exp(-dw*16*pi_sq*min/a_sq);
  term5 = (1/25)*exp(-dw*25*pi_sq*min/a_sq);

  model total = 1 - ((6/pi_sq) * (term1 + term2 + term3
                                + term4 + term5));
  title1 '5 terms, tmt = 60';

*****

```

```

proc nlin;
  where FR=60;
  parms dw = 1.0e-6;

  term1 = exp(-dw*pi_sq*min/a_sq);
  term2 = (1/4)*exp(-dw*4*pi_sq*min/a_sq);
  term3 = (1/9)*exp(-dw*9*pi_sq*min/a_sq);
  term4 = (1/16)*exp(-dw*16*pi_sq*min/a_sq);
  term5 = (1/25)*exp(-dw*25*pi_sq*min/a_sq);
  term6 = (1/36)*exp(-dw*36*pi_sq*min/a_sq);
  term7 = (1/49)*exp(-dw*49*pi_sq*min/a_sq);
  term8 = (1/64)*exp(-dw*64*pi_sq*min/a_sq);
  term9 = (1/81)*exp(-dw*81*pi_sq*min/a_sq);
  term10 = (1/100)*exp(-dw*100*pi_sq*min/a_sq);

  model total = 1 - ((6/pi_sq) * (term1 + term2 + term3
    + term4 + term5 + term6 + term7 + term8
    + term9 + term10));
  title '10 terms, tmt = 60';

proc nlin data=fungi;
  where FR=60;
  parms dw = 1.0e-6;

  term1 = exp(-dw*pi_sq*min/a_sq);
  term2 = (1/4)*exp(-dw*4*pi_sq*min/a_sq);
  term3 = (1/9)*exp(-dw*9*pi_sq*min/a_sq);
  term4 = (1/16)*exp(-dw*16*pi_sq*min/a_sq);
  term5 = (1/25)*exp(-dw*25*pi_sq*min/a_sq);
  term6 = (1/36)*exp(-dw*36*pi_sq*min/a_sq);
  term7 = (1/49)*exp(-dw*49*pi_sq*min/a_sq);
  term8 = (1/64)*exp(-dw*64*pi_sq*min/a_sq);
  term9 = (1/81)*exp(-dw*81*pi_sq*min/a_sq);
  term10 = (1/100)*exp(-dw*100*pi_sq*min/a_sq);
  term11 = (1/121)*exp(-dw*100*pi_sq*min/a_sq);
  term12 = (1/144)*exp(-dw*100*pi_sq*min/a_sq);
  term13 = (1/169)*exp(-dw*100*pi_sq*min/a_sq);

  model total = 1 - ((6/pi_sq) * (term1 + term2 + term3 + term4 + term5
    + term6 + term7 + term8 + term9 + term10 + term11
    + term12 + term13));

output out=fun60 p=yp60 r=res60;
proc plot; plot total*min yp60*min='*/overlay vpos=40;

```

```
*      plot res2*min/ vref=0 vpos=30;  
*      plot y2u95*min='u' y2l95*min='l'  
*      yp2*min='*'/overlay vpos=40;  
proc print data=fun60;  
  title1 '13 terms, tmt = 60';
```

VITA

Terry Hill Walker was born in Marion, Virginia, on March 19, 1966. He graduated from Marion Senior High School in 1984. He attended the University of Tennessee, Knoxville, and received a Bachelor of Science degree in Engineering Science and Mechanics in December, 1989 with a concentration in biomedical engineering. He accepted a research assistantship with the University of Tennessee Agricultural Engineering Department and received a Master of Science degree in December, 1992 with a concentration in food process engineering. He then accepted a position as Research Associate with the Food Science and Technology Department, while pursuing a Doctor of Philosophy degree in Biosystems Engineering with a concentration in bioprocess engineering.

He is a member of the American Society of Agricultural Engineers, American Institute of Chemical Engineers, Institute of Biological Engineers and the Institute of Food Technologists. He is also a member of the Phi Kappa Phi and Gamma Sigma Delta honor societies.

1014 9628 33
08/13/98 *sw* MAE

INFORMATION
CONSERVATION, INC.